INVESTIGATING INDOLE-MEDIATED MODULATION OF *SALMONELLA* VIRULENCE AND CHEMOTAXIS

A Dissertation

by

NANDITA KOHLI

Submitted to the Office of Graduate and Professional Studies of
Texas A&M University
in partial fulfillment of the requirements for the degree of

DOCTOR OF PHILOSOPHY

Chair of Committee,	Arul Jayaraman
Committee Members,	Robert C. Alaniz
	Katy Kao
	Zhilei Chen
Head of Department,	M. Nazmul Karim

May 2017

Major Subject: Chemical Engineering

ABSTRACT

The microbial community present in the gastrointestinal tract is an important component of the host defense against pathogen infections. Prior work from our lab demonstrated that indole, a microbial metabolite of tryptophan, reduces enterohemorrhagic *Escherichia coli* O157:H7 attachment to intestinal epithelial cells and biofilm formation, suggesting that indole may be an effector/attenuator of colonization for a number of enteric pathogens. Here, we show that indole attenuates *Salmonella* Typhimurium (*Salmonella*) virulence and invasion as well as increases resistance of host cells to *Salmonella* invasion. Indole-exposed *Salmonella* colonized mice less effectively compared to solvent-treated controls, as evident by competitive index values less than 1 in multiple organs. Indole-exposed *Salmonella* demonstrated 160-fold less invasion of HeLa epithelial cells and 2-fold less invasion of J774A.1 macrophages, compared to solvent-treated controls. However, indole did not affect *Salmonella* intracellular survival in J774A.1 macrophages, suggesting that indole primarily affects *Salmonella* invasion. The decrease in invasion was corroborated by a decrease in expression of multiple *Salmonella* Pathogenicity Island-1 (SPI-1) genes. Indole also reduced *Salmonella* motility and acts as a chemo-repellent through the Tsr chemoreceptor. We also identified that the effect of indole on *Salmonella* virulence was mediated by both PhoPQ-dependent and independent mechanisms. Further investigation of PhoPQ-dependent mechanism using Autodock Vina, Molecular Dynamic simulations and *in vitro* mutagenesis experiments revealed that indole does not bind to the periplasmic domain of PhoQ. Computational

analysis predicted indole-binding to the cytoplasmic catalytic domain. Indole also synergistically enhanced the inhibitory effect of a short chain fatty acid cocktail on SPI-1 gene expression. Lastly, indole-treated HeLa cells were 70% more resistant to *Salmonella* invasion suggesting that indole also increases resistance of epithelial cells to colonization. Our results demonstrate that indole is an important microbiota metabolite that has direct anti-infective effects on *Salmonella* and host cells, revealing novel mechanisms of pathogen colonization resistance.

In loving memory of my grandparents…

ACKNOWLEDGEMENTS

I am grateful to Dr. Arul Jayaraman for being patient with me and believing in my potential. As an advisor, he encouraged me to think and present my ideas in a logical and scientific manner. Without his guidance and support, the work in this dissertation would have been impossible and my training as a researcher incomplete. I also appreciate his mentorship in my teaching aspirations. I learnt a lot from his seasoned teaching style. He has been very understanding and supportive through the difficult times that I encountered during the course of my studies, and I am grateful.

I would also like to thank my committee—Dr. Alaniz, Dr. Kao and Dr. Chen—for their time and understanding. Dr. Alaniz's expertise in mouse infection models was crucial for the *in vivo* virulence studies, and I appreciated our discussions.

Words cannot do justice to the gratitude I feel towards my parents and family. I could not have accomplished the dream of pursuing my education towards a Ph.D. degree without their support and encouragement. Another family—that of my friends at Texas A&M—has been instrumental in helping me achieve my goals. They hold a special place in my heart, and I cannot describe my gratitude. With their support, I was able to swim through the turbulent times I faced during the course of my Ph.D.

My journey at Texas A&M University also introduced me to Vishal Mahindrakar, who is now my partner in life's journey. He has been my strength, and without his love and understanding, this journey would have been daunting.

CONTRIBUTORS AND FUNDING SOURCES

Contributors

This study was conducted under the advisement of Dr. Arul Jayaraman from the Department of Chemical Engineering and supervised by a dissertation committee consisting of Dr. Robert C. Alaniz (Department of Microbial Pathogenesis and Immunology), Dr. Katy Kao (Department of Chemical Engineering) and Dr. Zhilei Chen (Department of Microbial Pathogenesis and Immunology).

The *in vivo* mice experiments were carried out in collaboration with Dr. Robert C. Alaniz of the Department of Microbial Pathogenesis and Immunology. Also, the experiments for *Salmonella* invasion of indole-treated Hela cells were conducted by Zeni Crisp, an undergraduate in Dr. Alaniz's research group.

Michael Li (Department of Chemical Engineering) performed the experiments to determine the effect of tryptophan metabolites on *hilA* expression under my supervision.

Simulations and computational analysis of indole-binding to PhoQ receptor were carried out in collaboration with Dr. Phanourios Tamamis of the Department of Chemical Engineering. Asuka Orr in the Tamamis lab carried out the simulations and assisted with the analysis and interpretation of the results.

Anatara Dattagupta (Department of Chemical Engineering) assisted with expression and purification of the cytoplasmic domain of PhoQ for *in vitro* indole-binding experiments.

All other work conducted for the dissertation was completed by me under the supervision of Dr. Arul Jayaraman.

Funding Sources

This work was supported in part by grants from the National Science Foundation (NSF) to Dr. Arul Jayaraman and Dr. Robert C. Alaniz (MCB-1120827) and from the National Institutes of Health (NIH) to Dr. Arul Jayaraman and Dr. Robert C. Alaniz (1R21AI1095788). The funding agency had no role in study design, data collection and interpretation, or the decision to submit the work for publication.

I was also supported, for part of her graduate study, by the Graduate Teaching Fellowship from the Dwight Look College of Engineering at Texas A&M University.

NOMENCLATURE

Adenosine 5'-triphosphate	ATP
Angstrom	Å
Benzamidine Sepharose® Fast Flow	BSFF
Bicinchoninic acid	BCA
Cationic antimicrobial peptides	CAMPs
Centers for Disease Control and Prevention	CDC
Chemotaxis buffer	CB
Chloramphenicol	Cm
Colonization Resistance	CR
Colony Forming Unit	cfu
Competitive Index	CI
Dimethyl Sulfoxide	DMSO
Enterohemorrhagic *Escherichia coli*	EHEC
Facultative anaerobes (3 strains)	FA^3
Generalized Born with simple SWitching	GBSW
Glutathione S-transferase	GST
Glutathione Sepharose® 4B	GS4B
Gram	g
Green Fluorescent Protein	GFP
High Dose	HD

Hour	h
Hydrochloric acid	HCl
Inducible nitric oxide synthase	iNOS
Isopropyl β-D-thiogalactoside	IPTG
Liter	L
Low Dose	LD
Lysogeny broth/ Luria Bertani media	LB
Mesenteric Lymph Nodes	MLNs
Methyl-accepting Chemotaxis Protein	MCP
Microfold cells	M-cells
Microliter	µL
Microgram	µg
Micromolar	µM
Milliliter	mL
Molecular Dynamic	MD
Multiplicity of Infection	MOI
N-acylhomoserine lactones	AHLs
Nanometer	nm
Nanosecond	ns
New England Biolabs® Inc.	NEB
Nitrate	NO_3^-
Nitric oxide	NO

Oligo-Mouse-Microbiota (12 strains)	Oligo-MM[12]
Operational Taxonomic Units	OTUs
Peyer's Patches	PPs
Phenylmethanesulfonyl fluoride	PMSF
Phosphate buffer saline	PBS
Picosecond	ps
Polyacrylamide gel electrophoresis	PAGE
Protein Data Bank	PDB
Reactive oxygen species	ROS
Relative Centrifugal force	rcf
Reticuloendothelial system	RES
Revolutions per minute	rpm
Room Temperature	RT
Root Mean Square Deviation (or Distance)	RMSD
Salmonella containing vacuole	SCV
Salmonella induced filaments	Sifs
Salmonella Pathogenicity Island-1	SPI-1
Salmonella Pathogenicity Island-2	SPI-2
Salmonella plasmid virulence	*spv*
Salmonella sdiA deletion mutant	Δ*sdiA*
Salmonella SPI-1 deletion mutant	ΔSPI-1
Salmonella SPI-2 deletion mutant	ΔSPI-2

Salmonella Typhimurium	*Salmonella*
Short chain fatty acids	SCFAs
Sodium Chloride	NaCl
Sodium dodecyl sulfate	SDS
2’,3’-O-(2,4,6-Trinitrophenyl) adenosine	
5’-triphosphate tetrasodium salt	TNP-ATP
Tris(hydroxymethyl)aminomethane	Tris
Two-Component System	TCS
Type III Secretion Systems	TTSS
Wild Type	WT

TABLE OF CONTENTS

LIST OF FIGURES

Page

LIST OF TABLES

Page

1. INTRODUCTION

1.1 Overview

The human microbiota, or the microbial population (~10^{14} microorganisms) that inhabits multiple mucosal surfaces in the body, co-exists with human cells and outnumber host cells by a factor of 10 [2]. A major proportion of the microbiota reside in the gastrointestinal (GI) tract [3] with approximately 10^{12} organisms/mL, belonging to 30 genera and 500 species, present in the lumen of the large intestine alone [4]. These organisms share a mutualistic relationship with the host where they assist with metabolism of indigestible dietary compounds, synthesis of essential nutrients, help in defense against pathogen colonization, and promote development of the intestinal architecture of the host [5, 6]. The intestinal bacteria interact with the host's immune cells and participate in the development of the mucosal immune system [7] as well as condition and maintain a state of homeostasis in the gut [8, 9]. This indigenous human intestinal microflora has been referred to as an "essential organ" for its indispensable functional role in human physiology and health [10-12].

As a metabolically active "organ", the microbiota is extensively involved in the degradation and biotransformation of several dietary and non-dietary molecules in the GI tract [13]. This results in a broad range of metabolites that are generated, some of which are also substrates for other microorganisms. The roles for some of these metabolites such as short chain fatty acids (SCFAs) have been identified [14, 15]; however, a majority of

the metabolites produced by the microbiota have not been identified or characterized in terms of their function in the human GI tract.

Recent studies have identified the roles for a few classes of molecules (e.g., SCFAs, bile acids and bacteriocins), present in the GI tract, in the modulation of pathogenic microorganism virulence and infection [14]. Metabolites derived from the aromatic amino acid tryptophan have been recently recognized for their ability to prevent colonization of pathogenic microorganisms and promote homeostasis in the GI tract. One such tryptophan-derived metabolite is indole.

Indole is produced when bacteria use the tryptophanase enzyme (TnaA) to produce indole, pyruvate, and ammonia from tryptophan [16]. Indole regulates different aspects of bacterial physiology and has been accepted as an intercellular signal in microbial community development [17-19]. At least 85 bacterial species, some of which (*E. coli*, *Bacteroides thetaiotamicron*, *Bacteroides* sp. etc.) are present in the gut, are known to produce indole [18]. In the gastrointestinal tract, indole has been estimated to be present at a concentration of 0.3-6.64 mM based on a mean concentration of 2.59 mM in human fecal matter [20-22]. Previous studies in our lab showed that indole reduced motility, attachment to epithelial cells and biofilm formation by enterohemorrhagic *Escherichia coli* O157:H7 (EHEC) [23]. Indole has also been reported to attenuate virulence factors of the fungal pathogen *Candida albicans* that repressed the pathogen's ability to form biofilms and attach to epithelial cells [24]. However, the effect of indole on the virulence of a common food borne pathogen *Salmonella enterica* serovar Typhimurium has not been studied in detail.

Since the effect of indole on *Salmonella* virulence has not been investigated, the regulatory molecules and signaling network involved in the indole-mediated expression of virulence genes have also not been determined. This work builds on our knowledge of indole's effect on virulence of the enteric pathogen EHEC and aims to further our understanding on how the gut microbiota-metabolite indole modulates *Salmonella* virulence, an intra-kingdom signaling event occurring in the gut environment. This study also provides insight into the regulatory molecule(s) that are engaged by indole and the regulatory system involved in indole-mediated signal transduction within the pathogen.

1.2 Specific Aims

Specific aim 1: To determine the effect of indole on the virulence of the pathogenic microorganism *Salmonella enterica* serovar Typhimurium.

In this study, we investigated the effect of indole on the virulence of *Salmonella*. Specifically, we studied the competitiveness of indole treated *Salmonella* to cause infection *in vivo*, invasion of epithelial cells *in vitro*, invasion and survival within macrophages, and the effects of indole on motility of the bacterium. We also studied gene expression changes using β-gal reporter strains for four SPI-1 genes (*hilA*, *prgH*, *invF*, *sipC*).

Specific aim 2: To investigate the mechanism by which indole affects *Salmonella* virulence and chemotaxis.

SdiA has been shown to be involved in indole-mediated effects in *E.coli* [25] and we proposed that SdiA might be involved in indole-mediated virulence down-regulation in *Salmonella*; therefore, we investigated its role in indole-mediated effects on *Salmonella* virulence.

Virulence gene expression is known to be controlled by several regulators under the influence of different environmental signals [26-28] which may be involved in indole signaling as well. The PhoPQ two-component regulatory system has been shown to be involved in down-regulating SPI-1 gene expression [29-31]; therefore, we investigated the role of PhoPQ in indole mediated signaling.

Motility is an important virulence factor in pathogens such as *Campylobacter*, *Salmonella* and *E. coli* [32]. We investigated the effect of indole on *Salmonella* motility and chemotaxis as well as determine the chemoreceptor involved.

Specific aim 3: To study the interaction of the microbial signal- indole with the *Salmonella* membrane bound sensor protein PhoQ.

Environmental signals are detected by bacteria through membrane bound receptors that initiate signal transduction to regulate gene expression. The molecular level interaction between the ligand with the receptor results in conformational changes and modifications in the receptor that initiate signal transduction. A combination of computational modeling and *in vitro* experiments was used to investigate the interaction

of the microbial-metabolite indole, with the bacterial sensor PhoQ. The results from these experiments helped understand the nuances of signaling of microenvironments by bacterial protein sensors, specifically involving indole.

1.3 Novel Aspects

The gut milieu is extremely complex where several dietary molecules, hormones and microbial metabolites are present. An enteric pathogen will encounter these molecules when it enters the host GI tract. Few studies have been conducted to investigate the effect of the microbial metabolites and hormones on pathogen virulence. Thus, the first novel element in this work is investigating the effect of a specific metabolite, indole, on the virulence of a major enteric pathogen *Salmonella enterica* serovar Typhimurium (ie. cause-and-effect studies). Since the effect of indole on *Salmonella* virulence has not been extensively investigated previously, a second novel aspect is identifying the receptor involved in indole-mediated signaling. Third, developing a mechanistic understanding of the interaction of indole with specific amino acid residues in the identified membrane bound receptor using a combination of computational and experimental approaches is also novel.

2. LITERATURE REVIEW

2.1 Enteric Bacterial Pathogens

Foodborne illnesses in the Unites States are caused by 31 pathogenic agents- bacteria, viruses and parasites- amounting to 9.4 million cases each year according to the report by Scallan et al [33]. Norovirus was the most common reported causative agent followed by non-typhoidal *Salmonella* spp., *Clostridium perfringens* and *Campylobacter* spp. Of these, *Salmonella* spp., *Toxoplasma gondii*, *Listeria monocytogenes* and norovirus were also leading causes of hospitalizations and deaths due to foodborne illnesses in the Unites States [33].

Campylobacter, *Salmonella*, *E. coli* O157 and *Listeria* are the most common foodborne infection agents of adults ≥65 years of age in the United States [34], whereas, the 5-major bacterial enteric pathogens responsible for illnesses among children <5 years old are nontyphoidal *Salmonella*, *Campylobacter*, *Shigella*, *Yersinia enterocolitica* and *E. coli* O157. It is estimated that the most common cause of hospitalizations and deaths in children <5 years is nontyphoidal *Salmonella* [35]. The global burden of nontyphoidal salmonellosis is an estimated 93.8 million cases per year with a likelihood of 80.3 million cases being food-borne [36].

The symptoms for most of the enteric bacterial pathogen infections such as salmonellosis, shigellosis, *Campylobacter* enteritis, *Yersinia* and *E. coli* infections include diarrhea, abdominal cramps and vomiting, sometimes with associated fever [37]. The duration and severity of infection varies with the agent, host and treatment measures with

emergence of drug-resistant organisms being a cause of concern. Therefore, it is of importance to understand the disease causing mechanisms of pathogens as well as the role of microbiota in preventing infections.

2.2 *Salmonella*

Salmonella is a Gram-negative facultative anaerobe that causes intestinal infection commonly referred to as salmonellosis. The associated symptoms include diarrhea, fever and abdominal cramps and the effects are likely to be more severe in the elderly, infants and persons with an impaired immune system. *Salmonella enterica* serovar Typhimurium can cause inflammatory diarrhea in a range of hosts including humans such as cattle, pigs, sheep, horses, poultry and rodents [38].

Non-typhoidal *Salmonella* causes over one million cases of foodborne illness in the United States every year, averaging 19,000 hospitalizations and 380 deaths (Centers for Disease Control and Prevention, CDC). However, the global burden of non-typhoidal *Salmonella* gastroenteritis is estimated to be 93.8 million cases per year [36]. Consumption of the contaminated food (especially meats such as poultry and ground beef) culminates in disease in individuals who are more susceptible to *Salmonella* infection. In the year 2016, there have been 6 *Salmonella* outbreak investigations, currently underway by CDC, some traced back to eggs, Alfalfa sprouts and live poultry. *Salmonella* is one of the top five pathogens known to cause foodborne illness in the United States and it is the pathogen that causes the maximum deaths resulting from foodborne illnesses [33].

Salmonella is ingested upon consumption of contaminated food and it infects the small intestine. Invasion of the host's intestinal microfold cells (M-cells) has been suggested to be the first step for the establishment of a *Salmonella* infection [39]. The M-cells transport the bacteria to the underlying Peyer's patches where they encounter lymphoid (T and B) cells and macrophages. *Salmonella* can survive in the microbicidal environment of the macrophages and the internalized bacteria multiply intracellularly in endosomal compartments. A systemic infection may ensue when the infected immune cells disseminate throughout the reticuloendothelial system (RES) and spread to the spleen and liver (**Figure 1**) [1, 40].

Several virulence proteins are involved in the invasion and intracellular survival of *Salmonella* and these are encoded by genes present on SPI-1 (*Salmonella* Pathogenicity Island-1) and SPI-2, respectively which are part of the type III secretion system (TTSS). The TTSS forms a needle-like injection apparatus [41] that transports bacterial effectors to the host cell cytoplasm. The functions of these proteins have been studied extensively and reviewed in [42, 43].

The SPI-1 encoded TTSS translocates effector proteins to the host cell cytoplasm that induce membrane ruffling and cause bacterial mediated endocytosis of *Salmonella* in non-phagocytic cells. The effector proteins that are involved in this process include SipA, SipC, SopB, SopE and SopE2, and result in actin bundling and polymerization. The actin remodeling and cytoskeletal rearrangements result in the formation of membrane invaginations that allow bacterial internalization [43-48]. After bacterial uptake by the

host, the host cell membrane organization restoration is mediated by another effector protein SptP [49].

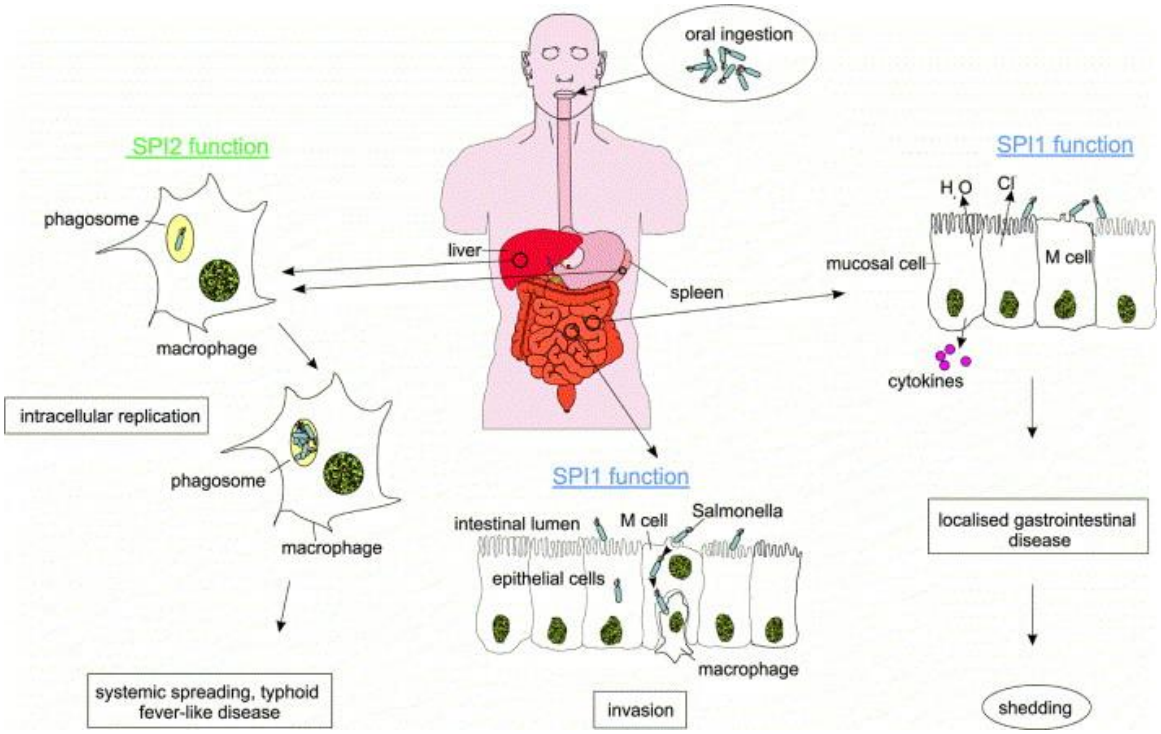

Figure 1. Schematic representation of host–pathogen interactions during pathogenesis of *Salmonella* infections. SPI-1 function is required for the initial stages of salmonellosis, i.e. the entry of *Salmonella* into non-phagocytic cells by triggering invasion and the penetration of the gastrointestinal epithelium. Furthermore, SPI-1 function is required for the onset of diarrheal symptoms during localized gastrointestinal infections. The function of SPI-2 is required for later stages of the infection, i.e. systemic spread and the colonization of host organs. The role of SPI-2 for survival and replication in host phagocytes appears to be essential for this phase of pathogenesis. Reprinted with permission from Elsevier from [1], Hansen-Wester I, Hensel M: *Salmonella* pathogenicity islands encoding type III secretion systems. *Microbes and infection* 2001, 3(7):549-559.

SPI-2 encoded TTSS translocates effectors essential for maintenance and maturation of *Salmonella* in the *Salmonella* containing vacuole (SCV). SifA induces the formation of tubular structures called *Salmonella* induced filaments (Sifs) and regulates the location of SCVs [50, 51]. The TTSS-1 effector SipA is also involved in localization of the SCV in the perinuclear region [51-53]. SseG and SseF form a complex that tethers the SCV to the Golgi apparatus which is essential for bacterial replication within the SCV [54, 55]. SseJ, SopD2, PipB and PipB2 are other effectors that localize to the SCV and modulate SCV tubulation [43, 51, 56].

The SPI-1 and SPI-2 TTSS along with the translocated effectors are important virulence factors that enable Salmonella to invade and survive within the host. These pathogenicity factors are expressed in response to environmental signals within the host microenvironments and their expression is controlled by several regulators [26-28].

2.3 Microbiota

The intestinal microbiota (the dynamic community of ~10^{14} microorganisms present in the human gastrointestinal (GI) tract) is an important mediator of several aspects of health, including promoting defense against pathogen colonization [57, 58]. The protective effect of the microbiota against pathogenic infections is termed as colonization resistance [59]. Several factors contribute to this phenomenon including competition between the indigenous microorganisms and the pathogen for nutrients [60, 61] and adhesion sites [62, 63], production of bacteriocins [64-66] and metabolites such as short chain fatty acids (SCFAs) [67-69] by the microbiota, and modulation of host defense

mechanisms [57, 70]. It is well documented that alterations in the abundance and composition of the microbiota leads to an increased susceptibility to pathogen colonization [70-72]. However, the underlying mechanisms are not completely understood.

Disruption of the mouse gut microbiota by streptomycin treatment has been shown to increase susceptibility of mice to *Salmonella* and reduce LD_{50} by several orders of magnitude [73-75]. The reduction in concentration of SCFAs in streptomycin-treated mice (due to a disruption of the normal microflora or dysbiosis) has been attributed to the increase in *Salmonella* proliferation in the mouse gut [73, 76]. Recent studies have used humanized mouse models [77] as well as defined microbial communities [78] to better understand the role of microbiota in human diseases. While a simple mono-association model does not capture complex community interactions, they are nevertheless useful to analyze the mechanisms underlying bacteria-host interactions.

Defined microbiota communities have been used to study factors affecting *Salmonella* infection in the mouse host [79, 80]. Germ-free mice colonized with a low complexity microbiota (Altered Schaedler flora [81]; low complexity is based on the number and diversity of operational taxonomic units (OTUs) detected post inoculation [82]) were more susceptible to *Salmonella* infection than mice with an intact microbiota suggesting that microbiota dysbiosis impacts pathogen colonization. Similarly, an enrichment of Enterobactericeae (*E. coli*) correlated with *Salmonella*-induced colitis [82]. A defined consortium of 15 murine intestinal bacteria (12 strains in the Oligo-Mouse-Microbiota, Oligo-MM^{12}, along with 3 facultative anaerobic strains FA^{3}) demonstrated conventional-like colonization resistance (CR) against *Salmonella* [80]. Oligo-MM^{12}

provided partial CR towards *Salmonella* in mice, which was enhanced upon co-transplantation with FA^3 consortium to the level existing in conventional mice. These facultative anaerobes may compete for the same niche as *Salmonella*, such as oxygen or other anaerobic electron acceptors such as nitrate, thereby boosting resistance to *Salmonella* colonization in mice.

Colonization resistance is just one of the roles of microbiota related to host health. Microbiota dysbiosis has been linked to several other diseases such as inflammatory bowel disease (IBD), diabetes, obesity, allergies and colorectal cancer [83, 84] and emphasizes the importance of microbiota in health and disease.

2.4 Environmental Factors Affecting *Salmonella* Virulence

Salmonella pathogenesis is widely studied using the mouse model of infection. The serovar Typhimurium is used as the infection agent because it causes a typhoid-like disease in mice which induces intestinal and extra-intestinal lesions similar to those of typhoid in humans [85]. Mice infected with *Salmonella* develop enteritis in the small intestine and spread to the mesenteric lymph nodes, liver and spleen to cause a systemic disease. Since *Salmonella* infections are mostly food-borne, the pathogen will encounter different signals in the GI tract. It is, therefore, important to understand the environmental cues as well as the *Salmonella*-induced changes in the gut that favor or impede this pathogen's ability to infect.

2.4.1 Modulation of Salmonella *infection by microbiota metabolites*

The intestinal microbiota community (and their metabolites) is encountered by enteric pathogens as they transit through the gastrointestinal tract of the host. Therefore, it is not surprising that microbiota-derived metabolites modulate pathogen virulence and infection. Several classes of microbiota metabolites, including SCFAs, bile acids, and bacteriocins have been identified as modulators of enteric pathogen infection. Of these, SCFAs are probably the most-studied class and has been shown to modulate *Salmonella*, *Listeria*, *Campylobacter*, *Shigella*, and *E. coli* infections (reviewed in [14]). Acetate, propionate and butyrate are the three SCFAs abundant in the cecum and the colon [86-88]. The SCFAs propionate [69] and butyrate [67] decrease virulence of the enteric pathogen *Salmonella*. However, not all SCFAs have the same effect on *Salmonella* infection. Lawhon et al reported acetate increases *Salmonella* invasion gene expression through SirA [89]. Formate is another signal present in the distal ileum that induces *Salmonella* invasion [90].

Other bioactive small molecules, such as bacteriocins, can also inhibit growth of competing bacteria. Plantaricin MG, a bacteriocin produced by *Lactobacillus plantarum* KLDS1.0391 has be shown to have bactericidal activity against *Salmonella* Typhimurium, by forming pores in the cytoplasmic membrane [65]. Plantaricin NC8, produced by *Lactobacillus plantarum* ZJ316 [91], and nisin, produced by *Lactococcus lactis* [92], are other examples of bacteriocins active against *Salmonella*.

The resident intestinal microbiota can also transform host molecules that can influence pathogen virulence and infection. An important example for this category are

bile acids (primary and secondary) that have been shown to repress *Salmonella* invasion gene expression [93, 94]. Cholate and chenodeoxycholate are the two primary bile acids in humans which undergo modification by the host and the intestinal microbiota to secondary bile acids [95]. The secondary bile acid deoxycholate (converted from cholate by the resident microflora possessing 7α-dehydroxylase activity [96, 97]) was reported to be the most potent bile acid to repress *Salmonella* invasion gene expression [94].

2.4.2 Microbiota metabolite indole

Another class of microbiota metabolites derived from tryptophan, such as indole, [98] have been recently identified as modulators of enteric pathogen virulence. The enzymatic action of tryptophanase on tryptophan yields indole, pyruvate and ammonia [16] (**Figure 2**). Indole is present in the GI tract at high concentrations ranging from 0.3-6.64 mM [20-22] and is likely encountered by enteric pathogens when ingested along with food. Bansal et al., showed that indole inhibits motility, biofilm formation, and *in vitro* attachment to epithelial cells of enterohemorrhagic *E. coli* (EHEC) [23]. Similarly, Oh et al reported that indole repressed *Candida albicans* biofilm formation and its attachment to epithelial cells [99]. On the contrary indole increases *Pseudomonas aeruginosa* biofilm formation but reduces expression of genes involved in synthesis of virulence factors that are regulated by quorum sensing [100]. Indole also decreases biofilm formation and exopolysaccharide production in the marine pathogen *Vibrio campbellii* [101].

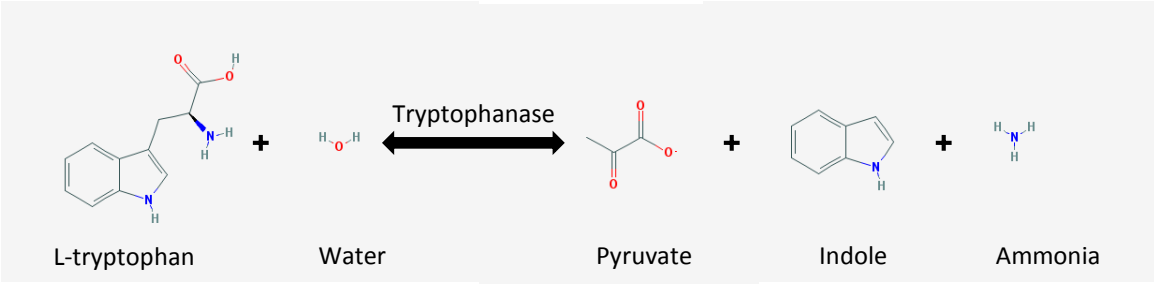

Figure 2. Tryptophanase reaction: conversion of tryptophan to indole, pyruvate and ammonia. The 2D structures were sourced from the open chemistry database: PubChem (https://pubchem.ncbi.nlm.nih.gov) CIDs: 6305 (L-tryptophan), 962 (water), 798 (indole), 107735 (pyruvate) and 222 (ammonia).

However, indole has also been suggested to indirectly promote pathogen colonization by enhancing antibiotic tolerance. Indole signaling induces persister formation in *E. coli* populations [102]. Vega et al demonstrated that exposure to low concentrations (0-500 µM) of indole improves the survival of *E. coli* and *Salmonella* to antibiotic exposure primarily through the OxyR regulon [102, 103]. Thus, pathogens that do not produce indole (such as *Salmonella*) have been proposed to potentially benefit from indole-mediated signaling leading to increased antibiotic resistance. Indole has also been reported to up-regulate expression of *Salmonella*'s AcrAB-TolC multidrug efflux system in a RamA/RamR dependent manner [104, 105] thus providing evidence for indole's involvement in efflux-mediated multidrug resistance.

Indole is an intercellular signaling molecule [18] that influences biofilm formation in *E. coli* through induction of *sdiA* [19, 106]. SdiA is a LuxR-homologue that

senses *N*-acylhomoserine lactones (AHLs) from other bacterial species [107-109]. Sabag-Daigle et al reported that indole, at concentrations higher than 100µM, inhibits AHL sensing by SdiA in *E. coli* and *Salmonella* [110]. The mechanisms of indole sensing are not well understood and further research is this area is required.

2.4.3 Salmonella *benefits from gut inflammation*

Intestinal microbiota impedes pathogen colonization through various mechanisms, collectively known as colonization resistance. However, *Salmonella* can compete with the microbiota and utilize the microenvironment to its advantage during infection [111]. For example, *Salmonella* can take advantage of pre-existing inflammatory state in the host intestinal tract to promote its growth and overcome colonization resistance conferred by the normal gut microbiota. *Salmonella* benefits from the reactive oxygen species generated during inflammation, by using the tetrathionate formed (from thiosulfate) as an electron acceptor [112]. Production and utilization of tetrathionate provides a growth advantage to *Salmonella* to compete with the luminal microbiota. *Salmonella* can also selectively utilize ethanolamine as a nutrient for growth in the presence of tetrathionate [113, 114], thereby gaining advantage over the competing microflora in the inflamed gut.

In addition to utilizing the pro-inflammatory molecules to its advantage, *Salmonella* can also directly induce inflammation in the GI tract and establish a foothold. *Salmonella* SPI-1 effector genes *sipA*, *sopE* and *sopE2* have also been shown to induce inflammatory responses in the mouse intestine [115]. SopE increases mucosal inducible nitric oxide (NO) synthase (iNOS) expression [116] that results in NO generation, which

on reaction with reactive oxygen species (ROS), produces nitrate (NO_3^-) [117]. Nitrate can be used as terminal electron acceptor by *Salmonella* [118, 119] and SopE induced host-derived nitrate production promotes *Salmonella* proliferation in the mouse lumen [116].

2.4.4 Signals in the Salmonella *containing vacuole*

Salmonella's infection lifecycle comprises of extracellular and intracellular phases. Once *Salmonella* breaches the intestinal epithelial barrier, it can survive and replicate within host cells. The survival of *Salmonella* within the phagosomal environment of macrophages is pertinent to its ability to cause systemic disease [120]. Acidic pH, reactive oxygen and nitrogen species as well as antimicrobial proteins and peptides are the antimicrobial features of phagosomes that the pathogen has to circumvent in order to survive in the SCV [121].

PhoP/PhoQ and OmpR/EnvZ are known modulators of SPI-2 gene expression in the intracellular microenvironment [122-124]. PhoPQ is a well-studied two-component regulatory system known to sense signals within the phagosome [125-131]. PhoQ gets activated in acidified phagosomes containing cationic antimicrobial peptides (CAMPs) and divalent cations [127, 129]. OmpR, was identified to respond to changes in osmolarity and regulate porin gene expression in *E. coli* [132]. However, it could also regulate porin gene expression in response to acidic pH [133, 134]. In *Salmonella*'s intracellular environment, OmpR/EnvZ regulate Sif formation [135] and translocon release for effector secretion [136] which are important for *Salmonella*'s survival.

3. INDOLE DOWN-REGULATES *SALMONELLA* VIRULENCE

3.1 Introduction

The intestinal microbiota (the dynamic community of ~10^{14} microorganisms present in the human gastrointestinal (GI) tract) is an important mediator of several aspects of health, including promoting defense against pathogen colonization [57, 58]. The protective effect of the microbiota against pathogenic infections is termed as colonization resistance [59]. Several factors contribute to this phenomenon including competition between the indigenous microorganisms and the pathogen for nutrients [60, 61] and adhesion sites [62, 63], production of bacteriocins [64-66] and metabolites such as short chain fatty acids (SCFAs) [67-69] by the microbiota, and modulation of host defense mechanisms [57, 70]. It is well documented that alterations in the abundance and composition of the microbiota [71, 72] leads to an increased susceptibility to pathogen colonization.

Non-typhoidal *Salmonella* is among the top five causative pathogens of foodborne illness in the United States (Centers for Disease Control and Prevention, 2011 estimates). It is also the primary cause of hospitalizations and deaths, resulting from foodborne illnesses. *Salmonella* infection involves activation of two distinct Type III Secretion Systems (TTSS), essential for bacterial invasion and intracellular survival. These TTSSs are virulence factors encoded by *Salmonella* pathogenicity island 1 (SPI-1) and SPI-2, respectively, and are required for *Salmonella* infections [1, 40].

Pathogen virulence factors are known to be modulated by several microbiota-derived compounds. Of these, SCFAs are a well-studied class with an established role in the modulation of enteric infections by *Salmonella*, *Listeria*, *Campylobacter*, *Shigella*, and *E. coli* [14]. While propionate [69] and butyrate [67] decrease virulence of the enteric pathogen *Salmonella*; formate [90] and acetate [89] have been shown to increase *Salmonella* virulence and infection. Previous work has shown that metabolites derived from tryptophan such as indole [98] are another class of molecules that inhibit colonization of pathogens like enterohemorrhagic *E. coli* (EHEC) and *Candida albicans* [23, 99]. On the other hand, indole has been shown to improve the survival of *E. coli* and *Salmonella* under antibiotic stress [17, 103]; thus, pathogens that do not produce indole (such as *Salmonella*) can potentially benefit from indole-mediated signaling and have been reported to have an increased antibiotic resistance primarily through the OxyR regulon [103].

The molecular basis for the effects of indole on pathogenic bacteria is not fully understood. Nikaido et al [104] reported that indole induced expression of multidrug efflux pumps in *Salmonella*. Using a genome-wide analysis, they determined that indole exposure leads to a decrease in the expression of SPI-1 genes, reduction in flagellar motility and *in vitro* invasion, along with an increase in the expression of genes involved in efflux-mediated multidrug resistance [105]. They demonstrated that while the indole-mediated up-regulation of the AcrAB-TolC multidrug efflux system was RamA/RamR dependent, the down-regulation of virulence genes was not. Therefore, the mechanism(s) involved in mediating the effects of indole on *Salmonella* virulence is not clear.

In this study, we investigated the effect of indole exposure on *Salmonella* virulence and infection. A competitive index assay was used to compare the fitness of indole-treated and non-treated *Salmonella* in infecting mice. In addition, the effect of indole on other *Salmonella* functions important for infection such as motility, invasion, intracellular survival, and SPI-1 gene expression was also investigated. Our results show a marked decrease in *Salmonella* motility, invasion of epithelial cells and macrophages, and down-regulation of virulence gene expression upon exposure to indole as well as lower competitiveness of indole-treated *Salmonella* in mice.

Another aspect studied was the combinatorial effect of indole on SPI-1 gene expression in the presence of SCFAs, another constituent of the gut environment. Since we previously reported that indole attenuates host cell inflammation and increases intestinal epithelial cell barrier integrity [22], we further investigated the susceptibility or resistance of indole-conditioned epithelial cells, to *Salmonella* invasion. Our results suggest that tryptophan-derived microbiota metabolites could be important mediators of colonization resistance to *Salmonella* infection in the GI tract.

3.2 Materials and Methods

3.2.1 Bacterial strains, cell lines, media and chemicals

Salmonella enterica serovar Typhimurium (ATCC 14028s) was grown and maintained in Luria-Bertani (LB) medium at 37°C supplemented with appropriate antibiotics where necessary. *Salmonella* SPI-1 reporter strains for *hilA*, *prgH*, *invF* and *sipC* [137] were a kind gift from Dr. Sara D. Lawhon. The ΔSPI-1, ΔSPI-2, Δ*motA* and

Δ*sdiA* deletion mutants [138] and the isogenic Nalidixic acid resistant (Nal^R) [139] strains were generous gifts from Dr. Helene Andrews-Polymenis.

For all indole exposure experiments, cells were grown in LB overnight with or without indole, diluted to an $O.D._{600nm}$ of ~0.05 and further grown for ~2 h in a shaker incubator (New Brunswick Scientific) at 37ºC, 250 rpm to obtain an exponential phase culture ($O.D._{600nm}$ of ~1.0), unless stated otherwise. 70% ethanol was used as the solvent control.

The murine macrophage cell line J774A.1 (ATCC), was maintained in the RPMI (Roswell Park Memorial Institute) 1640 medium with 10% fetal bovine serum, 1 mM sodium pyruvate, 10 mM HEPES, 2 g/L sodium bicarbonate, 0.05 mM 2-mercaptoethanol, 100 U/ml penicillin and 100 µg/ml streptomycin, at 37°C in 5% CO_2. The HeLa cell line (ATCC) was maintained in DMEM (Dulbecco's Modified Eagle Medium) supplemented with 10% bovine serum, 100 U/ml penicillin and 100 µg/ml streptomycin and 2 g/L sodium bicarbonate at 37°C in 5% CO_2 during normal growth and culture.

3.2.2 Motility assay

Motility assays were performed as described by Bansal et al [23]. Briefly, *Salmonella* was cultured in LB medium at 37°C or 30°C to exponential phase. Indole (1 mM) in 70% ethanol or the equivalent volume of solvent was added to motility agar plates (1% tryptone, 0.25% NaCl, and 0.3% agar), and the sizes of the motility halos were measured after 8 h. Four motility plates were used for each condition. A *motA* mutant was

used as the negative control. Images were obtained using the Bio Rad VersaDoc imaging system model 3000.

3.2.3 In vitro *invasion assay and intracellular survival assay*

HeLa cells were cultured in a 24-well tissue culture plate at a cell density of ~5×10^5 cells/well and infected with late log phase *Salmonella* cells at an MOI ~ 50:1 for 1 h to allow invasion. At the end of the incubation period, the media was replaced with medium containing gentamicin (100 μg/mL) and incubated for an additional hour to kill the *Salmonella* cells that did not invade. The HeLa cell monolayers were then washed twice with PBS and cells lysed with a 0.2% sterile solution of NP40 to release the invaded bacteria. The lysate was serially diluted and spread on LB agar plates to determine the number of invaded bacteria. The starting inoculum was also plated to obtain the initial count of bacterial cells used for infection. The percentage invasion was calculated as the ratio of bacterial cells invaded to cells inoculated.

J774A.1 macrophage cells were also used for invasion and intracellular survival assay. Cells were plated in a 24 well plate at a density of ~5×10^5 cells/well and treated with serum-free RPMI medium overnight to synchronize them in a quiescent state. Prior to infection, the serum-free medium was replaced with RPMI medium supplemented with 10% heat-inactivated serum. The protocol for the invasion assay was similar to that used for HeLa cells, except that a lower MOI ~10:1 was used since the macrophages are inherently phagocytic.

The intracellular survival of *Salmonella* at 4 h and 8 h post-invasion was determined by incubating the invaded J774A.1 cells in heat-inactivated serum RPMI media supplemented with 5μg/mL gentamicin at 37°C, 5% CO_2. Intracellular bacterial counts were obtained by lysing J774A.1 cells and plating serial dilutions on LB agar plates. The extent of survival was calculated as the ratio of the surviving intracellular bacteria to the number of bacteria that invaded.

3.2.4 Salmonella *SPI-1 reporter assays*

Salmonella SPI-1 reporter strains for *hilA*, *prgH*, *invF* and *sipC* with the β-galactosidase (β-gal) gene fused to each gene [137], were grown overnight in LB at 37°C and 250 rpm. Cells were diluted to an $O.D._{600}$ of ~0.05 in LB with 1 mM indole and grown to exponential phase, unless stated otherwise. β-gal activity measurements were made for the collected samples using a fluorogenic substrate (Resorufin β-D-galactopyranoside, AnaSpec) using a microplate scanning spectrofluorometer (SpectraMax, Gemini EM, Molecular Devices) with excitation and emission wavelengths as 544 nm and 590 nm, respectively. Fluorescence readings were normalized to the growth absorbance and fold changes were calculated with respect to the control. The effect of other tryptophan metabolites such as tryptamine, indole-3-acetic acid and indole-3-pyruvic acid was also investigated, on *hilA* expression at a concentration of 1 mM. For investigating synergism between indole and SCFAs, a mixture of SCFAs at published concentrations in cecal luminal contents (110 mM sodium acetate, 70 mM sodium propionate and 20 mM sodium butyrate) was used [89]. Cecal indole concentrations, as reported in [98], of 100 μM and

250 μM were tested. To control for osmolarity changes introduced by addition of sodium salts of SCFAs, 200 mM NaCl was used. All experiments were performed in duplicate and repeated with at least three biological replicates.

3.2.5 In vivo *competitive index experiment*

Female C57BL/6 mice (6-8 weeks old) were obtained from The Jackson Laboratories (Bar Harbor, ME). All mice were housed in specific pathogen-free conditions and cared for in accordance with Texas A&M Health Science Center and System Institutional Animal Care and Use Committee guidelines. Wild-type *Salmonella* and a naladixic acid resistant isogenic strain were cultured to exponential phase in the absence and presence of 1 mM indole, respectively. The two cultures were mixed together in equal ratio based on $O.D._{600}$ and the cell suspension was used for infection. Five mice were used for each group at each time point and the experiment was repeated for two infection doses. Approximately ~ 5×10^7 (low dose LD) and ~ 5×10^8 cells (high dose HD) were gavaged with feeding needles (22 × 11/2 with 11/4 mm ball, no. 7920, Popper & Sons, Inc., New Hyde Park, NY).

After bacterial challenge, bacterial burden in infected tissues was determined. At different time points (days 1 and 3 post-infection), fecal pellets, liver, spleen, mesenteric lymph nodes, Peyer's patches and cecum were harvested. The samples were homogenized in sterile 0.1% NP40 using a motorized homogenizer (Omni International), the homogenates were serially diluted in sterile 0.1% NP40, and multiple dilutions from each

organ were plated in duplicates. Two sets of plates, with and without naladixic acid at a concentration of 50µg/mL, were used to obtain total and Nal^R bacterial counts, respectively, in the different tissues. Two types of media (LB or XLD) were used depending on the organ and its inherent microflora. LB agar plates were used for plating samples from the spleen, liver, Peyer's patches and the mesenteric lymph nodes whereas XLD agar plates were used for fecal and cecum samples to differentiate *Salmonella* (black-colored colonies) from other microbes that are present. Colony forming unit (CFU) counts were determined after overnight incubation at 37°C.

The competitive index (CI) in each sample was calculated as [(cfu of indole-treated strain in the organ/cfu of control strain in the organ)]/[(cfu of indole treated strain used in the inoculum/cfu of control strain used in the inoculum)].

3.2.6 Statistical analysis

Graph Pad Prism, version 5.0, software was used for statistical analysis and plotting the competitive index data. Wilcoxon signed-rank non-parametric test was used to determine significance of difference between the numbers of two groups: indole-treated and the control (solvent-treated). Student's t-test was performed for the measured values of the *in-vitro* experiments and $p < 0.05$ was considered as statistically significant.

3.3 Results

3.3.1 Indole exposure decreases Salmonella *invasion* in vivo

A competitive index (CI) assay was used to determine the effect of indole on the ability of *Salmonella* to invade the murine GI tract. **Figure 3** shows the CI of indole-treated *Salmonella* on day 1 and day 3 after infection for a low dose (LD) and high dose (HD) *Salmonella* inoculum. For the LD group, no significant difference between the counts of indole- and solvent-treated bacteria was observed in the Peyer's patches (PPs) and feces on days 1 and 3 (**Figure 4** and **5**). However, the number of indole-treated bacteria in the cecum was significantly lower ($p < 0.05$) than the control, on days 1 and 3, (**Figure 3**, **4** and **5**Error! Reference source not found.). Beyond the GI tract, indole-treated *almonella* was not detectable in the spleen and liver on day 1 (**Figure 3** and **4**). On day 3, solvent-treated *Salmonella* were recovered from the spleen and liver of all mice but indole-treated *Salmonella* were recovered from livers and spleens of ~50% of the mice (**Figure 5)**. Both indole- and solvent-treated *Salmonella* were not recovered from mesenteric lymph nodes (MLN) on day 1. However by day 3, solvent-treated *Salmonella* were present in MLNs of all mice but indole-treated *Salmonella* were present in only 50% of the mice (**Figure 3** and **5**).

For the HD group, the number of indole-treated bacteria, recovered from the cecum was significantly lower ($p < 0.05$) than the number of solvent-treated bacterial numbers, on both day 1 and day 3, post inoculation (**Figure 3**, **6** and **7**). The counts of indole-treated bacteria were significantly lower ($p < 0.05$) in the PPs on day 1 and feces on day 3 (**Figure 6** and **7**). No difference in the counts of indole- and solvent-treated *Salmonella* was

observed in the spleen on days 1 and 3. The liver had significantly lower ($p < 0.05$) numbers of indole-treated bacteria compared to solvent-treated *Salmonella* on day 1, while the difference was less significant ($p < 0.10$) on day 3 (**Figure 3**, **6** and **7**). In the MLNs, significantly lower ($p < 0.05$) number of indole-treated *Salmonella* was detected compared to the solvent-treated *Salmonella* on days 1 and day 3.

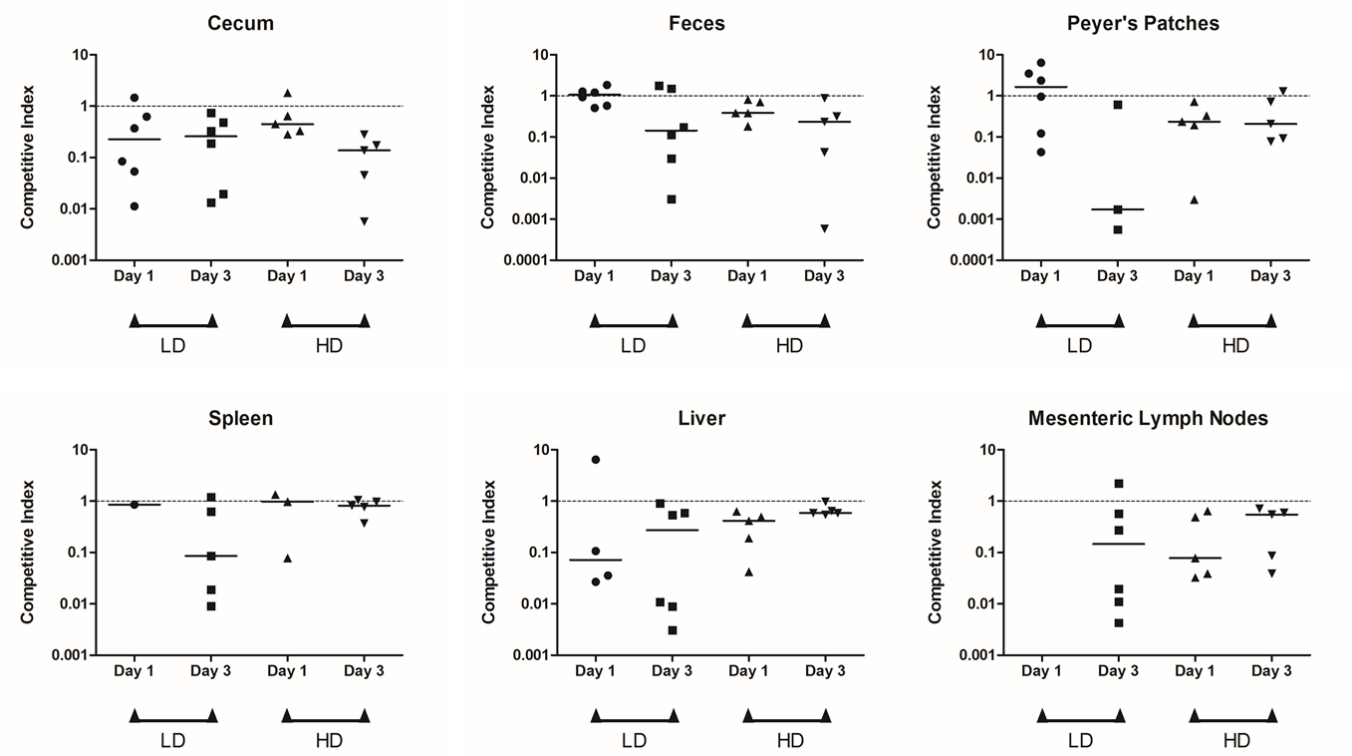

Figure 3. Competitive index values from i*n vivo* competition assays in C57BL/6 mice with indole treated *Salmonella.* Competitive index (CI) values for the indole treated *Salmonella* versus the control in different organs harvested from infected mice (n = 5) at days 1 and 3 post inoculation. Two inoculum doses were tested- low dose (LD; ~5×10^7 cfu) and high dose (HD; ~5×10^8 cfu) and several organs— cecum, Peyer's patches, spleen, liver and mesenteric lymph nodes— were harvested. Feces were collected prior to euthanization. The organs were homogenized and serial dilutions plated to obtain cfu counts that were used to calculate the CI values. Each dot (circle, square, upright triangle and downward triangle) on the plot represents a mouse from the respective group (LD day 1, LD day 3, HD day 1 and HD day 3, respectively). Lack of dots indicates that no colonies developed from that sample. For organs where indole treated *Salmonella* were absent but solvent treated *Salmonella* were present, CI was calculated assuming a cfu of 1 for the indole treated *Salmonella*. The horizontal bar represents the median of the observed CI values.

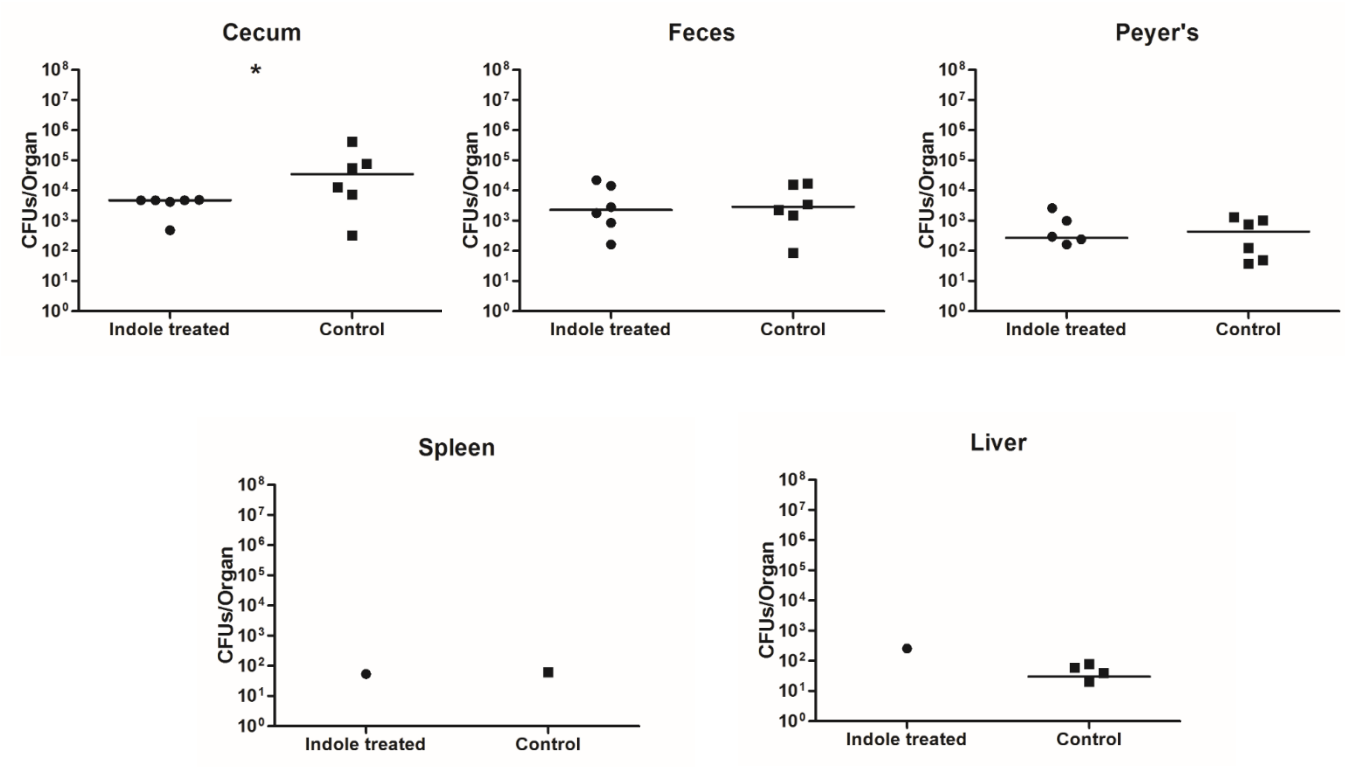

Figure 4. Comparative cfu counts from low dose *in vivo* competition assay in C57BL/6 mice with indole-treated *Salmonella*, day 1 post inoculation. The values of cfus/organ for the indole treated and non-treated *Salmonella* in different organs harvested from infected mice (n = 5) on day 1 using a low inoculum dose (~5×10^7 cfu). Several organs— cecum, Peyer's patches, spleen, liver and mesenteric lymph nodes— were harvested and feces were collected prior to euthanization. The organs were homogenized and dilutions were plated to obtain cfu counts. Each dot (circle and square) on the plot represents a mouse from the studied group (indole treated and control, respectively). Lack of dots indicates that no colonies developed from that sample. The horizontal bar represents the median of the observed cfu/organ values. (* indicates $p < 0.05$)

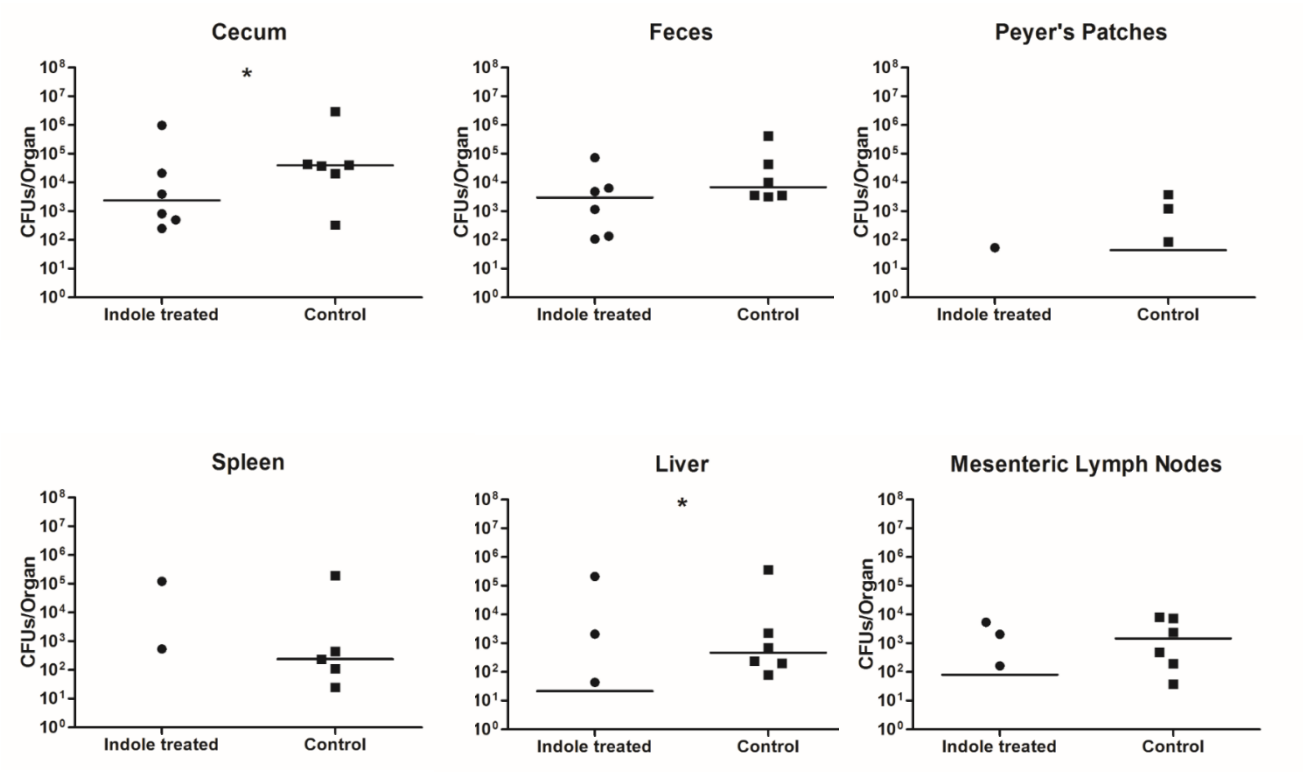

Figure 5. Comparative cfu counts from low dose *in vivo* competition assay in C57BL/6 mice with indole-treated *Salmonella*, day 3 post inoculation. The values of cfus/organ for the indole treated and non-treated *Salmonella* in different organs harvested from infected mice (n = 5) on day 3 using a low inoculum dose (~5 × 10^7 cfu). Several organs— cecum, Peyer's patches, spleen, liver and mesenteric lymph nodes— were harvested and feces were collected prior to euthanization. The organs were homogenized and dilutions were plated to obtain cfu counts. Each dot (circle and square) on the plot represents a mouse from the studied group (indole treated and control, respectively). Lack of dots indicates that no colonies developed from that sample. The

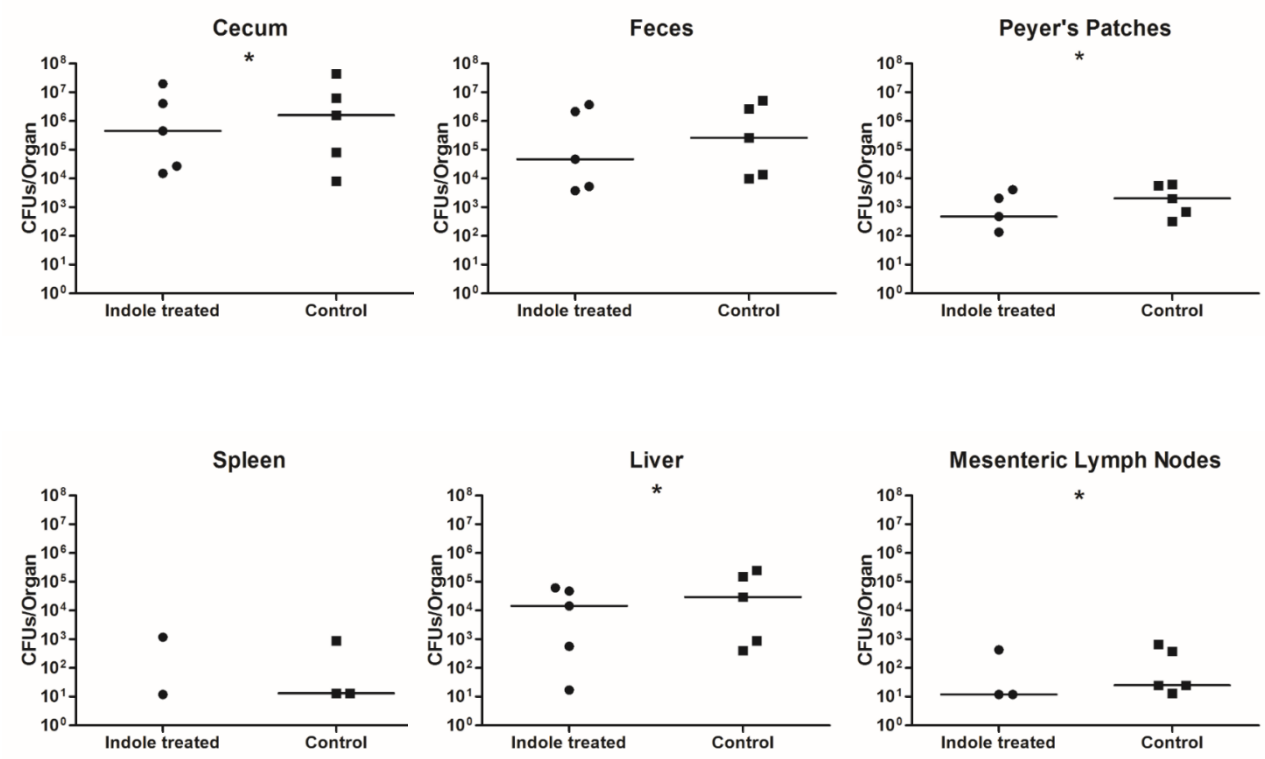

Figure 6. Comparative cfu counts from high dose *in vivo* competition assay in C57BL/6 mice with indole-treated *Salmonella*, day 1 post inoculation. The values of cfus/organ for the indole treated and non-treated *Salmonella* in different organs harvested from infected mice (n = 5) on day 1 using a high inoculum dose (~5×10^8 cfu). Several organs— cecum, Peyer's patches, spleen, liver and mesenteric lymph nodes— were harvested and feces were collected prior to euthanization. The organs were homogenized and dilutions were plated to obtain cfu counts. Each dot (circle and square) on the plot represents a mouse from the studied group (indole treated and control, respectively). Lack of dots indicates that no colonies developed from that sample. The horizontal bar represents the median of the observed cfu/organ values. (* indicates $p < 0.05$)

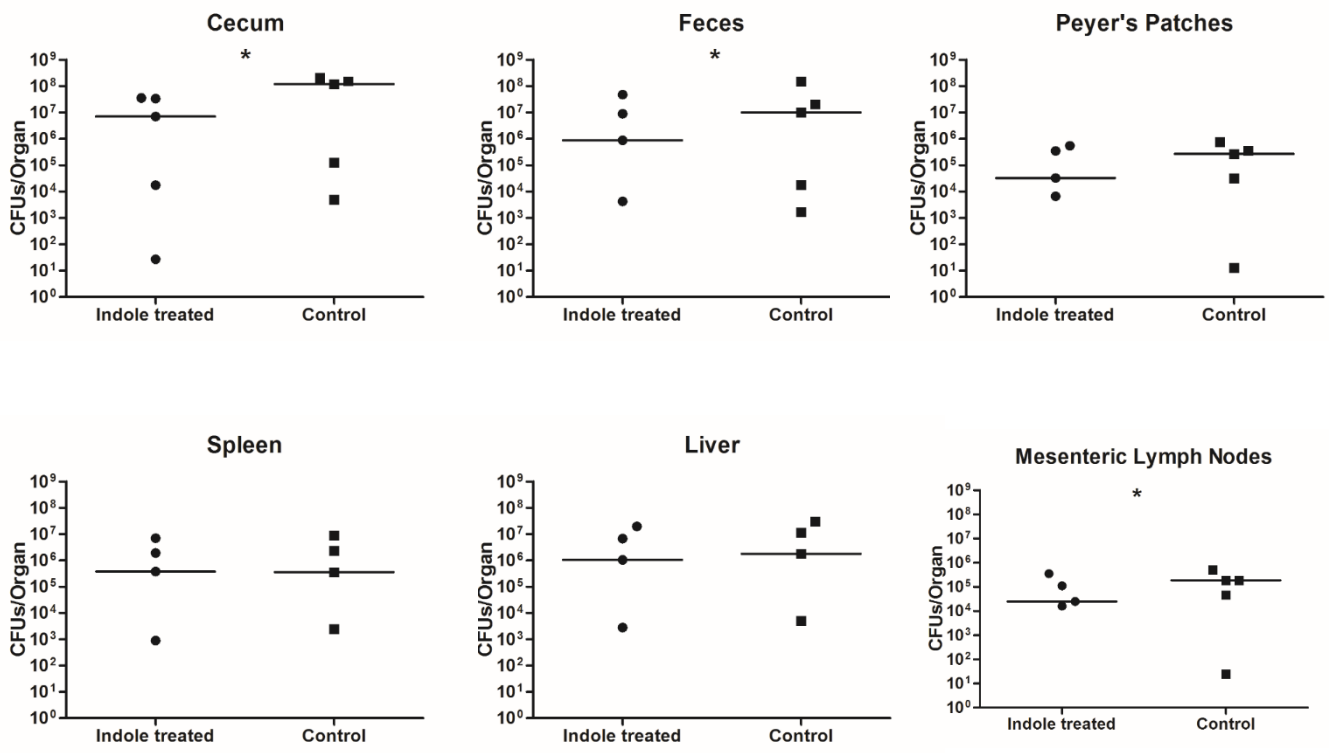

Figure 7. Comparative cfu counts from high dose *in vivo* competition assay in C57BL/6 mice with indole-treated *Salmonella*, day 3 post inoculation. The values of cfus/organ for the indole treated and non-treated *Salmonella* in different organs harvested from infected mice (n = 5) on day 3 using a high inoculum dose (~5×10^8 cfu). Several organs— cecum, Peyer's patches, spleen, liver and mesenteric lymph nodes— were harvested and feces were collected prior to euthanization. The organs were homogenized and dilutions were plated to obtain cfu counts. Each dot (circle and square) on the plot represents a mouse from the studied group (indole treated and control, respectively). Lack of dots indicates that no colonies developed from that sample. The horizontal bar represents the median of the observed cfu/organ values. (* indicates $p < 0.05$)

3.3.2 Indole decreases Salmonella *motility*

Since motility is a virulence factor for enteric pathogens [32], we determined the effect of indole on *Salmonella* motility *in vitro* by measuring the halo diameter in the presence or absence of indole as a measure of motility. Exposure to indole reduced *Salmonella* motility by ~ 60% upon exposure to indole at 37°C as compared to solvent-treated controls (**Figure 8**). A similar inhibition in motility was also observed when *Salmonella* were exposed to 1 mM indole at 30°C (~ 40% decrease in motility as compared to controls; see **Figure 9**).

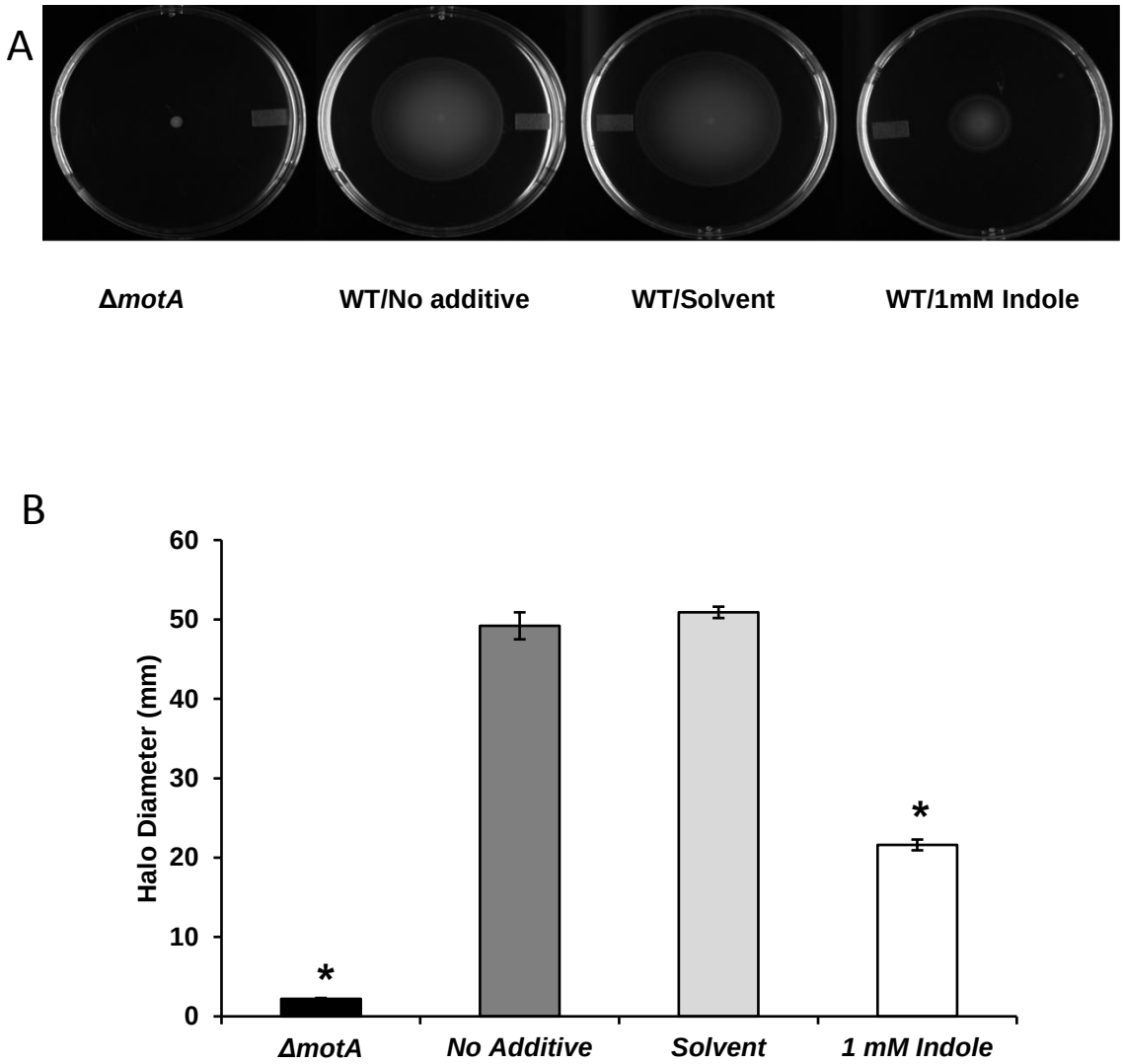

Figure 8. Effect of indole on *Salmonella* swimming motility at 37°C. (A) Representative photographs of the swimming motility agar plates spotted with WT *Salmonella*. (B) Measured halo diameters for the different test conditions. Diameters were measured using Vernier calipers, 8 hours post spotting. Δ*motA* was spotted on swimming motility agar plates as a negative control for motility. (* indicates $p < 0.05$)

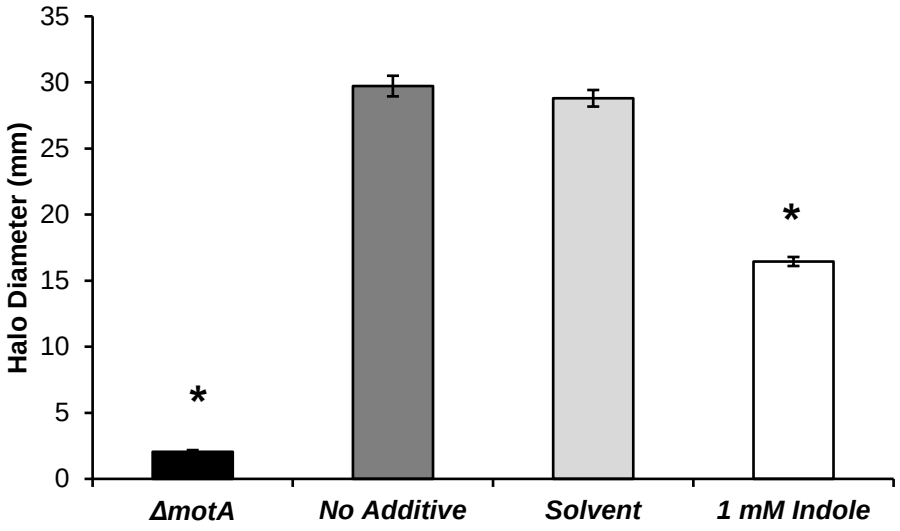

Figure 9. Effect of indole on *Salmonella* swimming motility at 30°C. Measured halo diameters for the different test conditions. Diameters were measured using Vernier calipers, 8 hours post spotting. Δ*motA* was spotted on swimming motility agar plates as a negative control for motility. (* indicates $p < 0.05$)

3.3.3 Indole decreases Salmonella *invasion but not its intracellular survival*

We investigated the effect of indole on invasion of epithelial cells by *Salmonella*. A 160–fold decrease in invasion of the HeLa epithelial cell line was observed when *Salmonella* was treated with 1 mM indole prior to *in vitro* infection (**Figure 10)**. No change in invasion was observed with a SPI-1 mutant (ΔSPI-1) upon indole treatment. Since *Salmonella* invades and replicates inside macrophages after breaching the epithelial cell layer, we also investigated the effect of indole exposure on invasion and intracellular survival of macrophages. **Figure 11A** shows that *Salmonella* exposed to 1mM indole invaded J774A.1 murine macrophages approximately 2-fold less than the untreated controls. **Figure 11B** shows that indole exposure did not significantly alter intracellular survival in J774A.1 macrophages up to 8 h.

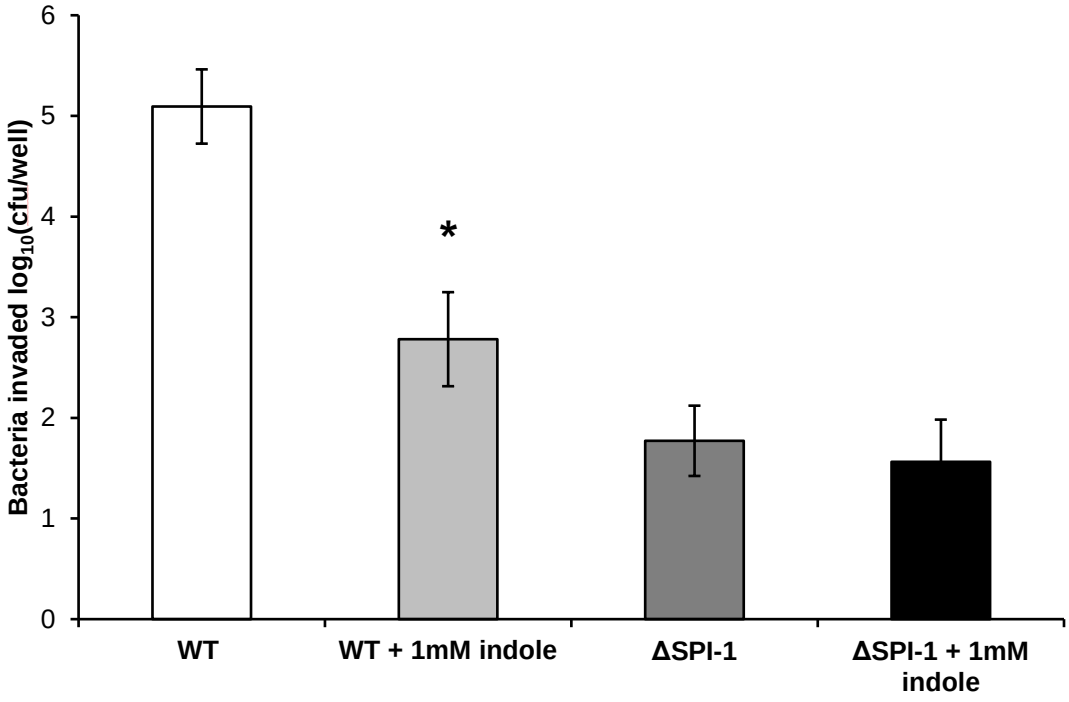

Figure 10. Invasion of epithelial cells with indole-treated *Salmonella*. Invasion in HeLa epithelial cell line with *Salmonella* treated with or without 1mM indole. Infection with the ΔSPI-1 strain was used as control. A MOI of 50:1 was used for HeLa cells and the data shown is intracellular bacteria recovered. (* indicates $p < 0.05$)

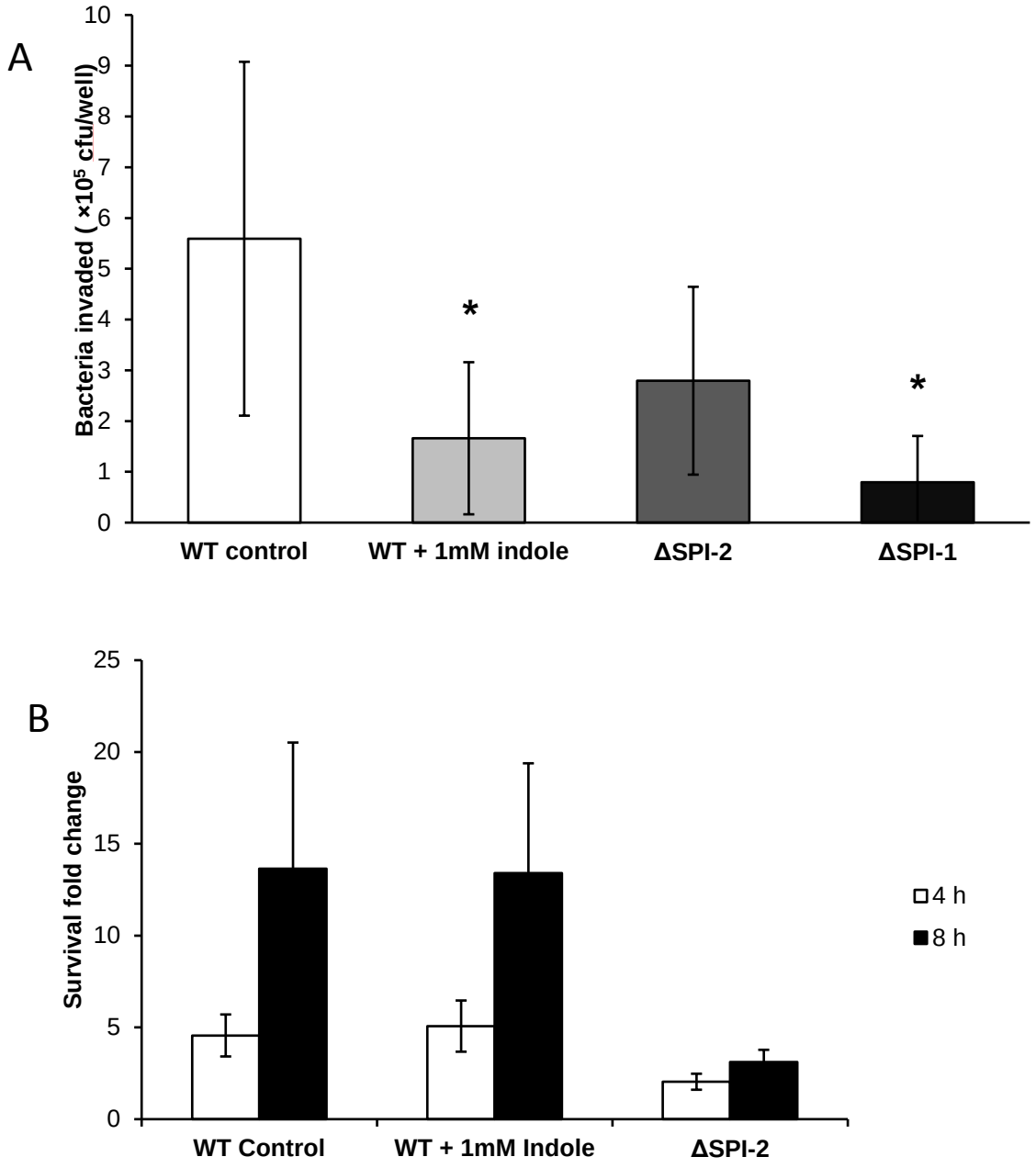

Figure 11. Invasion and intracellular survival within macrophages with indole-treated *Salmonella*. Invasion (A) and intracellular survival (B) in J774A.1 cells. Infection with the ΔSPI-1 and ΔSPI-2 strains were used as controls. A MOI of 10:1 was used and data shown are intracellular bacteria recovered and fold changes in survival (at 4 and 8 h post invasion) relative to the invasion. (* indicates $p < 0.05$)

3.3.4 Indole decreases Salmonella *virulence gene expression*

A β-gal reporter assay was used to determine whether the decrease in invasiveness of *Salmonella* was mirrored by changes in the expression of genes in the *Salmonella* pathogenicity island. **Figure 12** shows that the expression of *hilA*, *sipC*, *invF*, and *prgH* were all down-regulated to different degrees upon exposure to 1 mM indole. The expression of *hilA* was decreased significantly by 23-fold upon exposure to indole, whereas the expression of *prgH*, *invF*, and *sipC* decreased by 12-, 8-, and 3-fold, respectively. Therefore, the reduced expression of genes involved in the invasion process was consistent with the decrease in invasion of epithelial cells by *Salmonella* upon indole treatment.

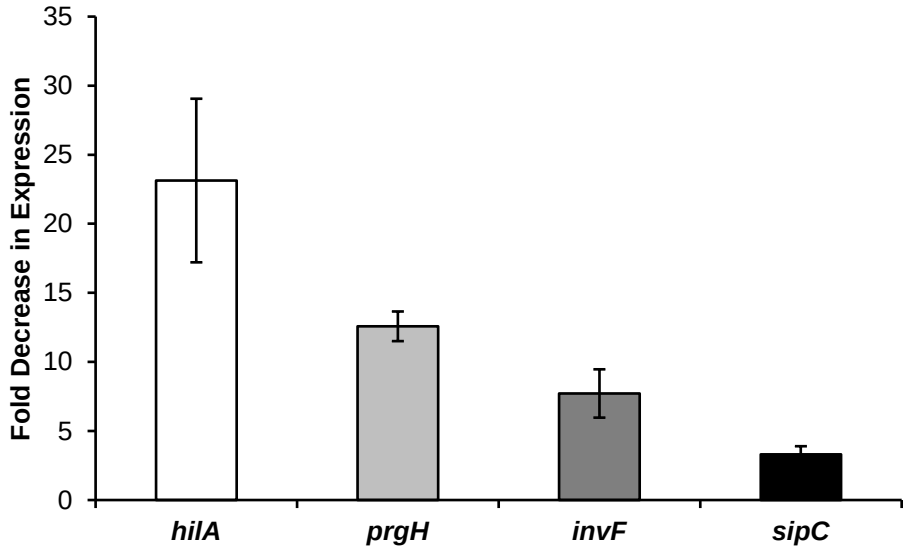

Figure 12. SP I-1 virulence gene expression change in WT *Salmonella* upon treatment with 1 mM indole. SPI-1 reporter strains for *hilA*, *prgH*, *invF* and *sipC* were treated overnight with and without 1 mM indole and the β-gal activity was measured in exponential phase cultures after dilution. Data shown are the fold decrease in expression with indole-treatment relative to the solvent-treated control which was statistically significant with $p < 0.05$.

3.3.5 Indole synergizes with SCFAs

Given the likely interactions among GI tract metabolites to mediate colonization resistance, we hypothesized indole's effect on *Salmonella* virulence may be augmented when present along with other GI tract microbiota metabolites. We specifically focused on short chain fatty acids (SCFAs) as they are abundant in the GI tract [86-89] and are important modulators of pathogen virulence [14]. Therefore, we investigated the combined effect of indole (100 μM and 250 μM) and SCFAs (110 mM acetate, 70 mM propionate and 20 mM butyrate for a total concentration of 200 mM) on *hilA* expression. The average fold decrease in *hilA* expression upon treatment with cecal SCFAs alone was 1.8-fold and the decrease in *hilA* expression with 100 μM and 250 μM indole alone was 1.6- and 5.0-fold, respectively (**Figure 13**). However, when 100 μM or 250 μM indole was present with cecal SCFAs, the observed average decrease in *hilA* expression was 3.7-fold and 19.3-fold, respectively. These observations suggest that 250 μM indole and cecal SCFAs synergistically enhance the down-regulation of *hilA* in a dose-dependent manner.

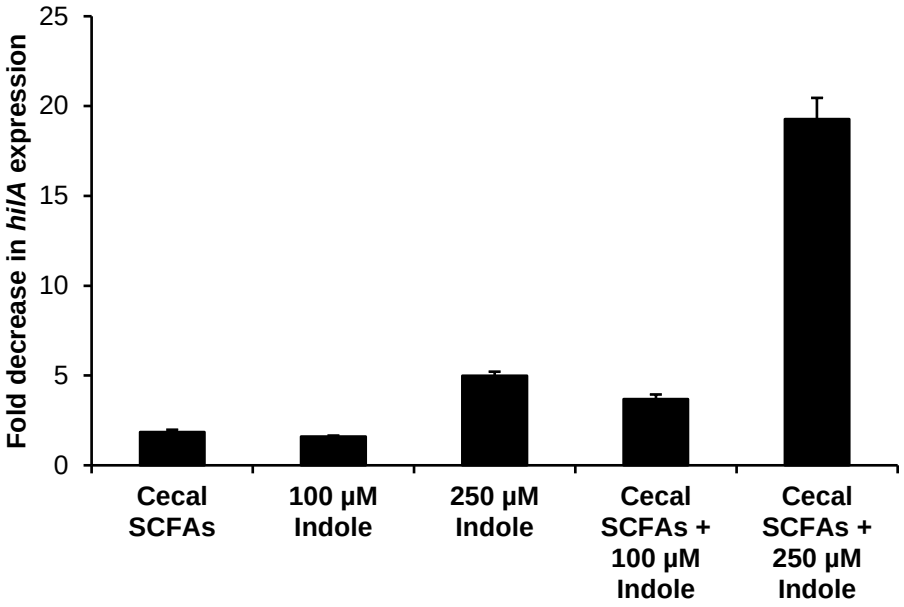

Figure 13. Effect of indole in combination with cecal SCFAs on *hilA* expression. SPI-1 reporter strain for *hilA* was treated overnight with and without indole (100 µM and 250 µM) in the presence of 200 mM cecal SCFAs or 200 mM NaCl, and the β-gal activity was measured in exponential phase cultures after dilution. Data shown are the fold decrease in expression of *hilA* with treatment relative to the control: *hilA* expression in presence of 200 mM NaCl, and was statistically significant with $p < 0.05$.

3.3.6 Effect of other tryptophan metabolites on hilA expression

Indole is not the only microbiota metabolite of tryptophan metabolism. Several other tryptophan metabolites have been detected in murine cecal contents such as indole-3-pyruvate, indole-3-acetate and tryptamine [98] (see **Table 5** for structure information), which we tested for effect on *hilA* expression. Indole-3-pyruvic acid decreased *hilA* expression by 3-fold whereas tryptamine and indole-3-acetic acid down-regulated *hilA* expression by 1.3- and 1.5-fold, respectively (**Figure 14**).

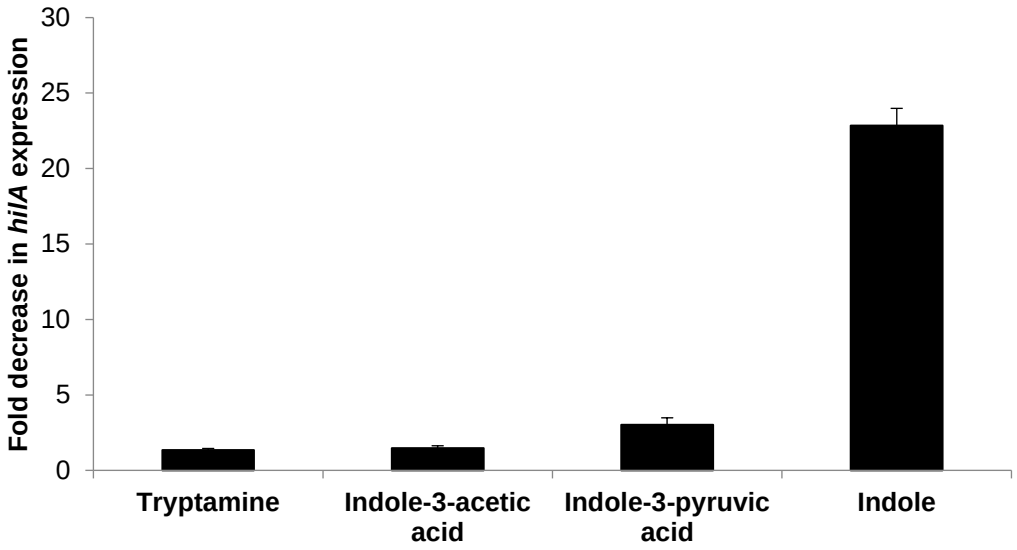

Figure 14. Effect of tryptophan metabolites on *hilA* expression. SPI-1 reporter strain for *hilA* was treated overnight with and without 1 mM tryptophan metabolites: tryptamine, indole-3-acetic acid, indole-3-pyruvic acid and indole, and the β-gal activity was measured. Data shown are the fold decrease in expression of *hilA* with treatment relative to the solvent-treated control which was statistically significant with $p < 0.05$.

3.3.7 Indole increases epithelial cells resistance to Salmonella *invasion*

To determine whether indole also impacted the ability of host cells to resist *Salmonella* invasion, we exposed HeLa epithelial cells to indole prior to infection with *Salmonella* (not exposed to indole) and determined the extent of *Salmonella* invasion. **Figure 15** shows that, compared to untreated HeLa cells, a statistically-significant 70% decrease in invasion was observed when indole-conditioned epithelial cells were infected

with wild type *Salmonella*. This suggests that indole increases resistance of host cells to *Salmonella* invasion in addition to attenuating *Salmonella* virulence.

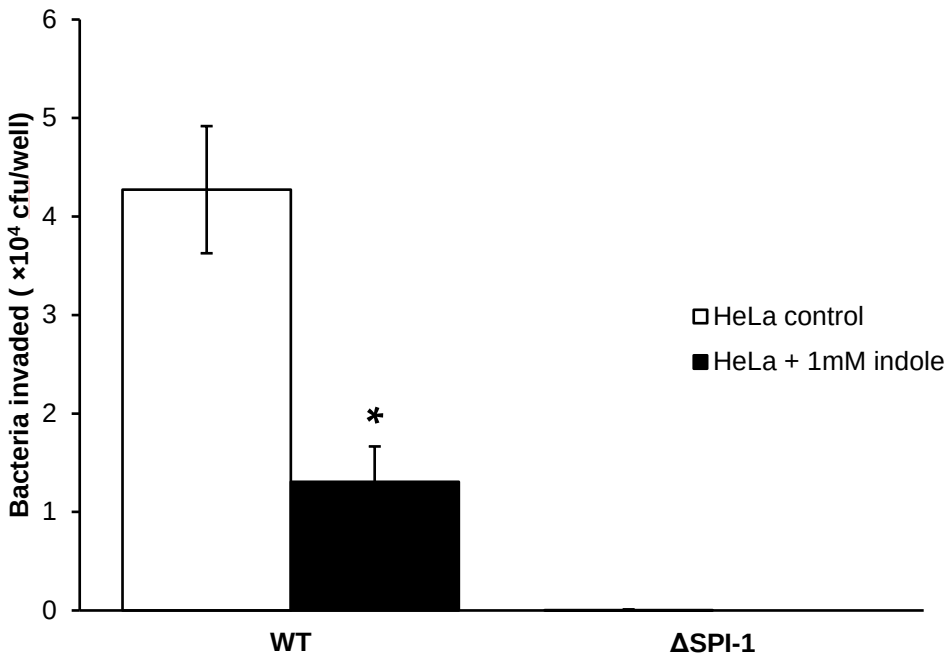

Figure 15. Effect of indole on resistance of HeLa epithelial cells to *Salmonella* invasion. HeLa cells were seeded in a 24 well plate and conditioned with 1 mM indole for 24 h prior to infection. A MOI of 10:1 was used for infection. Data shown are intracellular bacteria recovered from infected HeLa monolayers with indole treatment or control (solvent treatment). (* indicates $p < 0.05$)

3.4 Discussion

The link between prevention of pathogen colonization and the GI tract microbiota has been long established [59], and a number of contributing factors such as nutrient competition [61], steric hindrance [140], production of bacteriocins [64-66] and specific metabolites such as SCFAs [67-69] have been reported to play a role in this phenomenon [57, 58]. However, besides SCFAs, few other specific classes of molecules have been

identified that impact pathogen colonization. Here, we report that indole, an abundant tryptophan-derived microbiota metabolite, attenuates *Salmonella* infectivity *in vivo* and virulence *in vitro,* as well as increases resistance of host cells to *Salmonella* invasion *in vitro*.

Indole is produced from tryptophan by the enzyme trytophanase (TnaA) [16] that is present in *E. coli* and several other microorganisms present in the GI tract belonging to the phyla- *Bacteroidetes*, *Firmicutes*, *Proteobacteria* and *Actinobacteria*- [18]. Indole is an abundant microbiota metabolite in the GI tract luminal microenvironment where pathogen colonization is initiated. Indole concentrations of ~40 nmol/g tissue in murine cecum were reported by Whitt et al. using an enzymatic assay [141]. Recently, we used mass spectrometry to determine that indole is present at 10 - 40 nmol/g sample wet weight in murine cecum; based on unpublished data from our lab that the extraction efficiency of indole from cecal contents is ~15% and assuming that cecal contents have a density similar to that of water, the effective concentration of indole in cecal contents is ~100-300 μM. Another recent study determined fecal indole levels in 53 healthy adults to vary from 0.3 mM to 6.64 mM with a mean of 2.59 mM [21] (i.e., comparable to concentrations at which a response was observed in this study).

The reduced colonization *in vivo* by indole-treated *Salmonella* in mice is apparent from the statistically significant difference in the number of indole-treated and non-treated *Salmonella* detected in the cecum for both the LD and HD groups post infection (**Figure 4**, **5**, **6** and **7**). Since *Salmonella* were exposed to indole prior to infection, our observations suggest that comparatively fewer indole-treated *Salmonella* invaded the intestinal

epithelium and colonized the cecum. Since the cecum is reportedly a reservoir for *Salmonella* intestinal persistence and fecal shedding in mice [142, 143], it is interesting to observe the lower competitiveness of indole-treated *Salmonella* to colonize the cecum with CI < 1 (**Figure 3**).

The marked decrease in *Salmonella* motility, invasion of epithelial cells and macrophages, and decrease in virulence gene expression upon exposure to indole is similar to our previous report on indole's effect on EHEC motility, biofilm formation, and its colonization of epithelial cells [23]. However, to our knowledge, this is the first *in vivo* study demonstrating that indole's effect on pathogen virulence translates to reduced infectivity in mice. A striking aspect of our results is the concordance between observations at multiple levels or stages of *Salmonella* infection. Another interesting observation is the temporal coordination in the effect of indole on SPI-I gene expression. The *hilA* gene is the master regulator of the SPI-I regulon [144] and an indole-mediated decrease in expression of *hilA* was observed first, when a time-course study was conducted, followed by decrease in expression of *prgH*, *invF* and *sipC*. HilA is a transcriptional regulator which activates the expression of structural type III secretion genes such as *prgH* and the transcription factor *invF* [144]. *SipC*, on the other hand, is a secreted effector (translocase) that is activated by *invF*. Thus the reduced invasion *in vitro* and infectivity *in vivo* are likely the result of coordinated decrease in SPI-1 gene cluster expression.

While indole markedly attenuated invasion and the expression of SPI-I genes, it did not significantly affect intracellular survival of *Salmonella* in macrophages. The lack

of effect on intracellular survival suggests that indole impacts functions related to extracellular infection. The intracellular phase of *Salmonella*'s infection cycle allows *Salmonella* within macrophages to escape from Peyer's patches to the lymph nodes and spread to the liver and spleen resulting in systemic disease. Distal ileum (in proximity to the cecum), with Peyer's patches rich in lymphoid cells, is considered to be the primary enteric site for *Salmonella* infection causing systemic disease [145]. The CI < 1 observed for the systemic organs such as liver, spleen and mesenteric lymph nodes (**Figure 3**), is likely a result of the initial lower invasion and colonization by indole-treated *Salmonella*, based on our *in vitro* results showing that indole did not modulate intracellular survival.

The mechanism(s) underlying indole's effects on pathogen virulence are poorly understood. Few transcriptional regulators and two-component systems have been reported to be involved in indole signaling. Kanamaru et al., [146] showed that the expression of virulence factors in EHEC is controlled by *sdiA* and that indole acts through *sdiA* [19]. Therefore, we were interested in investigating whether SdiA is involved in indole-mediated down-regulation of *Salmonella* virulence (Section 4).

Although we observed strong attenuation of *Salmonella* virulence and invasion with indole, it should be noted that several other metabolites can be derived by the microbiota from dietary tryptophan, and are present in the lumen of the GI tract such as indole-3-acetate, indole-3-pyruvate and tryptamine [98]. However, not all tested metabolites had the same effect on *Salmonella* as indole. Indole-3-pyruvic acid decreased *hilA* expression by 3-fold whereas tryptamine and indole-3-acetic acid down-regulated *hilA* expression by 1.3- and 1.5-fold, respectively. Thus, there appears to be some

variability in the anti-infective effect of microbiota-derived tryptophan metabolites. Further structure-function studies are required to identify feature(s) that are required to elicit the observed phenotype.

Apart from tryptophan metabolites, SCFAs constitute the other major class of microbiota metabolites abundant in the gut lumen. The total concentration of the SCFAs varies along the length of the GI tract- low (~20 mM) in the ileum and high (~140-200 mM) in the cecum and the colon [86-88]. The relative concentration of the individual components- acetate, propionate and butyrate- also varies in the ileal and colonic segments. Since SCFAs are known modulators of *Salmonella* virulence [67, 69, 89, 90], our data on the synergy between indole (at a concentration of 250 μM) and SCFAs in down-regulating *hilA* expression further underscores the importance of indole as a potent virulence-attenuating signal in the GI tract.

In addition to decreasing pathogen virulence phenotypes, we also observed that exposing epithelial cells to indole decreased *Salmonella* invasion. This suggests that indole (and presumably, other microbiota metabolites) could attenuate pathogen invasion and colonization by both inhibiting virulence factors directly in the pathogen while, simultaneously, increasing the resistance of host cells. This observation is also consistent with previous work from our laboratory and another research group showing that indole increased anti-inflammatory cytokine production and epithelial cell tight junction resistance in HCT-8 enterocytes [22, 147]. In this regard, indole is similar to the SCFA butyrate in its scope of action. Butyrate is a major source of energy for colonocytes [148, 149] and inhibits bacterial pathogenesis through its effect on colonocytes as demonstrated

by studies with *Campylobacter jejuni* [68]. Current work in our laboratory is focusing on elucidating the mechanism(s) underlying indole's effect on host cells.

In summary, our observations demonstrate indole's role in inhibiting *Salmonella* virulence and colonization. Taken together with our prior work showing that indole attenuates inflammatory gene expression in intestinal epithelial cells, our results suggest that microbiota metabolites such as indole could play an important role in determining the susceptibility of the host to pathogen infection in the GI tract.

4. MECHANISM OF INDOLE-MEDIATED DOWNREGULATION OF VIRULENCE AND CHEMOTAXIS IN *SALMONELLA*

4.1 Introduction

Indole is a microbiota product secreted into the gut lumen and will be encountered by *Salmonella* inside the host. Our results show that indole reduces *Salmonella* motility and down-regulates SPI-1 gene expression, invasion and virulence *in vivo*. However, the mechanism of indole's action is not known.

Several groups have reported the effect of indole on the virulence of multiple pathogens, including EHEC [23], *Candida albicans* [99], *Pseudomonas aeruginosa* [100] and *Vibrio campbellii* [101]. SdiA (suppressor of cell division inhibition) has been shown to be involved in reducing EHEC biofilm formation, controlling expression of virulence factors and reducing adherence to epithelial cells [19, 146, 150]. SdiA is a LuxR homologue encoded by *E. coli* and *Salmonella* Typhimurium that detects quorum sensing signals, such as *N*-acylhomoserine lactones (AHLs), from other species [107-109]. The SdiA homolog in *Salmonella* Typhimurium regulates genes on the virulence plasmid encoding the *Salmonella* plasmid virulence locus (*spv*) [151]. Therefore, we tested whether *sdiA* was involved in indole mediated down-regulation of *Salmonella* virulence.

Two component regulatory systems mediate bacterial signal transduction in response to environmental stimuli. TCSs consist of a sensor kinase and a cognate response regulator that modulate gene expression in response to environmental changes of the bacterium. One such regulatory system is the PhoPQ two-component system where PhoQ

is the sensor kinase and PhoP is the cognate response regulator. The PhoPQ system has been extensively studied and senses signals such as divalent cations (Mg^{2+} and Ca^{2+}) [128, 152], cationic antimicrobial peptides [127] and pH changes [129]. PhoPQ has also been reported to down regulate SPI-1 gene expression [29-31].

In this work, we investigated whether SdiA and the PhoPQ system are involved in mediating the decrease in epithelial cell invasion and *Salmonella* virulence upon indole exposure. Deletion mutants for different regulatory genes were constructed and their effect on invasion and expression of SPI-1 genes was determined to assess the role for each regulator.

Another aspect of virulence is the motility of the pathogen and the ability to find the appropriate niche to infect, where chemotaxis plays an important role. Indole is a chemorepellent for EHEC [23] and is sensed by the chemoreceptor Tsr in *E. coli* [153]. We observed that indole reduces *Salmonella*'s motility and chemotaxis and, therefore, investigated whether *tsr* homolog in *Salmonella* was the chemoreceptor involved in indole's repellent response.

4.2 Materials and Methods

4.2.1 Bacterial strains, cell lines, media and chemicals

Salmonella enterica serovar Typhimurium (ATCC 14028s) was grown and maintained in Luria-Bertani (LB) medium at 37°C supplemented with appropriate antibiotics where necessary. *Salmonella* SPI-1 reporter strains for *hilA*, *prgH*, *invF* and *sipC* [137] were a kind gift from Dr. Sara D. Lawhon. The ΔSPI-1, ΔSPI-2, Δ*tsr*, Δ*motA*

and Δ*sdiA* deletion mutants [138] were generous gifts from Dr. Helene Andrews-Polymenis. *Salmonella* Typhimurium LT2 (ATCC 700720) strain [154] was a kind gift from Dr. Mustafa Akbulut. *Salmonella* LT2 was electroporated with pCM18 gfpmut3-encoding plasmid [155] and used in chemotaxis plug assays.

For all indole exposure experiments, cells were grown in LB overnight with or without indole, diluted to an $O.D._{600nm}$ of ~0.05 and further grown for ~2 h in a shaker incubator (New Brunswick Scientific) at 37°C, 250 rpm to obtain an exponential phase culture ($O.D._{600nm}$ of ~1.0), unless stated otherwise. 70% ethanol was used as the solvent control.

The murine macrophage cell line J774A.1 (ATCC), was maintained in the RPMI (Roswell Park Memorial Institute) 1640 medium with 10% fetal bovine serum, 1 mM sodium pyruvate, 10 mM HEPES, 2 g/L sodium bicarbonate, 0.05 mM 2-mercaptoethanol, 100 U/ml penicillin and 100 µg/ml streptomycin, at 37°C in 5% CO_2. The HeLa cell line (ATCC) was maintained in DMEM (Dulbecco's Modified Eagle Medium) supplemented with 10% bovine serum, 100 U/ml penicillin and 100 µg/ml streptomycin and 2 g/L sodium bicarbonate at 37°C in 5% CO_2 during normal growth and culture.

4.2.2 Generation of Salmonella *deletion mutants*

The Δ*phoPQ* mutations were generated in the *Salmonella* wild type and SPI-1 reporter strains using the Datsenko and Wanner method [156]. Briefly, gene deletion fragments encoding the kanamycin resistance gene flanked by upstream and downstream

regions of gene to be deleted were generated using the designed primers and pKD13 plasmid as template (**Table 1**). The DNA fragments were purified and the desired fragment length product was digested with *DpnI* followed by purification. These were then electroporated into the wild-type *Salmonella* and SPI-1 reporter strains containing the pKD46 plasmid encoding recombinase. The recombinant deletion mutants were then selected using kanamycin and verified for the gene deletion using PCR.

Table 1. Primers for generation and verification of *phoPQ* deletion in *Salmonella*.

Primer name	Sequence (5' - 3')
Primers for generation of *phoPQ* deletion	
phoP::Kan Forward	CATAATCAACGCTAGACTGTTCTTATTGTTAACACAAGGGAGAAGAGATGATTCCGGGGATCCGTCGACC
phoQ::Kan Reverse	GAGATGCGTGGAAGAACGCACAGAAATGTTTATTCCTCTTTCTGTGTGGGTGTAGGCTGGAGCTGCTTCG
Primers for verification of *phoPQ* deletion	
phoP Upstream Forward	ATTATATCGGTCGCGCTGTG
phoQ Downstream Reverse	AGAAAGTCGGGCCAGTTAAG
phoP Forward	GATGAAGACGGCCTTTCCTT
phoQ Reverse	GGCGATCCACAGTAAAGGAA
K1 Reverse [156]	CAGTCATAGCCGAATAGCCT

4.2.3 Motility assay

Motility assays were performed as described by Bansal et al [23]. Briefly, *Salmonella* was cultured in LB medium at 37°C or 30°C to exponential phase. Indole (1 mM) in 70% ethanol or the equivalent volume of solvent was added to motility agar plates (1% tryptone, 0.25% NaCl, and 0.3% agar), and the sizes of the motility halos were measured after 8 h. Four motility plates were used for each condition. A *motA* mutant was used as the negative control. Images were obtained using the Bio Rad VersaDoc imaging system model 3000.

4.2.4 In vitro *invasion assay and intracellular survival assay*

HeLa cells were cultured in a 24-well tissue culture plate at a cell density of ~5×10^5 cells/well and infected with late log phase *Salmonella* cells at an MOI ~ 100:1 for 1 h to allow invasion. At the end of the incubation period, the media was replaced with medium containing gentamicin (100 μg/mL) and incubated for an additional hour to kill the *Salmonella* cells that did not invade. The HeLa cell monolayers were then washed twice with PBS and cells lysed with a 0.2% sterile solution of NP40 to release the invaded bacteria. The lysate was serially diluted and spread on LB agar plates to determine the number of invaded bacteria. The starting inoculum was also plated to obtain the initial count of bacterial cells used for infection. The percentage invasion was calculated as the ratio of bacterial cells invaded to cells inoculated.

J774A.1 macrophage cells were also used for invasion and intracellular survival assay. Cells were plated in a 24 well plate at a density of ~5×10^5 cells/well and treated with serum-free RPMI medium overnight to synchronize them in a quiescent state. Prior to infection, the serum-free medium was replaced with RPMI medium supplemented with 10% heat-inactivated serum. The protocol for the invasion assay was similar to that used for HeLa cells, except that a lower MOI ~10:1 was used since the macrophages are inherently phagocytic.

The intracellular survival of *Salmonella* at 8 h post-invasion was determined by incubating the invaded J774A.1 cells in heat-inactivated serum RPMI media supplemented with 5μg/mL gentamicin at 37°C, 5% CO_2. Intracellular bacterial counts were obtained by lysing J774A.1 cells and plating serial dilutions on LB agar plates. The extent of survival was calculated as the ratio of the surviving intracellular bacteria to the number of bacteria that invaded.

4.2.5 Salmonella *SPI-1 reporter assays*

Salmonella SPI-1 reporter strains for *hilA*, *prgH*, *invF* and *sipC* with the β-galactosidase (β-gal) gene fused to each gene [137], were grown overnight in LB at 37°C and 250 rpm. Cells were diluted to an $O.D._{600}$ of ~0.05 in LB with 1 mM indole and grown to exponential phase, unless stated otherwise. β-gal activity measurements were made for the collected samples using a fluorogenic substrate (Resorufin β-D-galactopyranoside, AnaSpec) using a microplate scanning spectrofluorometer (SpectraMax, Gemini EM, Molecular Devices) with excitation and emission wavelengths as 544 nm and 590 nm,

respectively. Fluorescence readings were normalized to the growth absorbance and fold changes were calculated with respect to the control.

4.2.6 Chemotaxis plug assay

The *Salmonella* LT2 strain expressing GFP from the pCM18 plasmid was used for the qualitative plug assay to investigate the repellent response to indole as pCM18 was not stable in 14028s strain and was being lost resulting in non-fluorescent cells. Briefly, overnight culture was diluted in LB to an $O.D._{600nm}$ ~ 0.05 and grown to $O.D._{600nm}$ ~ 0.5 at 37°C, 250 rpm. The cells were harvested by centrifuging at 400 rcf for 10 min at RT. The supernatant was discarded and cells were re-suspended in CB at $O.D._{600nm}$ ~ 0.25. Plugs were prepared with low melting agarose (Sigma) by dissolving in CB at 55°C. Plugs were formed by sandwiching 5-10 µL of signal containing agarose between a slide and a coverslip (raised using double sided tape) [23, 157]. It was then allowed to cool before introducing cells. The plug boundary was imaged using Zeiss microscope.

4.2.7 Capillary assay

The capillary assay was modified for *Salmonella* chemotaxis from a previous report for *E. coli* [158]. Briefly, an overnight culture was grown at 37ºC, 250 rpm and back diluted to an $O.D._{600nm}$~ 0.05 and grown to $O.D._{600nm}$ ~ 0.5. The cells were centrifuged (in round bottom tubes), at 400g for 10 minutes, gently resuspended in 2/3rd volume of chemotaxis buffer (CB: 1× PBS, 0.1 mM EDTA (pH 8.0), 0.01 mM L-methionine and 10 mM DL-lactate). Chemotaxis chambers were prepared using C-rings

sandwiched between a glass slide and cover slip and the cell suspension was loaded into the chambers. Chemoeffector signals were prepared fresh and loaded in MICROCAPS capillaries prior to inserting into the culture-filled chambers. The capillaries were incubated for 45 minutes at 37°C and the contents were expelled into tubes containing 500 µL of CB on ice. Serial dilutions were prepared and plated on LB plates. Colonies were counted after overnight incubation at 37°C and bacterial accumulation in each capillary was calculated.

4.3 Results

4.3.1 Indole's effect on motility of sdiA *mutant*

The Δs*diA* mutant also demonstrated comparable decrease in motility to the wild-type strain upon indole exposure at 37°C (65% and 42% decrease, respectively; **Figure 16**). These results indicate that indole's effect on *Salmonella* motility is not mediated through *sdiA*.

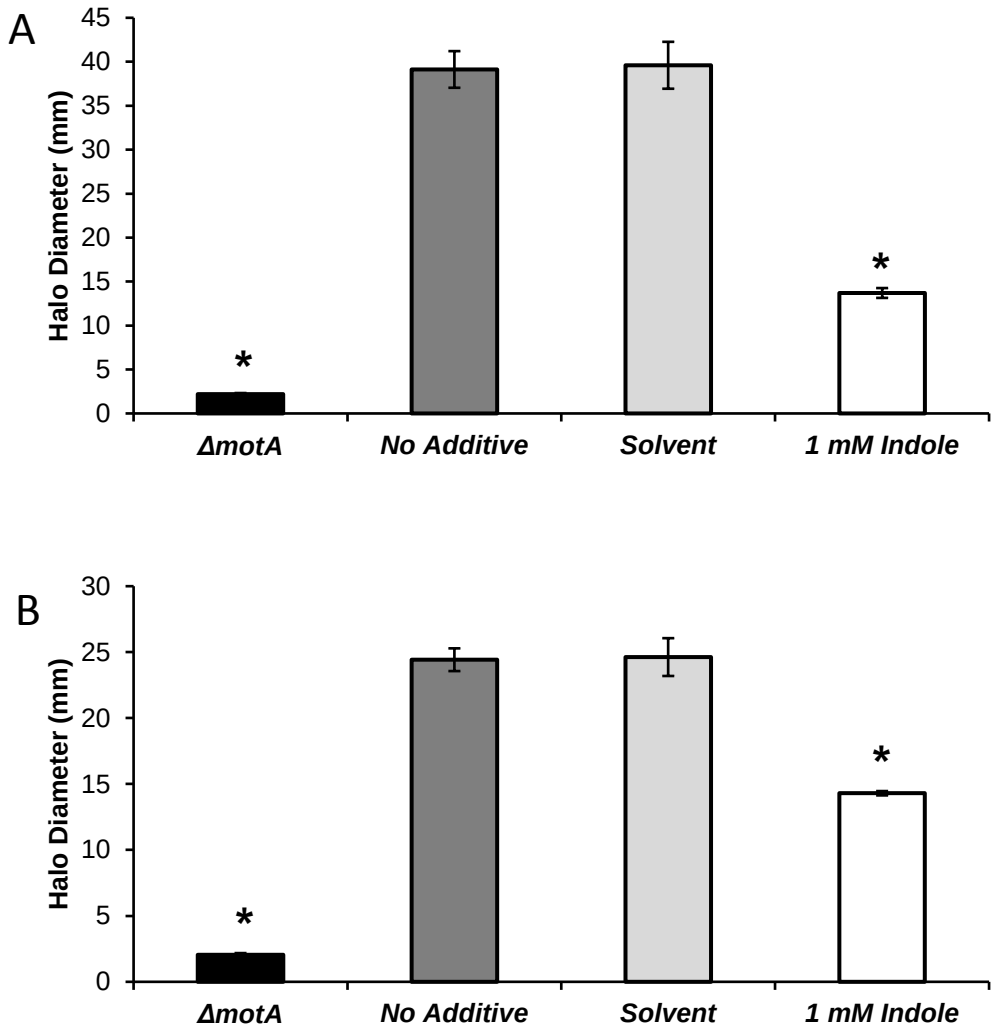

Figure 16. Effect of indole on *Salmonella* swimming motility in Δ*sdiA* strain. Swimming motility assay observations of *Salmonella* (A) Δ*sdiA* strain at 37°C and (B) Δ*sdiA* strain at 30°C. Data shown are the measured halo diameters for the different test conditions - no additive, solvent and 1 mM indole at 8 h post-spotting. Diameters were measured using Vernier calipers. Δ*motA* was spotted on swimming motility agar plates as a negative control for motility. (* indicates $p < 0.05$)

4.3.2 Indole's effect on invasion and survival of sdiA *mutant*

The decrease in invasion of HeLa epithelial cells due to indole exposure by Δ*sdiA* strain was to the same extent as WT (**Figure 17**). A 2.8-fold decrease in invasion of macrophages and no significant change in intra-cellular survival was observed with the Δ*sdiA* strain (**Figure 18**). This decrease in invasiveness and the lack of effect on intra-cellular survival in J774.A1 macrophages, observed with the Δs*diA* strain, was comparable to that observed with the WT which further confirmed that *sdiA* is not involved in indole-mediated effects on *Salmonella*.

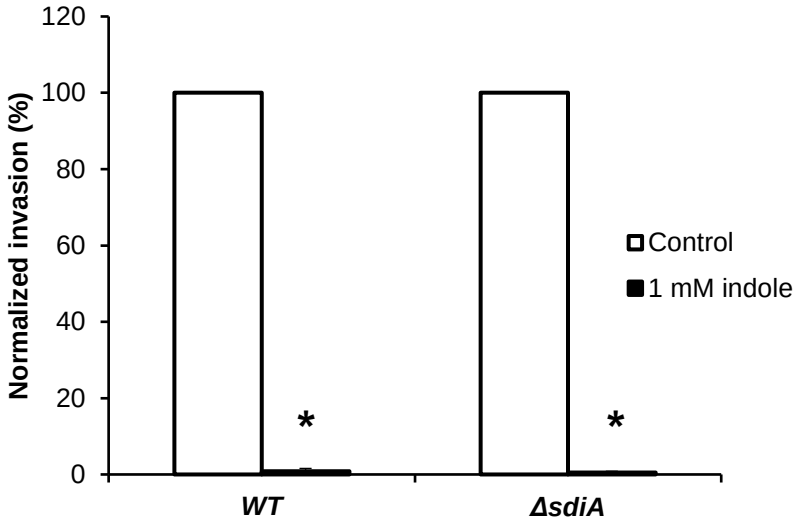

Figure 17. Invasion of epithelial cells with indole-treated *Salmonella* Δ*sdiA*. Invasion in HeLa epithelial cell line with *Salmonella* treated with or without 1mM indoleA MOI of 100:1 was used and data shown are % invasion, normalized to the solvent-treated control. (* indicates $p < 0.05$)

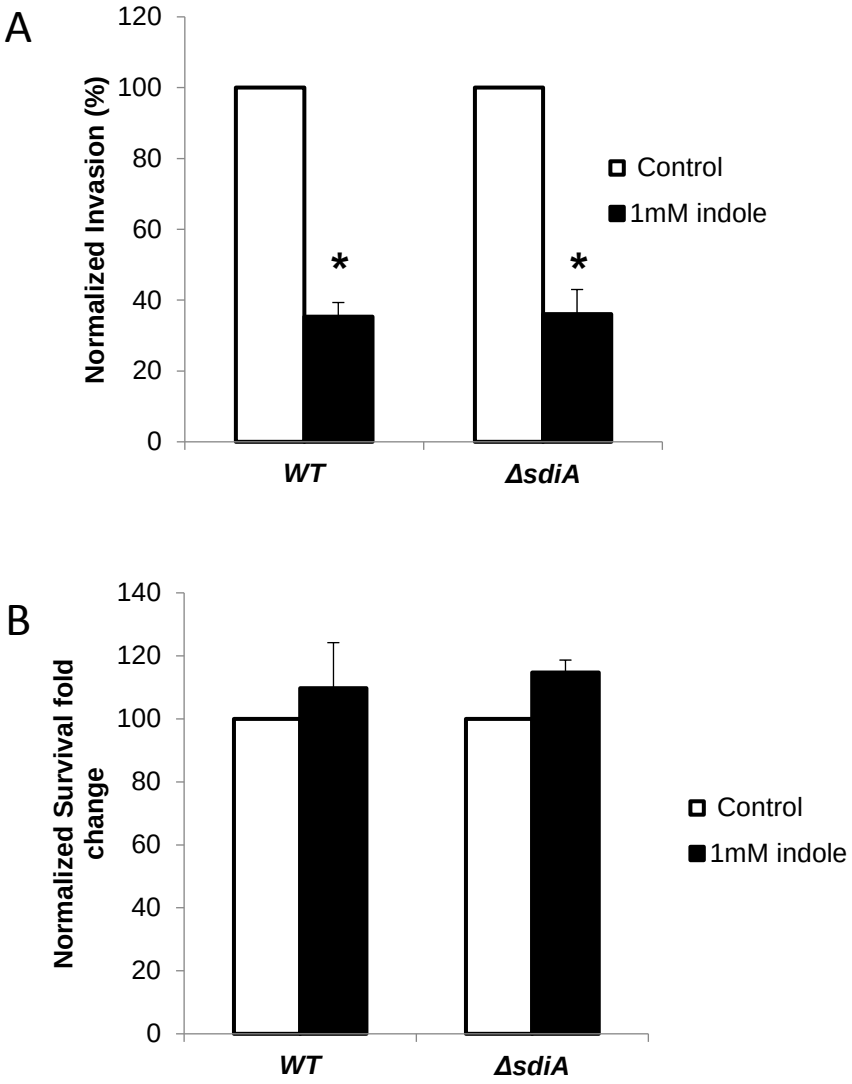

Figure 18. Invasion and intracellular survival within macrophages with indole-treated *Salmonella* Δ*sdiA*. Invasion (A) and intracellular survival (B) in J774A.1 cells. A MOI of 10:1 was used and data shown are % invasion or survival fold changes, relative to the invasion, normalized to the solvent-treated control. (* indicates $p < 0.05$)

4.3.3 Indole's effect on SPI-1gene expression in phoPQ *mutant*

Salmonella with a constitutively expressed *phoP* (part of the *phoPQ* two-component signaling system) is known to reduce the expression of *prg* loci genes that are part of SPI-1 [29]. We investigated whether the effect of indole was mediated through the *phoPQ* two-component system by investigating the effect of indole on SPI-1 gene expression in a *phoPQ* deletion mutant. Exposure to 1 mM indole decreased the expression of the four SPI-1 genes tested (*hilA*, *prgH*, *invF* and *sipC*) by 8-, 11-, 8- and 4-fold, respectively, in the Δ*phoPQ* mutant; however, the magnitude of attenuation was ~2-fold less than that observed in wild type cells i.e. 23-, 20-, 13- and 6-fold, respectively, for *hilA*, *prgH*, *invF* and *sipC* (**Figure 19**). This suggests that *phoPQ* decreases SPI-I gene expression and *Salmonella* virulence using PhoPQ-dependent and independent mechanisms.

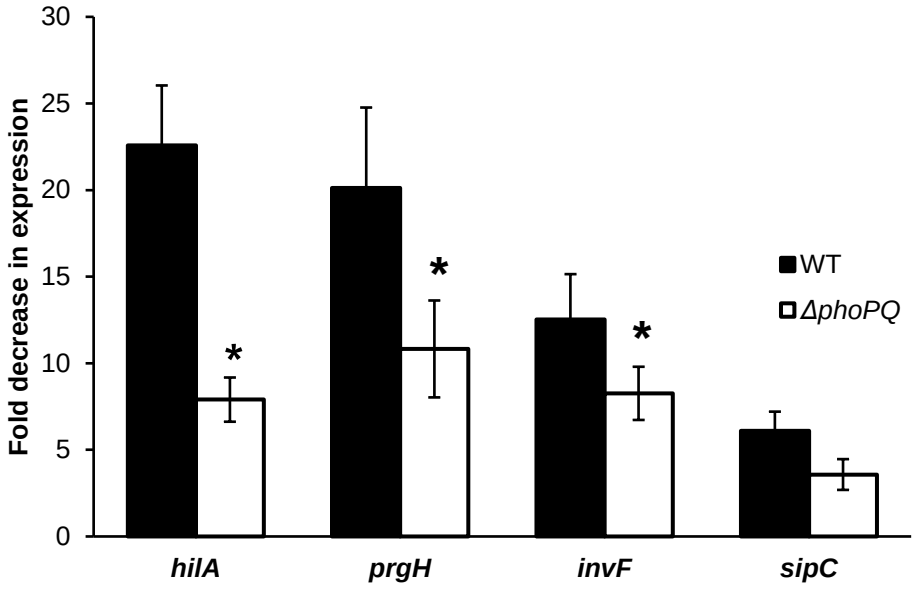

Figure 19. Role of *phoPQ* in indole mediated down-regulation of SPI-1 gene expression using β-gal assay. The Δ*phoPQ* mutation was generated in the four SPI-1 reporter strains for *hilA*, *prgH*, *invF* and *sipC*. The WT and the Δ*phoPQ* reporter strains were treated overnight with and without 1 mM indole and the β-gal activity was measured in exponential phase cultures after dilution. Data shown are the fold decrease in expression with indole-treatment relative to the solvent-treated control. (* indicates $p < 0.05$)

4.3.4 Indole's effect on invasion by phoPQ *mutant*

Epithelial cell invasion assays with the Δ*phoPQ* mutant were consistent with the previous observation on SPI-1 gene expression. The decrease in invasion with the Δ*phoPQ* mutant upon indole treatment was ~ 9-fold, which was ~ 3-fold less than that observed for the WT strain (~ 26-fold) **(Figure 20**).

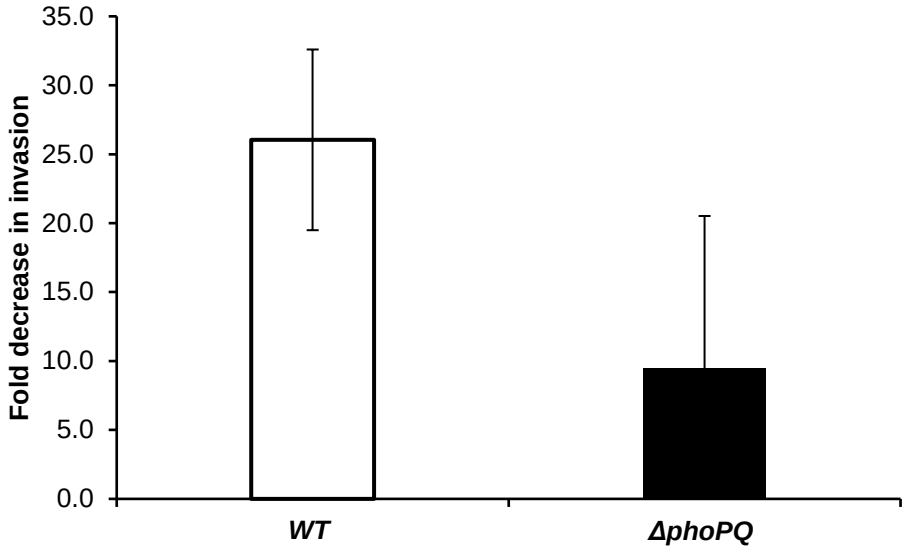

Figure 20. Role of *phoPQ* in indole mediated down-regulation of epithelial cell invasion. Invasion in HeLa epithelial cell line with *Salmonella* WT and Δ*phoPQ* strain treated with or without 1mM indole. A MOI of 100:1 was used and the data shown is the fold decrease in invasion by indole-treated relative to solvent-treated *Salmonella* and was statistically significant with $p < 0.05$.

4.3.5 Indole's effect on Salmonella *chemotaxis*

We observed that indole treatment reduces *Salmonella* motility (**Figure 8**) and were interested in further investigating whether indole acts as a repellent using a plug assay. We observed that *Salmonella* LT2 cells expressing GFP accumulated at the boundary of the plug containing 1 mM serine whereas no accumulation was observed at the interface of the plug containing 1 mM indole or the CB control (**Figure 21**). This suggests either no response or a chemorepellent response to indole by *Salmonella* cells. To further confirm the chemorepellent response and determine the chemoreceptor involved, capillary assays were conducted.

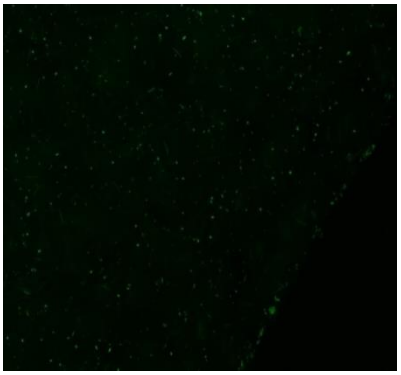

CB

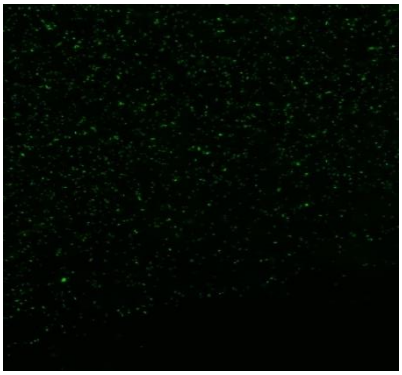

1 mM Indole

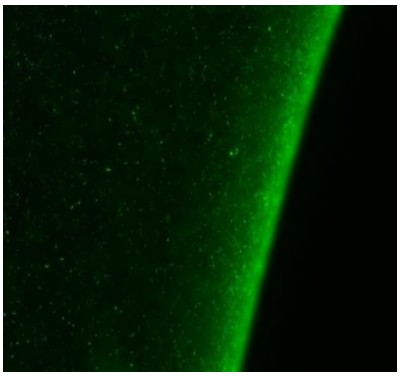

1 mM Serine

Figure 21. Indole's chemorepellent response in a plug assay. Motile *Salmonella* Typhimurium LT2 cells, expressing GFP from pCM18, were introduced in a chamber with a plug containing either 1 mM indole or 1 mM serine (or no signal i.e. CB). Accumulation or the lack thereof, of cells at the plug boundary represent a chemoattractant or chemorepellent/no response, respectively. Images were taken after 20 min incubation at 37°C using a 10× objective.

4.3.6 Indole's repellent response in capillary assay

Capillary assays were performed with *Salmonella* 14028s with indole, serine and aspartate as signals; however, based on accumulation numbers in response to 1 mM indole, it was difficult to distinguish the lack of response from a repellent response. Therefore, the experimental design was modified to determine indole's repellent response by introducing it along with an attractant such as serine or aspartate and probe for a reduction in accumulation when indole is present along with an attractant (compared to attractant alone). We observed that 1 mM indole when present along with an attractant, i.e. 10 mM serine or 1 mM aspartate, decreased bacterial accumulation in the capillary by ~2-fold (**Figure 22**). These results suggested that indole acts as a repellent for *Salmonella* chemotaxis.

Indole is a known chemorepellent for *E. coli* and Tsr was identified as the chemoreceptor that senses indole in *E. coli* [153]. Therefore, we investigated whether *Salmonella* with a *tsr* deletion would respond to indole in a capillary assay. Our results show that 1 mM indole did not significantly reduce accumulation in the capillary when present along with 1 mM aspartate (an attractant) (**Figure 23**) and, therefore, suggests that indole is sensed by Tsr in *Salmonella* as well.

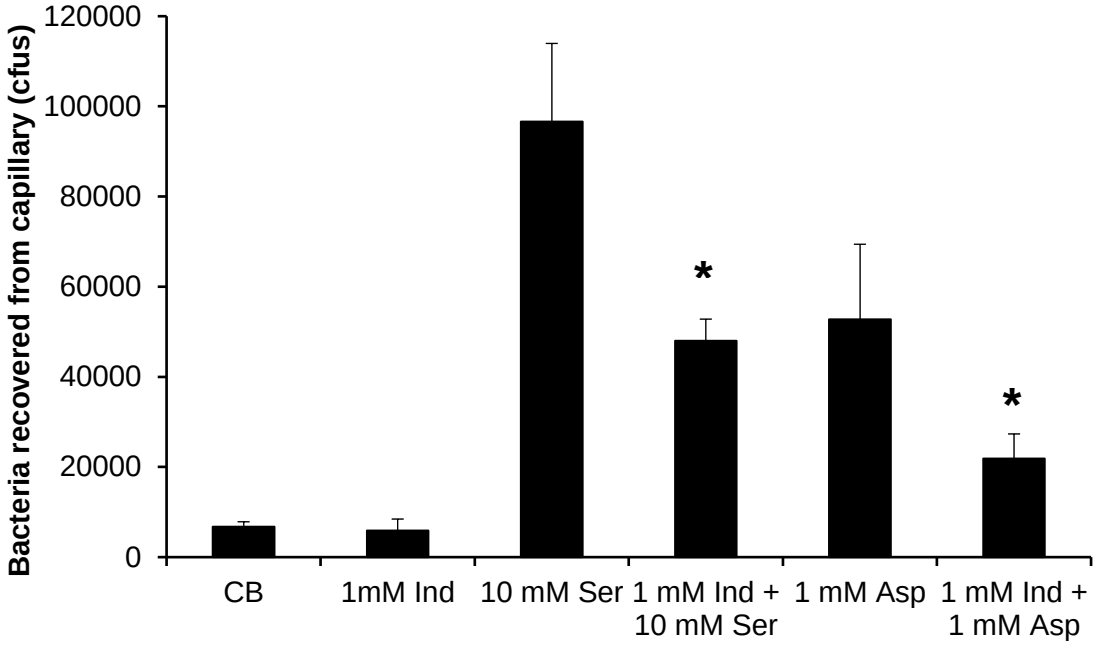

Figure 22. Capillary assay with *Salmonella* Typhimurium 14028s. Bacterial accumulation in capillaries in response to 1mM indole (Ind), 10 mM serine (Ser), 1 mM aspartate (Asp) and their combinations after 45 minute incubation at 37°C. (* indicates $p < 0.05$)

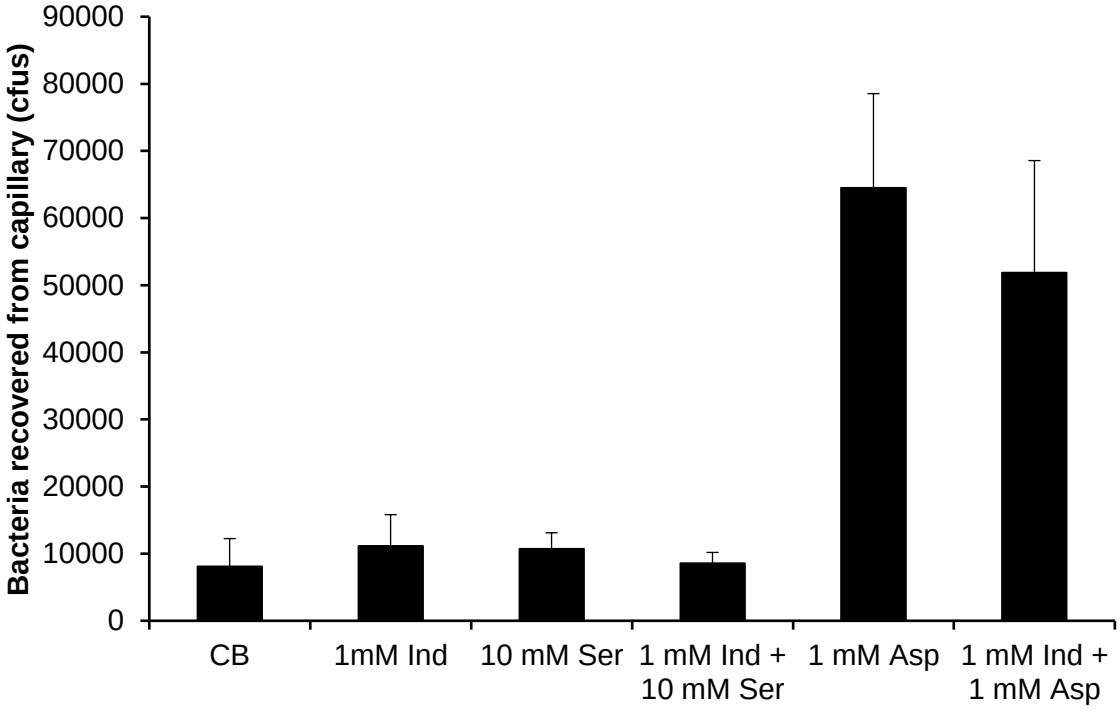

Figure 23. Capillary assay with *Salmonella* Typhimurium 14028s Δ*tsr*. Bacterial accumulation in capillaries in response to 1mM indole (Ind), 10 mM serine (Ser), 1 mM aspartate (Asp) and their combinations, after 45 minute incubation at 37°C.

4.4 Discussion

The mechanism(s) underlying indole's effects on pathogen virulence are poorly understood. Few transcriptional regulators and two-component systems have been reported to be involved in indole signaling. Kanamaru et al., [146] showed that the

expression of virulence factors in EHEC is controlled by *sdiA* and that indole acts through *sdiA* [19]. It has also been reported that high indole concentrations inhibit detection of AHLs by SdiA [110]. However, our *in vitro* data with motility and invasion suggest that SdiA is not involved in mediating indole's effects in *Salmonella*. The decrease in motility of a Δs*diA* mutant upon indole treatment was comparable to the wild-type strain at 37°C and 30°C (**Figure 16**). These results indicate that indole's effect on *Salmonella* motility is not mediated through *sdiA*. The decrease in invasion of HeLa epithelial cells and J774A.1 macrophages (and the lack of effect on intra-cellular survival) with indole-treated Δs*diA* mutant was also similar to that observed by the WT strain (**Figure 17** and **18**), which further confirmed that *sdiA* is not involved in indole-mediated effects on *Salmonella*.

Several bacterial two-component systems sense environmental signals (such as pH, cations, cationic antimicrobial peptides, osmolarity, etc) and one such regulatory system, *phoPQ*, has been reported to down regulate SPI-1 gene expression [29-31]. Our data indicate that the *phoPQ* two-component system is at least partially involved in mediating the effects of indole in *Salmonella*, as the change in expression of SPI-I genes upon indole exposure was neither unaltered nor completely abrogated in the Δ*phoPQ* mutant strains compared to the WT. These results also suggest that other pathways are involved in indole mediated signaling that regulate virulence gene expression. Nikaido et al [105] found that while *ramA* is involved in indole signaling, the down-regulation of virulence gene expression with indole was independent of RamA/RamR. Vega et al., reported that pathogens such as *Salmonella* (which do not produce indole) may benefit from indole-mediated signaling through the OxyR regulon, increasing their antibiotic

resistance [103]; however, OxyR has been reported to not influence *Salmonella* virulence [159]. Therefore, while our data clearly shows a role for *phoPQ* in the down-regulation of *Salmonella* virulence by indole, further work needs to be done to fully elucidate the additional underlying mechanism(s).

Motility is an important virulence factor in pathogens such as *Campylobacter*, *Salmonella* and *E. coli* [32]. Presence of flagella was required for efficient colonization by *Salmonella* in mice and has been attributed to chemotaxis [160]. Three chemoreceptors: Trg, Tsr and Aer, have been reported to be important in *Salmonella* colonization in the mice infection model [161]. Trg is a methyl-accepting chemotaxis protein (MCP) that senses galactose, an abundant residue in the cecal mucosa [162]. Tsr and Aer were determined to provide a luminal growth advantage to *Salmonella* in an inflamed intestine and were involved in energy taxis. Tsr and Aer mediated chemotaxis towards electron acceptors nitrate and tetrathionate (present in the inflamed gut), respectively [161]. Most of the studies involved in identifying luminal signals are focused on attractants. In this study we show that microbiota-metabolite indole is a repellent for *Salmonella* chemotaxis and is sensed by the Tsr chemoreceptor. Indole might, therefore, play a role in preventing *Salmonella* colonization in the cecum by reducing the directed migration of the pathogen towards the epithelium.

5. INTERACTION OF INDOLE WITH PHOQ

5.1 Introduction

Bacteria can sense environmental signals via two-component systems, comprising a transmembrane sensor kinase and a cytosolic response regulator. The signal transduction pathway for such two-component systems is well studied. Briefly, the sensor kinase is autophosphorylated at the histidine residue in an ATP-dependent manner. When a signal from the environment such as a chemical molecule, interacts with the periplasmic domain of the sensor kinase, structural changes are induced that are transmitted across the transmembrane segment of the sensor, and the phosphoryl group is transferred from the sensor kinase to an aspartate residue in the response regulator protein. This activates the response regulator, which then binds to promoter regions of target genes and regulates gene expression.

In order to determine the mechanism by which indole is sensed by *Salmonella* through the PhoQ sensor kinase, a computational approach was used to scan the PhoQ receptor for possible binding sites using AutoDock Vina [163] and SwissDock [164] programs. Molecular dynamic simulations were employed to assess the stability of the ligand interaction with the receptor based on free energy calculations. Application of these computational tools provided a list of candidate amino acid targets, narrowing the scope of search for the mutagenesis experiments.

We explored indole's interaction with the periplasmic and cytoplasmic domains of PhoQ using computational modeling and tested the predictions *in vitro* using alanine

substitutions of amino acids that were predicted to interact with indole. Our results suggest that indole most likely interacts with the cytoplasmic domain of PhoQ in the ATP-binding pocket.

5.2 Materials and Methods

5.2.1 Bacterial strains and cloning

Salmonella enterica serovar Typhimurium (ATCC 14028s) was grown and maintained in Luria-Bertani (LB) medium at 37°C supplemented with appropriate antibiotics where necessary. *Salmonella* SPI-1 reporter strains for *hilA* [137] was a kind gift from Dr. Sara D. Lawhon (Department of Veterinary Pathobiology, Texas A&M University). The Δ*phoQ* mutation were generated in the *Salmonella* WT and SPI-1 *hilA* reporter strain using the Datsenko and Wanner method [156]. Briefly, gene deletion fragments encoding the kanamycin resistance gene flanked by upstream and downstream regions of gene to be deleted were generated using the designed primers and pKD13 plasmid as template (**Table 2**). The DNA fragments were purified and the desired fragment length product was digested with *DpnI* followed by purification. These were then electroporated into the wild-type *Salmonella* and SPI-1 reporter strains containing the pKD46 plasmid encoding recombinase. The recombinant deletion mutants were then selected using kanamycin and verified for the gene deletion using PCR.

Table 2. Primers for generation and verification of *phoQ* deletion in *Salmonella* and cloning *Salmonella phoQ* on pCA24N.

Primer name	Sequence (5' - 3')
Primers for generation of *phoQ* deletion	
phoQ::Kan Forward	GTCATTACCACCGTACGCGGACAAGGATATCTTTTTGAATTGCGCTAATGATTCCGGGGATCCGTCGACC
phoQ::Kan Reverse	GAGATGCGTGGAAGAACGCACAGAAATGTTTATTCCTCTTTCTGTGTGGGTGTAGGCTGGAGCTGCTTCG
Primers for verification of *phoQ* deletion	
phoQ Upstream Forward	ATCCGCACGATGTCATTACC
phoQ Forward	ATGACGATGATGCCGAGATG
phoQ Reverse	GGCGATCCACAGTAAAGGAA
K1 Reverse [156]	CAGTCATAGCCGAATAGCCT
Primers for cloning *phoQ* in pCA24N	
StmPhoQ_N-terminal	[Phos]GCCAATAAATTTGCTCGCCATTT
StmPhoQ_C-terminal	[Phos]CCTTCCTCTTTCTGTGTGGGATG

The *Salmonella phoQ* gene was cloned in pCA24N using the strategy reported in [165] for PhoQ complementation and periplasmic domain-mutagenesis studies. pCA24N was a generous gift from Dr. Katy Kao (Department of Chemical Engineering, Texas A&M University). Briefly, genomic DNA was isolated from the *Salmonella* Typhimurium WT strain using the PowerSoil DNA isolation kit from MO BIO laboratories Inc. The gDNA was then used as template for amplifying the *phoQ* gene using the high fidelity Phusion DNA polymerase (NEB) and the StmPhoQ_N-terminal and StmPhoQ_C-terminal primers (**Table 2**). The PCR product was run on 1% agarose gel and the amplified fragment was gel extracted using the Promega Wizard gel extraction and PCR clean up kit. The pCA24N plasmid was extracted using the Promega plasmid isolation kit and digested with the NEB restriction enzyme *StuI*. The restricted ends were then dephosphorylated using the NEB alkaline phosphatase, CIP, followed by clean up using the Promega PCR clean up kit. Ligation of the insert in the vector was carried out using T4 DNA ligase (NEB) at 16°C, overnight followed by heat inactivation at 65°C, 10 minutes (Insert:Vector ~3:1 was used). The ligation reaction product was transformed into chemically competent *E. coli* DH5α cells (NEB C2992) using heat shock method. The desired clones were selected on LB agar plates containing 30 µg/mL chloramphenicol (Cm) verified by digesting the plasmid with *SfiI* at 50°C, 1 h and the digest was run on 1% agarose gel. The appropriate clones resulted in 2 bands corresponding to ~1.5 kb band for the gene and ~5 kb band corresponding to the vector backbone. Since pCA24N vector contains a gfp tag, the desired clone of pCA24NStmPhoQ was digested using *NotI*, followed by purification using gel extraction and self-ligation using T4 DNA ligase. The

ligated reaction mixture, now comprising pCA24NStmPhoQ -gfp, was transformed into chemically competent *E. coli* DH5α cells (NEB C2992). The desired clones were verified using *SfiI* digestion and agarose gel electrophoresis. The verified pCA24NStmPhoQ –gfp plasmid was then used for PhoQ complementation as well as site-directed mutagenesis studies and was electroporated into *Salmonella* Δ*phoQ* strains.

Studies with the cytoplasmic domain of PhoQ were conducted using the pGEX-KG construct encoding the catalytic domain of *Salmonella* PhoQ (Stm $PhoQ_{cat}$) residues 332-487, kindly provided by Dr. Rui Zhao at University of Colorado, Denver [166, 167]. The construct was verified using PCR (see **Table 3** for primers used) for the presence of the following gene sequences: *tac* promoter, GST tag, thrombin cleavage site and sequence corresponding to $PhoQ_{cat}$; and transformed into *E. coli* BL21 cells for overexpression and purification.

Table 3. Primers for verification of Stm $PhoQ_{cat}$ cloned in pGEX-KG.

Primer name	Sequence (5' - 3')
GST Forward	TTAAGGGCCTTGTGCAACC
GST Reverse	GGCACATTGGGTCCATGTATAA
Tac promoter Forward	TGACAATTAATCATCGGCTCGTATAATGT
Thrombin site Forward	TCTGGTTCCGCGTGGAT
$StmPhoQ_{cat}$ Forward	AAGTGATGGGCAACGTACTG
$StmPhoQ_{cat}$ Reverse	CCGGCGTATTGTTCCGTAAT

For all indole exposure experiments, cells were grown in LB overnight with or without indole, diluted to an $O.D._{600nm}$ of ~0.05 and further grown for ~2 h in a shaker incubator (New Brunswick Scientific) at 37°C, 250 rpm to obtain an exponential phase culture ($O.D._{600nm}$ of ~1.0), unless stated otherwise. 70% ethanol was used as the solvent control.

5.2.2 Indole-PhoQ periplasmic domain interaction

Possible binding sites of indole to the periplasmic domain of *Salmonella*'s PhoQ receptor were determined using two open source molecular docking programs: AutoDock Vina [163] and SwissDock [164]. The crystal structures of *Salmonella*'s PhoQ periplasmic domain were obtained from Protein Data Bank (PDB) [168, 169]. PDB ID: 1YAX [128] is the crystal structure of *Salmonella* PhoQ periplasmic domain in the Ca2+ bound state and the PDB ID: 4UEY [130] is the structure of the periplasmic domain of PhoQ double mutant W104C and A128C engineered for restrained conformational flexibility by forming a disulfide bond. The 4UEY structure was used for docking after computationally correcting the mutations to WT amino acids in the structure, using SCWRL4 [170]. The entire receptor was used as the search space for docking using the SwissDock server and the AutoDock Vina program. Indole's structure (ZINC ID:14516984) was obtained from the ZINC database [171, 172].

5.2.3 Site-directed mutagenesis

The key amino acid, in the identified binding pockets of the PhoQ periplasmic domain where indole was predicted to interact, was mutated to alanine using the NEB Q5® site-directed mutagenesis kit. Briefly, primers (**Table 4**) were designed using NEBaseChanger™ v1.2.4 tool to substitute the codons corresponding to the identified key charged amino acids to the codon encoding alanine, thereby switching the key amino acid with alanine upon translation. "GCG" was the codon used for alanine as it was determined to have the highest frequency (32.4 per thousand) in the *Salmonella* Typhimurium genome (http://www.kazusa.or.jp/codon/cgi-bin/showcodon.cgi?species=602) [173].

Table 4. Primers designed for site-directed alanine mutagenesis.

Substitution	Primer name	Sequence (5' - 3')
R100A CGC → GCG	StmPhoQ_R100A_F	ATGGACGCAGgcgAACATTCCCTGG
	StmPhoQ_R100A_R	AATAATTTGCCCGTTTCATC
R50A CGU → GCG	StmPhoQ_R50A_F	AACCACCTTTgcgTTGCTGCGCG
	StmPhoQ_R50A_R	TTATCAAAACTTACGCTATAGC
K186A AAA → GCG	StmPhoQ_K186A_F	GATAGAACTAgcgCGCTCCTATATGGT GTG
	StmPhoQ_K186A_R	GGAATGGTATCGACCACC
K115A AAA → GCG	StmPhoQ_K115A_F	GGAATGGTTAgcgACGAACGGCTTC
	StmPhoQ_K115A_R	GGTTGAATGCTTTTAATCAGC
Primers for sequencing pCA24NStmPhoQ mutants		
F-CA [165]		CATTAAAGAGGAGAAATTAACTATGA GAGG
pCA24N-gfpR		CGTCAGTCAGTCACGATGAA

The primers designed for alanine site-directed mutagenesis were used to amplify the plasmid pCA24N clone encoding the *Salmonella phoQ* gene using the Q5 Hot Start High-Fidelity master mix as recommended by manufacturer (NEB). The KLD mixture, provided in the kit, was then used to phosphorylate and ligate the ends of the amplified product (comprising the mutation) and circularize the plasmid clone as well as to digest the parent plasmid backbone, according to manufacturer's protocol. The ligated plasmid

was then transformed into chemically competent *E. coli* cells (NEB C2992) using heat shock. The clones were streaked on a fresh LB agar plates containing 30 µg/mL chloramphenicol to purify and were verified by sequencing using primers specified in **Table 4**.

5.2.4 Effect of site-directed alanine mutations on hilA *expression using β-galactosidase reporter assay*

Site-directed mutagenesis of identified amino acids in the PhoQ periplasmic domain was carried out by substituting the codon for the key amino acid with the codon GCG, coding for alanine, in the *Salmonella phoQ* genetic sequence cloned in pCA24N. The verified clones (pCA24NStmPhoQ WT as well as those with single amino acid alanine substitutions) were transformed into the *Salmonella* Δ*phoQ* HilA reporter strain. The *Salmonella* Δ*phoQ* strains harboring pCA24N, encoding either the WT or the mutant PhoQ, were grown overnight in LB at 37°C and 250 rpm. Cultures were diluted to an $O.D._{600}$ of ~0.05 in LB with 1 mM indole and grown to exponential phase, unless stated otherwise. β-gal activity measurements were made for the collected samples using a fluorogenic substrate (Resorufin β-D-galactopyranoside, AnaSpec) using a microplate scanning spectrofluorometer (SpectraMax, Gemini EM, Molecular Devices) with excitation and emission wavelengths as 544 nm and 590 nm, respectively. Fluorescence readings were normalized to the growth absorbance and fold changes were calculated with respect to the control.

5.2.5 Indole's interaction with the PhoQ cytoplasmic domain

AutoDock Vina [163] was used to determine possible binding sites of indole to the cytoplasmic domain of *Salmonella* PhoQ. The crystal structure for the *Salmonella* PhoQ cytoplasmic domain (residues 331 – 485) was obtained from PDB (PDB ID: 3CGZ but residues 423 – 444 are unresolved) [166] and used for simulation studies. The structure for the unresolved residues (423 – 444) was built using SWISS-MODEL [174]. The docking poses generated by AutoDock Vina were equilibrated for 1 nanosecond (ns) and underwent 10 ns explicit solvent MD simulations with 20 picosecond (ps) snapshots. Interaction free energy between PhoQ residue R and indole (L) was calculated, for 2.5 ns segments (125 snapshots), for the most stable binding pose using the following equation (**Eq. 1**) [175-177]:

$$\Delta G_{RL}^{\text{inte}} = \frac{1}{f}\sum_{k\in f}\left(\sum_{i\in R}\sum_{j\in L}\left(E_{ij}^{\text{Elec}} + E_{ij}^{\text{GB}}\right) + \sum_{i\in R}\sum_{j\in L}E_{ij}^{\text{vdW}} + \gamma\sum_{i\in R,L}\Delta\left(\text{SASA}_i\right)\right)$$

Eq. 1

Where, the polar component of the interaction free energy between *R* and *L* is represented by the sum of the electrostatic, E_{ij}^{Elec}, and polar solvation, E_{ij}^{GB}, free energy terms. The non-polar component of the interaction free energy between *R* and *L* is represented by the sum of the Van der Waals, E_{ij}^{vdW}, and non-polar solvation, $g\times\text{SASA}$

, free energy terms. The sum of the per residue interaction free energies across the 2.5 ns segment is averaged over the number of snapshots used in the calculation, *f* (=125).

The electrostatic interaction contribution represents the interaction between residue *R* and *L*, and the polar solvation contribution represents the interaction of residue *R* with the solvent polarization potential induced by *L*. The van der Waals contribution represents the non-polar interaction between residue *R* and *L*, and the non-polar solvation contribution represents the non-polar interactions with the surrounding solvent and cavity contributions due to binding. The solvation terms were determined using the Generalized Born with simple SWitching (GBSW) model [178]. The interaction free energy calculations were performed using a non-polar surface tension coefficient, γ, of 0.03 kcal/(molÅ^2).

5.2.6 Expression and purification of Salmonella *PhoQ cytoplasmic catalytic domain*

E. coli BL21 cells carrying pGEX-KG plasmid encoding Stm PhoQcat tagged with GST was used for overexpression of the desired protein. Briefly, an overnight culture was grown in LB media (containing ampicillin at 100µg/mL concentration) at 30°C, 250 rpm and diluted 1:100 in 200 mL LB media (in 5 flasks amounting to 1L) containing ampicillin and incubated at 30°C, 250 rpm until an $O.D._{600nm}$ ~ 0.4-0.6 was achieved. The culture was then induced with 100 µM IPTG (Isopropyl β-D-galactopyranoside) overnight at RT. The cells were harvested by centrifugation at 10,000g, 4°C for 15 min and resuspended in 50mM Tris-HCl, pH 7.5, 50mM NaCl containing 200 µM of the protease inhibitor PMSF (phenylmethanesulfonyl fluoride). The suspension was sonicated using BRANSON

Digital Sonifier and centrifuged at 10,000 ×g, 4°C for 1 h and the supernatant containing the soluble fraction was collected for purifying the desired protein.

The StmPhoQ$_{cat}$ domain is fused to the Glutathione S-transferase (GST) tag through a thrombin cleavage site; therefore, a strategy involving affinity purification with Glutathione Sepharose® 4B (GS4B), followed by on-column cleavage of GST tag using thrombin protease, and thrombin removal using Benzamidine Sepharose® Fast Flow (BSFF) was employed [166, 179]. GE products were used for the purification steps and manufacturer recommended protocols were followed. Samples were collected at various steps and protein concentrations were determined based on the absorbance at 280 nm on a Nanodrop (Thermo Scientific). Samples were analyzed using SDS-PAGE to assess purity of the the desired protein. A 12.5% resolving gel was cast to obtain separation and gels were stained using LabSafe GEL Blue™ (G-BIOSCIENCES®) as per recommended procedure. The Pierce™ BCA (bicinchoninic acid) protein assay kit (Thermo Scientific™) was used to determine concentration of purified protein samples.

5.2.7 TNP-ATP displacement assay

The fluorometric TNP-ATP displacement assay was used to investigate indole binding to the PhoQ catalytic domain, as described in [166, 167]. Briefly, the purified Stm PhoQ$_{cat}$ protein was mixed with the fluorogenic substrate TNP-ATP (2',3'-O-(2,4,6-Trinitrophenyl) adenosine 5'-triphosphate tetrasodium salt) in the ratio ~100 µM:100 µM. Aliquots of the premixed protein and substrate were then incubated in the presence of test signals/controls (1 mM indole, 1 mM radicicol or DMSO) for 15 min followed by

recording fluorescence readings using Mithras LB 940 multimode microplate reader from Berthold Technologies with 405nm excitation and 535nm emission filters. A reduction in fluorescence, compared to DMSO control, in the presence of a test chemical was used as the indicator of competitive binding to the catalytic site.

5.3 Results

5.3.1 Identification of the indole binding sites in the PhoQ periplasmic domain

We used AutoDock Vina and SwissDock to scan the PhoQ periplasmic domain for possible binding sites and over 500 potential binding pockets were identified (**Figure 24**). The key charged residues in the top 4 potential binding pockets (based on lowest AutoDock Vina score) were: Arg100 (R100), Arg50 (R50), Lys186 (K186) and Lys115 (K115) (**Figure 25**).

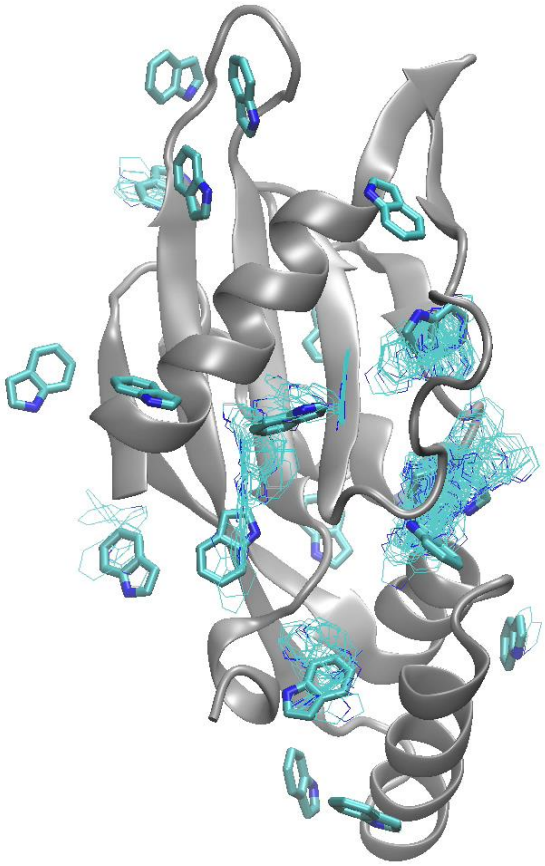

Figure 24. PhoQ crystal structure with representative indole-binding sites determined using docking algorithms such as AutoDock Vina and SwissDock. Generated binding poses of indole were clustered (shown in line representation) and the most favorable conformation within each cluster is shown in licorice representation. The PhoQ periplasmic crystal structure is shown in grey cartoon representation.

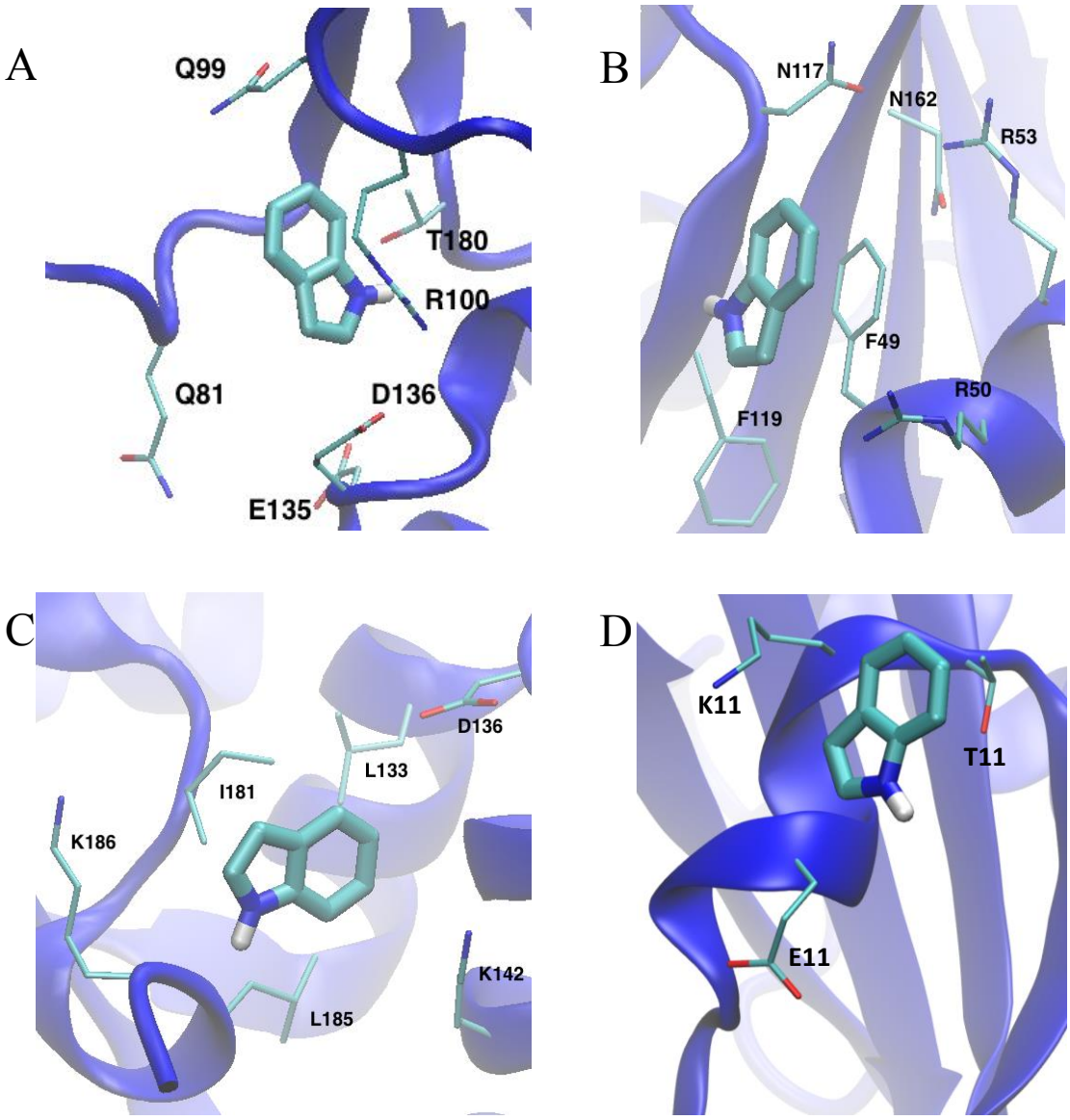

Figure 25. Indole docking representations for the four key binding pockets using AutoDock Vina. A candidate pose for indole in the binding pocket with the key charged residue A) Arg100 (R100), B) Arg50 (R50), C) Lys186 (K186) and D) Lys115 (K115**).**

5.3.2 Indole's effect on hilA *expression in PhoQ periplasmic alanine mutants*

The key residues, in the PhoQ periplasmic domain, potentially interacting with indole, were changed to alanine in *Salmonella phoQ* gene cloned on pCA24N. The Q5® Site-directed mutagenesis kit (NEB) was used to substitute arginine 100, lysine 186, and lysine 115 to alanine (R100A, K186A and K115A). The plasmids encoding the WT and mutant *phoQ* were transformed into the *hilA*- reporter *Salmonella* Δ*phoQ* strain. The effect of indole on *hilA* expression was observed using the β-gal reporter assay to determine the influence of the alanine substitutions in PhoQ's periplasmic domain on indole-mediated virulence. Our data (**Figure 26**) suggested that these are not the binding sites as the response to indole with the alanine-substituted PhoQ was not significantly different compared to that observed with the native PhoQ.

We further investigated the stability of indole's interaction with these residues in the binding pockets using Molecular Dynamics (MD) simulations. Our analysis suggested that indole did not interact with PhoQ stably in these four binding pockets. Briefly, the two docking programs/servers (SwissDock and AutoDock Vina) were used to search indole binding to the PhoQ crystal structures: 1YAX and 4UEY. For 1YAX and 4UEY, SwissDock produced 256 structures and AutoDock Vina produced 9 poses. The 9 binding poses predicted by AutoDock Vina for both structures were investigated through short (5 ns) MD simulations. For SwissDock produced structures, clustering analysis was carried out. The SwissDock structures were first scored using AutoDock Vina's scoring function and then ranked based on energy (lowest, most favorable to highest energy). WORDOM [180, 181] was used to conduct RMSD based clustering using leader method with cutoff

RMSD of 5 Å (Angstrom). The lowest energy structure, per cluster, was then investigated using short 5 ns MD simulations. A total of 21 binding poses from SwissDock were evaluated after clustering. The MD simulations showed indole leaving the binding site for all of the binding pockets investigated indicating that indole's interaction with the periplasmic domain was unstable.

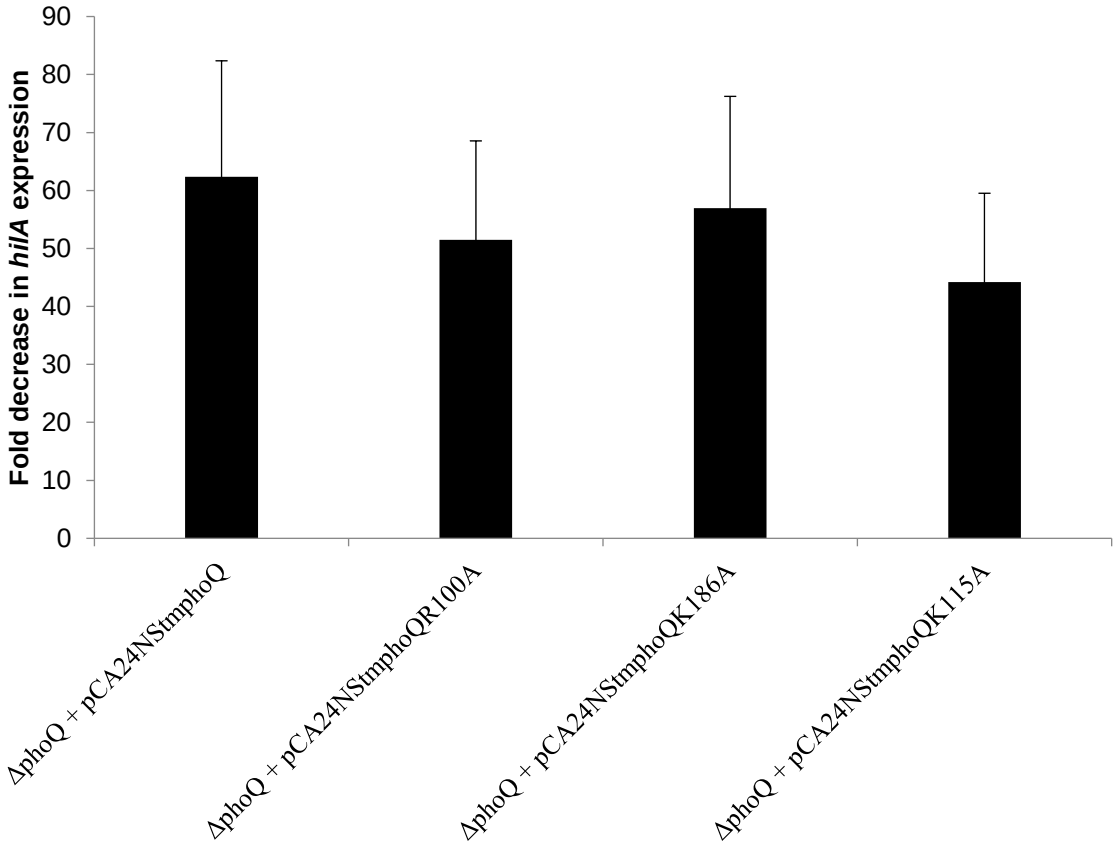

Figure 26. Effect of indole on *hilA* expression in PhoQ single amino acid mutants. *hilA* virulence gene expression using β-gal assay. The Δ*phoQ* mutation was generated in the *hilA* reporter and transformed with pCA24N plasmid encoding WT *phoQ*, *phoQ*R100A, *phoQ*K186A and *phoQ*K115A. The reporter strains were treated overnight with and without 1 mM indole and the β-gal activity was measured in exponential phase cultures after dilution. Data shown are the fold decrease in expression with indole-treatment relative to the solvent-treated control.

5.3.3 Investigation of indole interaction with the cytoplasmic domain of Salmonella *PhoQ*

We extended our computational analysis of indole-PhoQ interactions to the cytoplasmic domain. AutoDock Vina [163] was used to determine possible indole-binding sites in the cytoplasmic PhoQ domain (residues 331 – 485). Nine docking poses were generated by AutoDock Vina and eight of these shared the same binding site as ATP. The predicted poses were equilibrated for 1 ns and short 10 ns explicit solvent MD simulations were conducted. Interaction free energy was calculated using **Eq. 1** between the PhoQ residue R and indole (L). The average interaction free energies per PhoQ residue and their standard deviation is represented in **Figure 27**.

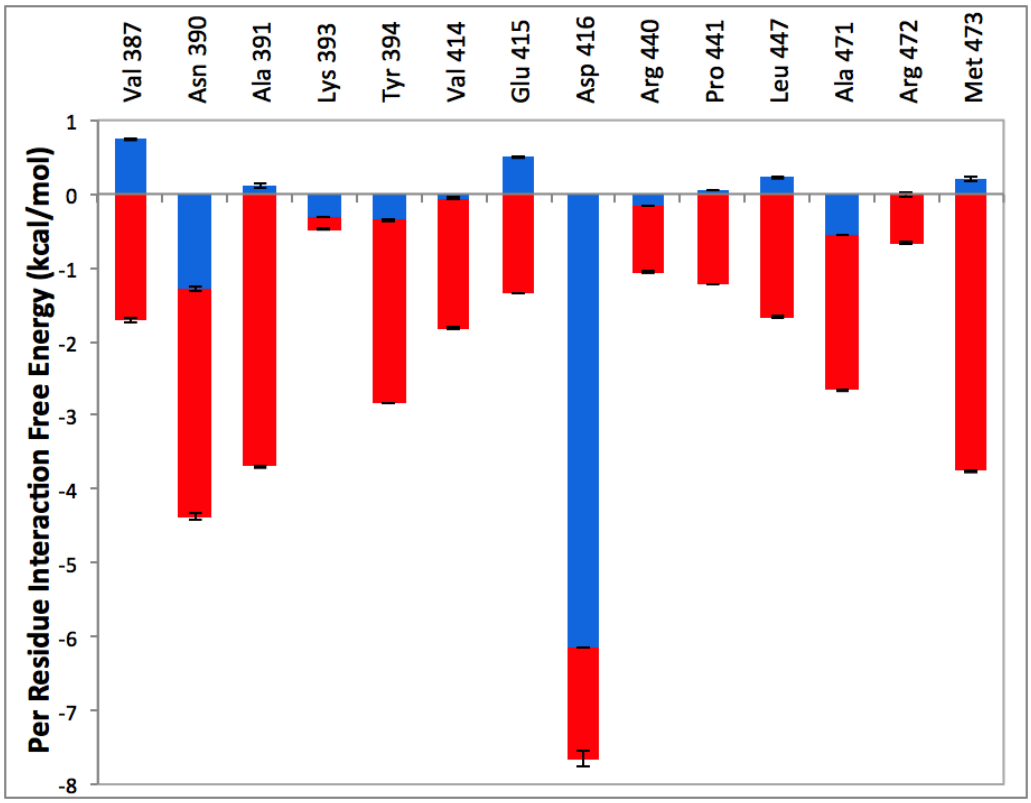

Figure 27. Preliminary average interaction free energies (kcal/mol) per residue for indole binding to the PhoQ cytoplasmic domain. Red bars and blue bars represent the non-polar and polar components of the total per residue interaction free energies, respectively.

Preliminary results show that indole is primarily stabilized by non-polar interactions. The aromatic ring of Tyr394 forms π-π interactions with the aromatic rings of indole. The side chains of Val387, Asn390, Ala391, Val414, Arg440, Pro441, Ala471, Met473, and Leu447 as well as the backbone atoms of Glu415 and Arg442 form the walls of the binding site and, due to their proximity to indole, interact with indole through non-polar interactions. These results also indicate that the position of Tyr394 is stabilized by cation-π interactions between the aromatic ring of Tyr394 and the charged group of

Lys393. The orientation of indole is largely guided by the strong, stable hydrogen bond formed between the amide group of indole and the carboxyl side chain of Asp416 (**Figure 28**).

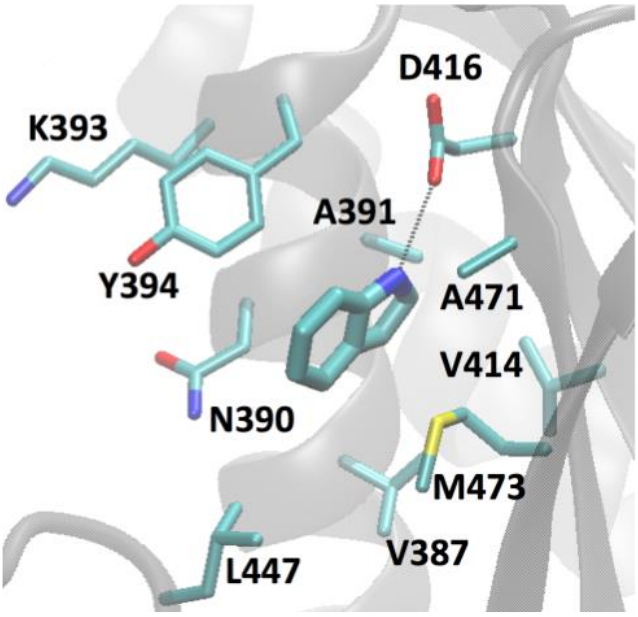

Figure 28. Simulation of indole binding to the cytoplasmic domain of *Salmonella* PhoQ. The PhoQ receptor is shown in gray, new cartoon representation. Key receptor residues are shown in thin licorice representation, labeled in black. The hydrogen bond between indole and Asp416 (D416) is shown by a dotted black line.

Other tryptophan metabolites such as indole-3-acetic acid, indole-3-pyruvic acid and tryptamine did not decrease *hilA* expression in *Salmonella* to the extent exhibited by indole treatment (**Figure 14**). Therefore, to test whether these other tryptophan metabolites interact with PhoQ in the ATP-binding pocket, we docked the three

compounds to the crystal structure of PhoQ using AutoDock Vina and conducted short MD simulations. Preliminary simulations showed that indole-3-acetic acid and indole-3-pyruvic acid were being pulled out of the ATP-binding site (**Figure 29**). Tryptamine, on the contrary, was stable in the ATP-binding site; however, it is likely trapped in the periplasmic domain that is rich in negatively charged residues such as aspartic and glutamic acid (**Figure 30**). Tryptamine's transport to the cytoplasm might be limited due to its interaction with PhoQ's periplasmic domain, thereby restricting its access to the cytoplasmic domain of PhoQ. This may explain why we do not observe a significant decrease in *hilA* expression with tryptamine treatment.

A

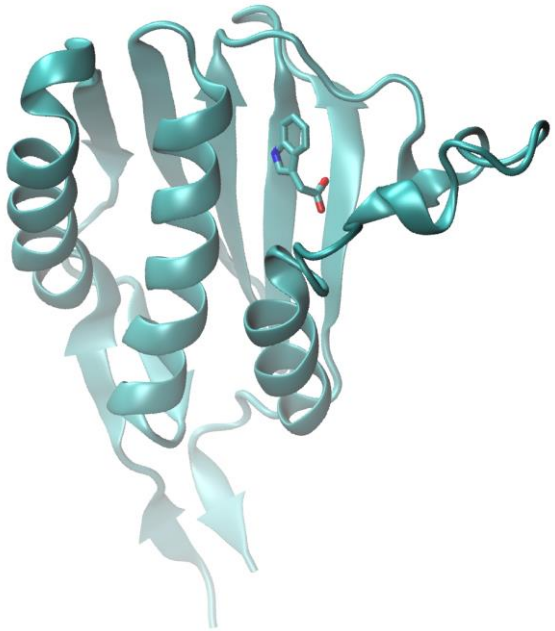

B

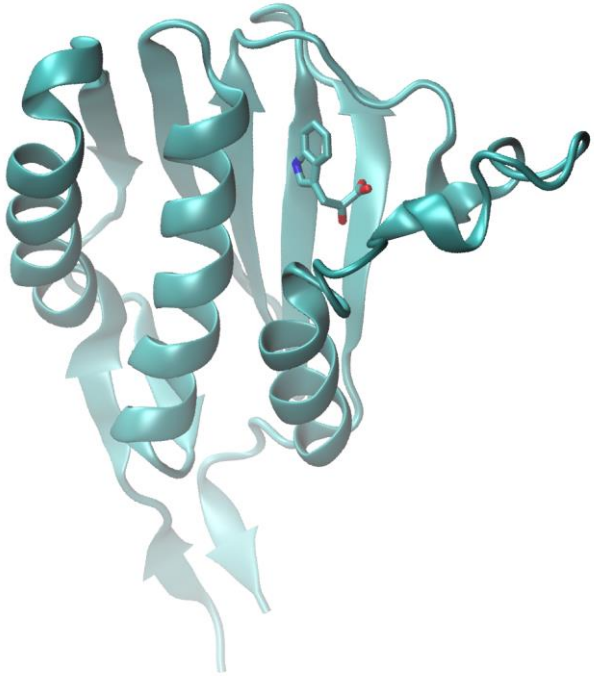

Figure 29. Docking of tryptophan metabolites with PhoQ cytoplasmic domain using AutoDock Vina. A candidate pose for A) indole-3-acetate and B) indole-3-pyruvate in the ATP-binding pocket of PhoQ crystal structure. Indole-3-acetate and indole-3-pyruvate are in licorice representation and PhoQ in new cartoon representation.

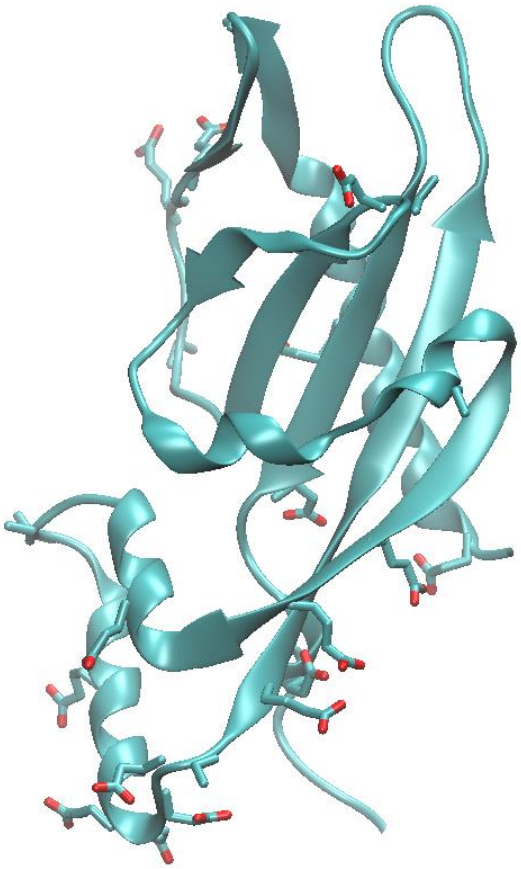

Figure 30. Experimentally resolved crystal structure of PhoQ's periplasmic domain with aspartic and glutamic acids shown in licorice representation. The negatively charged amino acid residues likely trap tryptamine in the periplasmic domain.

Table 5. Chemical structures (2D) of indole, other tryptophan metabolites, radicicol and ATP analogs. (Sourced from the open chemistry database: PubChem, https://pubchem.ncbi.nlm.nih.gov)

Chemical Name	Chemical Structure	PubChem CID
Indole	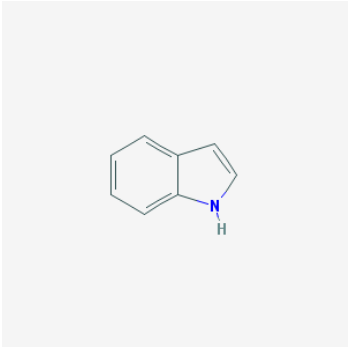	798
Indole-3-acetic acid	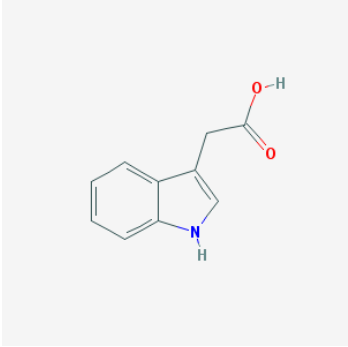	802
Indole-3-pyruvic acid	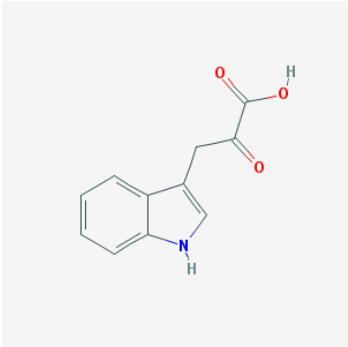	803

Table 5. Continued

Chemical Name	Chemical Structure	PubChem CID
Tryptamine	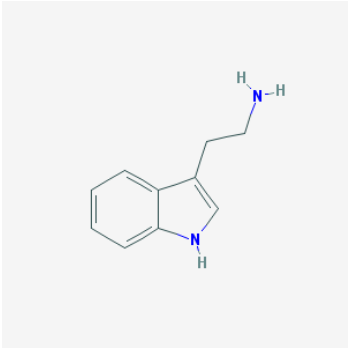	1150
Radicicol	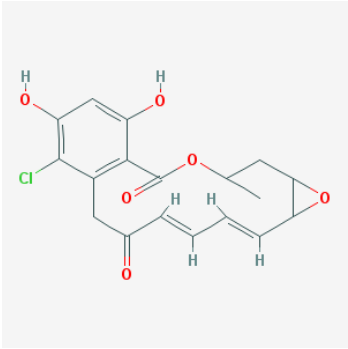	5359013
ATP	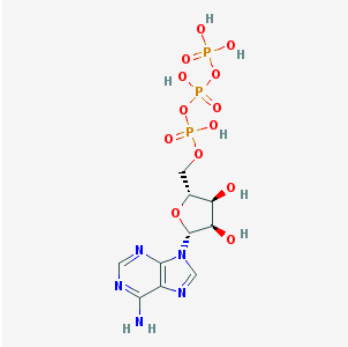	5957
TNP-ATP	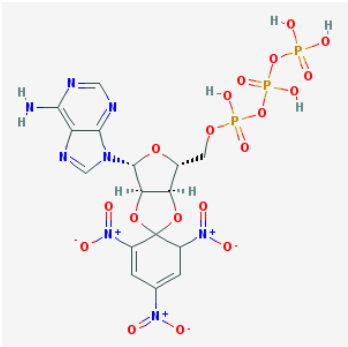	24820759

5.3.4 Indole's interaction with the catalytic domain of Salmonella *PhoQ*

Computational analysis of indole binding to the PhoQ cytoplasmic domain predicted that indole occupies the ATP binding site in the PhoQ catalytic domain. We used the TNP-ATP displacement assay to determine indole's interaction with the catalytic domain of *Salmonella* PhoQ (Stm $PhoQ_{cat}$) *in vitro*. The ~17 kDa Stm $PhoQ_{cat}$ protein was expressed in *E. coli* BL21 and purified as described in the methods section. Samples from purification steps were collected and run on SDS PAGE to verify presence of the desired protein (**Figure 31**).

The purified fraction containing Stm $PhoQ_{cat}$ was used in the TNP-ATP displacement assay to determine indole's interaction with PhoQ. Radicicol was used as a control because it is a known to bind *Salmonella* PhoQ in the ATP-binding site and reduce fluorescence by 50% in the TNP-ATP displacement assay [166]. Our observations with radicicol and indole in the TNP-ATP displacement assay were not as expected. The decrease in fluorescence was ~10% with 1 mM radicicol compared to the expected ~50% (**Figure 32**). Indole did not show a decrease in fluorescence at either of the concentrations tested (1 and 5 mM). The observations from the TNP-ATP displacement assay are inconclusive as the control (1 mM radicicol) did not result in the expected decrease in fluorescence. Future experiments will be aimed at optimizing the assay with respect to testing a range of concentrations (protein and ligand) as well as interaction time i.e. incubation period of the TNP-ATP:PhoQ complex with indole. We also propose to investigate radicicol in the *hilA* reporter assay to determine whether radicicol can downregulate *hilA* expression in a manner similar to that observed for indole.

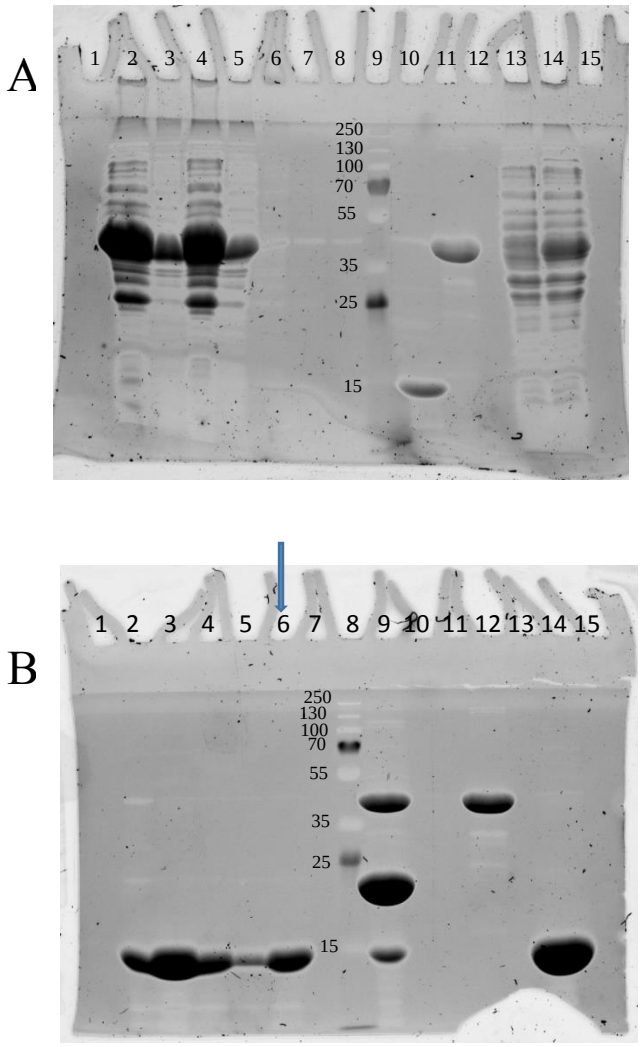

Figure 31. SDS PAGE images of Stm PhoQ$_{cat}$ purification fractions. A) Sonicated lysate (lanes 2, 3), unbound fractions from GS4B (lanes 4,5), washes from GS4B (lanes 6-8), PageRuler™ Plus ladder (lane 9), thrombin cleavage fraction (lane 10), GS4B matrix bound to Stm PhoQ$_{cat}$-GST (lane 11), uninduced whole cell lysate (lane 13) and induced whole cell lysate (lane 14).
B) Fractions containing Stm PhoQ$_{cat}$ post thrombin cleavage (lanes 2-5), purified Stm PhoQ$_{cat}$ post thrombin removal (lane 6), PageRuler™ Plus ladder (lane 8), GS4B matrix post thrombin cleavage (lane 9), GS4B matrix bound to Stm PhoQ$_{cat}$-GST (lane 12) and BSFF matrix post thrombin removal (lane 14).

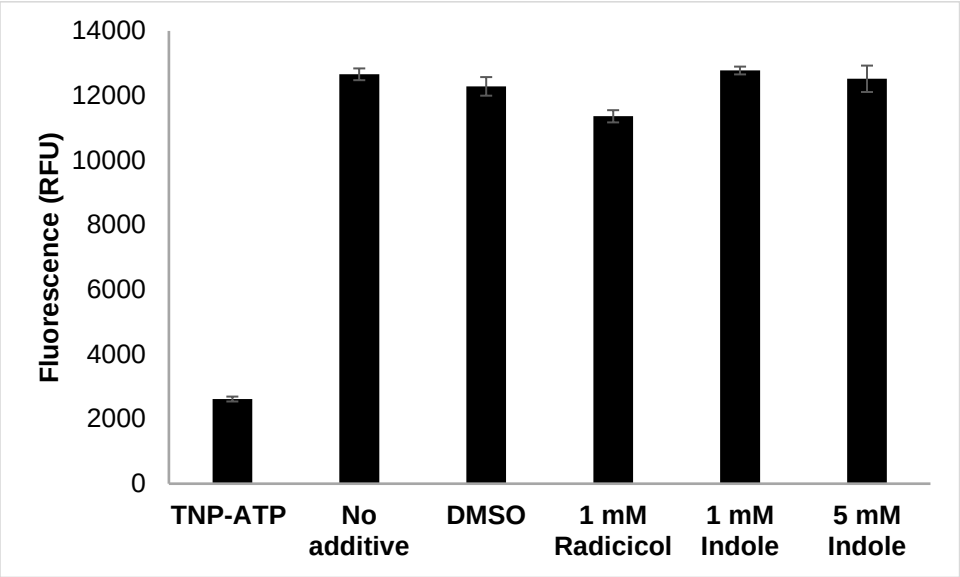

Figure 32. TNP-ATP displacement assay to assess indole's interaction with Stm PhoQ$_{cat}$ cytoplasmic domain in the ATP-binding pocket. TNP-ATP was mixed with Stm PhoQ$_{cat}$ in the ratio of 1:1 and fluorescence intensity was recorded after addition of control and test signals. Data shown is representative of two independent measurements from a single batch of purified Stm PhoQ$_{cat}$.

5.4 Discussion

Microorganisms sense changes in their environments through two-component systems (TCSs). These two-component systems are encoded in genomes of most bacteria with an average of 52 TCSs [182, 183] consisting of a sensor kinase and a cognate response regulator pair. About thirty putative sensor kinases have been identified in the *Salmonella* Typhimurium genome [184] and some of these TCS genes, such as *phoPQ* [29], *ompR*/*envZ* [185], *pmrAB* [186] and *ssrAB* [187], are important for systemic infection in mice.

The β-gal reporter and invasion assay data with Δ*phoPQ* mutants provided evidence for PhoPQ involvement in indole-mediated down-regulation of *Salmonella* virulence. PhoQ is the sensor for cations and cationic antimicrobial peptides that interact with the periplasmic domain [128, 130]. In order to determine the indole sensing mechanism for *Salmonella*, we used computational analysis of indole's interaction with the sensor kinase PhoQ followed by *in vitro* experiments to verify predictions. Since TCSs sense a wide range of environmental signals [183] and the most common mode of interaction occurs through binding to the periplasmic domain, we first scoped PhoQ's periplasmic domain for indole binding. Our simulations and *in vitro* data for indole binding to PhoQ suggest that indole does not interact with the periplasmic domain of PhoQ. Further computational analysis of PhoQ-indole interaction indicated that indole might interact with the cytoplasmic domain of PhoQ in the ATP-binding pocket (**Figure 33A**).

Free energy calculations for indole's interaction with the PhoQ catalytic domain (**Figure 27**) as well as reported interaction of radicicol with the PhoQ catalytic domain (**Figure 33B**) strongly support the possibility of indole's interaction with the PhoQ cytoplasmic region. However, further experimentation is required to verify these predictions.

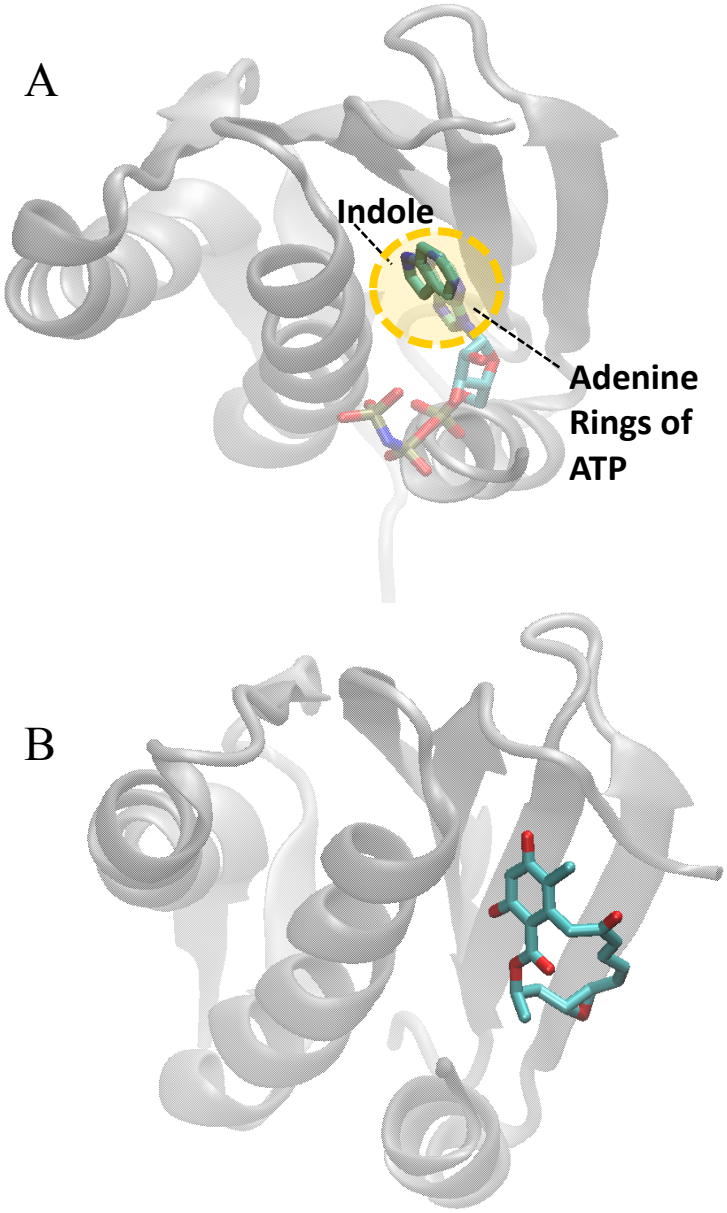

Figure 33. Molecular modeling of indole and radicicol binding to cytoplasmic domain of PhoQ in comparison to ATP. A) Binding pose of indole (opaque licorice representation) in the ATP-binding site of cytoplasmic domain of PhoQ (grey new cartoon representation). According to simulations, indole binds in the same location as the adenine rings of ATP (transparent licorice representation from protein alignment using Match Maker in Chimera).
B) Radicicol (opaque licorice representation) binding to the cytoplasmic domain of PhoQ (grey new cartoon representation). Loop residues 420-446 in PhoQ are omitted for clarity.

Although most of the ligands studied are known to interact with their receptor at the periplasmic domain, there is evidence that the EnvZ receptor mediates signal sensing via the cytoplasmic domain instead of the periplasmic domain [188]. Contingent upon verification, indole sensing by PhoQ may be another example of signal sensing through the cytoplasmic domain.

6. CONCLUSIONS AND FUTURE DIRECTIONS

Exposure to indole reduced the extent of *Salmonella* infection in mice. We observed lower competitiveness of indole treated *Salmonella* in the cecum, which is a known site for intestinal persistence and fecal shedding. The decrease in *Salmonella* virulence is due, in part, to the reduced motility and competence in invasion of mammalian cells. The phenotype of reduced epithelial cell invasion is a result of down-regulation of SPI-1 genes due to indole treatment. We also demonstrated that indole-mediated decrease in invasion is not limited to the bacterial cells but also extends to the mammalian cells, and indole-treated epithelial cells were found to be partially resistant to *Salmonella* invasion.

Indole's modulation of *Salmonella* virulence gene expression was not exhibited by other tryptophan metabolites such as indole-3-acetic acid, indole-3-pyruvic acid and tryptamine, suggesting a structure-function relationship for the different tryptophan metabolites in regulating SPI-1 gene expression. Indole also synergized with SCFA's (cecal concentrations) to down-regulate *hilA* expression *in vitro*, further supporting indole's importance as a virulence-mitigating signal in the gut.

We were also interested in determining the regulatory proteins involved in indole-mediated down-regulation of *Salmonella* invasion and virulence. Our current data shows that SdiA is not involved in the indole-mediated decrease in *Salmonella* invasion. A well-studied two-component regulatory system, PhoPQ, was determined to be partially involved in mediating indole's down-regulatory effect on *Salmonella* virulence as

determined by *in vitro* invasion and β-gal reporter assays. This leads us to surmise that other regulatory systems may also contribute to indole-mediated modulation of *Salmonella* virulence. We further investigated the mechanism of indole's interaction with PhoQ using computational approaches, such as ligand docking and molecular modeling, followed by *in vitro* experimentation. Our data suggests that indole might interact with the cytoplasmic catalytic domain of the PhoQ receptor rather than the periplasmic domain.

Indole also reduced *Salmonella* motility *in vitro* and acts as a chemorepellent. We confirmed that the repellent response to indole is mediated via indole sensing through the MCP Tsr in *Salmonella*. The chemorepellent property may be responsible in mitigating *Salmonella*'s migration to the infection niche in the GI tract, thereby strengthening colonization resistance *in vivo*.

Future directions for this work include further investigation into the role of indole *in vivo* as well as other mechanisms of indole-mediated modulation of *Salmonella* virulence. It would also be interesting to study indole's interaction with Tsr to understand the molecular mechanism underlying *Salmonella*'s chemorepellent response to indole. Some of the proposed future work is as follows:

1. *Investigate the role of indole in colonization resistance* in vivo

Gut microbiota protect the host from enteric infections using a phenomenon termed colonization resistance, however, the underlying mechanisms are not completely understood. It will be interesting to investigate whether indole plays a role in colonization resistance towards *Salmonella* infection *in vivo*. In order to test this, a defined microbiota community such as the Oligo-MM^{12} along with FA^{3} [80] can be used that confers

conventional-like colonization resistance against *Salmonella* infection. However, the consortium member strains would need to either not have *tnaA* activity or be genetically modified to delete the *tnaA* gene so that the gut environment is devoid of indole. The colonization ability of *Salmonella* in the presence of the modified Δ*tnaA* microbiota can be evaluated to understand indole's role *in vivo* pathogen colonization resistance.

SCFAs have been attributed to colonization resistance and a reduction in concentration of SCFAs in streptomycin-treated mice (due to a disruption of the normal microflora) resulted in an increase in *Salmonella* proliferation in the mouse gut [73, 76]. We observed that indole synergistically enhanced the down-regulation of *hilA in vitro*. This could be another factor contributing towards/enhancing colonization resistance and it would be interesting to ascertain the mechanism of indole's synergistic behavior on SPI-1 gene expression and regulation.

2. Investigate role of indole as a chemorepellent with respect to Salmonella *colonization*

The motility-apparatus flagella and the ability of directed movement, i.e. chemotaxis, are important for efficient colonization by *Salmonella* in mice [160]. Chemoreceptors can sense luminal signals and guide pathogens to favorable niches in the host to colonize and infect. Trg, Tsr and Aer are three such chemoreceptors that sense galactose, nitrate and tetrathionate, respectively, and promote *Salmonella* colonization in the mouse infection model [161]. In the present study, we demonstrate that indole is a chemorepellent sensed by the Tsr chemoreceptor. It would be interesting to investigate

whether indole's repellent response is stronger than the attractant response of the gut luminal signals such as galactose, nitrate and tetrathionate. Capillary assay with competing signals can be used to determine indole's potency as a chemorepellent in the presence of attractant signals that *Salmonella* encounters in the gut environment.

3. Determine indole-binding site on the Tsr chemoreceptor using docking and in vitro *experimentation*

We showed that indole is sensed by Tsr in *Salmonella* but little is known about how indole interacts with the chemoreceptor. A docking approach can be used to predict the sites of molecular interaction of the ligand indole with the protein chemoreceptor Tsr. The predictions can be verified experimentally by generating mutations in Tsr at the positions predicted to be important for indole interaction. These mutants can be evaluated for their chemotactic response using capillary assays to further our understanding on molecular interactions between indole and Tsr. Indole might play a role in preventing *Salmonella* colonization in the cecum and it will be worthwhile to further investigate the role of indole-Tsr interaction *in vivo* using the *tsr* mutants that do not respond to indole.

4. Investigate other mechanisms of indole-mediated down-regulation of Salmonella *virulence:*

In the present study we show that PhoPQ is only partially involved the indole-mediated down-regulation of *Salmonella* virulence. Therefore, further investigation to completely understand the other underlying mechanisms is needed. Bacteria sense

environmental signals using two component systems that signal their preparation for survival or infection. *Salmonella* Typhimurium genome has about thirty putative sensor kinases [184] which can be examined for their involvement in indole-mediated down-regulation of *Salmonella* virulence. An exploratory approach can be employed using sensor kinase gene deletion mutants for evaluation of indole's effect on *hilA* (master regulator of SPI-1 genes) expression. Abrogation of indole's response in a deletion mutant would suggest involvement of the deleted gene in indole-mediated modulation of *hilA* expression, hence *Salmonella* virulence.

REFERENCES

1. Hansen-Wester I, Hensel M. *Salmonella* pathogenicity islands encoding type III secretion systems. Microbes and Infection. 2001;3(7):549-59.

2. Savage DC. Microbial ecology of the gastrointestinal tract. Annual Reviews in Microbiology. 1977;31(1):107-33.

3. Ley RE, Peterson DA, Gordon JI. Ecological and evolutionary forces shaping microbial diversity in the human intestine. Cell. 2006;124(4):837-48.

4. Simon G, Gorbach S. Normal alimentary tract microflora. Infections of the gastrointestinal tract. 1995:53-69.

5. Bäckhed F, Ley RE, Sonnenburg JL, Peterson DA, Gordon JI. Host-Bacterial Mutualism in the Human Intestine. Science. 2005;307(5717):1915-20. doi: 10.1126/science.1104816.

6. Hooper LV, Gordon JI. Commensal host-bacterial relationships in the gut. Science. 2001;292(5519):1115-8.

7. Macpherson AJ, Harris NL. Interactions between commensal intestinal bacteria and the immune system. Nature Reviews Immunology. 2004;4(6):478-85.

8. Round JL, Mazmanian SK. The gut microbiota shapes intestinal immune responses during health and disease. Nature Reviews Immunology. 2009;9(5):313-23.

9. Artis D. Epithelial-cell recognition of commensal bacteria and maintenance of immune homeostasis in the gut. Nature Reviews Immunology. 2008;8(6):411-20.

10. Manson J, Rauch M, Gilmore M. The Commensal Microbiology of the Gastrointestinal Tract. In: Huffnagle G, Noverr M, editors. GI Microbiota and Regulation

of the Immune System. Advances in Experimental Medicine and Biology. 635: Springer New York; 2008. p. 15-28.

11. Eckburg PB, Bik EM, Bernstein CN, Purdom E, Dethlefsen L, Sargent M, et al. Diversity of the human intestinal microbial flora. Science. 2005;308(5728):1635-8.

12. O'Hara AM, Shanahan F. The gut flora as a forgotten organ. EMBO reports. 2006;7(7):688-93.

13. Hooper LV, Midtvedt T, Gordon JI. How host-microbial interactions shape the nutrient environment of the mammalian intestine. Annual review of nutrition. 2002;22(1):283-307.

14. Sun Y, O'Riordan MX. Regulation of bacterial pathogenesis by intestinal short-chain fatty acids. Advances in applied microbiology. 2013;85:93-118.

15. Tan J, McKenzie C, Potamitis M, Thorburn AN, Mackay CR, Macia L. The role of short-chain fatty acids in health and disease. Advances in immunology. 2014;121:91-119.

16. Snell EE. Tryptophanase: structure, catalytic activities, and mechanism of action. Advances in enzymology and related areas of molecular biology. 1975;42:287-333.

17. Lee HH, Molla MN, Cantor CR, Collins JJ. Bacterial charity work leads to population-wide resistance. Nature. 2010;467(7311):82-5.

18. Lee JH, Lee J. Indole as an intercellular signal in microbial communities. FEMS microbiology reviews. 2010;34(4):426-44.

19. Lee J, Jayaraman A, Wood TK. Indole is an inter-species biofilm signal mediated by SdiA. BMC microbiology. 2007;7:42.

20. Karlin D, Mastromarino A, Jones R, Stroehlein J, Lorentz O. Fecal skatole and indole and breath methane and hydrogen in patients with large bowel polyps or cancer. Journal of cancer research and clinical oncology. 1985;109(2):135-41.

21. Darkoh C, Chappell C, Gonzales C, Okhuysen P. A rapid and specific method for the detection of indole in complex biological samples. Applied and environmental microbiology. 2015;81(23):8093-7.

22. Bansal T, Alaniz RC, Wood TK, Jayaraman A. The bacterial signal indole increases epithelial-cell tight-junction resistance and attenuates indicators of inflammation. Proceedings of the National Academy of Sciences of the United States of America. 2010;107(1):228-33.

23. Bansal T, Englert D, Lee J, Hegde M, Wood TK, Jayaraman A. Differential effects of epinephrine, norepinephrine, and indole on *Escherichia coli* O157: H7 chemotaxis, colonization, and gene expression. Infection and immunity. 2007;75(9):4597-607.

24. Oh S, Go G, Mylonakis E, Kim Y. The bacterial signalling molecule indole attenuates the virulence of the fungal pathogen *Candida albicans*. Journal of applied microbiology. 2012;113(3):622-8.

25. Lee J, Jayaraman A, Wood T. Indole is an inter-species biofilm signal mediated by SdiA. BMC microbiology. 2007;7(1):42.

26. Ellermeier JR, Slauch JM. Adaptation to the host environment: regulation of the SPI1 type III secretion system in *Salmonella enterica* serovar Typhimurium. Current opinion in microbiology. 2007;10(1):24-9.

27. López-Garrido J, Casadesús J. Crosstalk between virulence loci: regulation of *Salmonella enterica* pathogenicity island 1 (SPI-1) by products of the std fimbrial operon. PloS one. 2012;7(1):e30499.

28. Jones BD. *Salmonella* invasion gene regulation: a story of environmental awareness. J Microbiol. 2005;43:110-7.

29. Miller SI, Mekalanos JJ. Constitutive expression of the PhoP regulon attenuates *Salmonella* virulence and survival within macrophages. Journal of bacteriology.

30. Bajaj V, Lucas RL, Hwang C, Lee CA. Co-ordinate regulation of *Salmonella typhimurium* invasion genes by environmental and regulatory factors is mediated by control of *hilA* expression. Molecular microbiology. 1996;22(4):703-14.

31. Groisman EA, Mouslim C. Sensing by bacterial regulatory systems in host and non-host environments. Nature reviews Microbiology. 2006;4(9):705-9.

32. Josenhans C, Suerbaum S. The role of motility as a virulence factor in bacteria. International journal of medical microbiology : IJMM. 2002;291(8):605-14.

33. Scallan E, Hoekstra RM, Angulo FJ, Tauxe RV, Widdowson MA, Roy SL, et al. Foodborne illness acquired in the United States--major pathogens. Emerging infectious diseases. 2011;17(1):7-15.

34. Scallan E, Crim SM, Runkle A, Henao OL, Mahon BE, Hoekstra RM, et al. Bacterial Enteric Infections Among Older Adults in the United States: Foodborne Diseases Active Surveillance Network, 1996–2012. Foodborne pathogens and disease. 2015;12(6):492-9.

35. Scallan E, Mahon BE, Hoekstra RM, Griffin PM. Estimates of illnesses, hospitalizations and deaths caused by major bacterial enteric pathogens in young children in the United States. The Pediatric infectious disease journal. 2013;32(3):217-21.

36. Majowicz SE, Musto J, Scallan E, Angulo FJ, Kirk M, O'Brien SJ, et al. The global burden of nontyphoidal *Salmonella* gastroenteritis. Clinical infectious diseases : an official publication of the Infectious Diseases Society of America. 2010;50(6):882-9.

37. Chao HC, Chen CC, Chen SY, Chiu CH. Bacterial enteric infections in children: etiology, clinical manifestations and antimicrobial therapy. Expert review of anti-infective therapy. 2006;4(4):629-38.

38. Kingsley RA, Baumler AJ. Host adaptation and the emergence of infectious disease: the *Salmonella* paradigm. Molecular microbiology. 2000;36(5):1006-14.

39. Jones BD, Ghori N, Falkow S. *Salmonella typhimurium* initiates murine infection by penetrating and destroying the specialized epithelial M cells of the Peyer's patches. The Journal of experimental medicine. 1994;180(1):15-23.

40. Haraga A, Ohlson MB, Miller SI. Salmonellae interplay with host cells. Nature Reviews Microbiology. 2008;6(1):53-66.

41. Kubori T, Sukhan A, Aizawa SI, Galan JE. Molecular characterization and assembly of the needle complex of the *Salmonella typhimurium* type III protein secretion system. Proceedings of the National Academy of Sciences of the United States of America. 2000;97(18):10225-30.

42. Moest TP, Méresse S. *Salmonella* T3SSs: successful mission of the secret (ion) agents. Current opinion in microbiology. 2013;16(1):38-44.

43. Agbor TA, McCormick BA. *Salmonella* effectors: important players modulating host cell function during infection. Cellular microbiology. 2011;13(12):1858-69.

44. Hayward RD, Koronakis V. Direct modulation of the host cell cytoskeleton by *Salmonella* actin-binding proteins. Trends in cell biology. 2002;12(1):15-20.

45. McGhie EJ, Brawn LC, Hume PJ, Humphreys D, Koronakis V. *Salmonella* takes control: effector-driven manipulation of the host. Current opinion in microbiology. 2009;12(1):117-24.

46. McGhie EJ, Hayward RD, Koronakis V. Control of actin turnover by a *Salmonella* invasion protein. Molecular cell. 2004;13(4):497-510.

47. Patel JC, Galan JE. Manipulation of the host actin cytoskeleton by *Salmonella*--all in the name of entry. Current opinion in microbiology. 2005;8(1):10-5.

48. Patel JC, Galan JE. Differential activation and function of Rho GTPases during *Salmonella*-host cell interactions. The Journal of cell biology. 2006;175(3):453-63.

49. Galan JE, Zhou D. Striking a balance: modulation of the actin cytoskeleton by *Salmonella*. Proceedings of the National Academy of Sciences of the United States of America. 2000;97(16):8754-61.

50. Stein MA, Leung KY, Zwick M, Garcia-del Portillo F, Finlay BB. Identification of a *Salmonella* virulence gene required for formation of filamentous structures containing lysosomal membrane glycoproteins within epithelial cells. Molecular microbiology. 1996;20(1):151-64.

51. Malik-Kale P, Jolly CE, Lathrop S, Winfree S, Luterbach C, Steele-Mortimer O. *Salmonella* - at home in the host cell. Frontiers in microbiology. 2011;2:125.

52. Brawn LC, Hayward RD, Koronakis V. *Salmonella* SPI1 effector SipA persists after entry and cooperates with a SPI2 effector to regulate phagosome maturation and intracellular replication. Cell host & microbe. 2007;1(1):63-75.

53. Wasylnka JA, Bakowski MA, Szeto J, Ohlson MB, Trimble WS, Miller SI, et al. Role for myosin II in regulating positioning of *Salmonella*-containing vacuoles and intracellular replication. Infection and immunity. 2008;76(6):2722-35.

54. Salcedo SP, Holden DW. SseG, a virulence protein that targets *Salmonella* to the Golgi network. The EMBO Journal. 2003;22(19):5003-14.

55. Hallstrom K, McCormick BA. *Salmonella* Interaction with and Passage through the Intestinal Mucosa: Through the Lens of the Organism. Frontiers in microbiology. 2011;2:88.

56. Ohlson MB, Huang Z, Alto NM, Blanc MP, Dixon JE, Chai J, et al. Structure and function of *Salmonella* SifA indicate that its interactions with SKIP, SseJ, and RhoA family GTPases induce endosomal tubulation. Cell host & microbe. 2008;4(5):434-46.

57. Buffie CG, Pamer EG. Microbiota-mediated colonization resistance against intestinal pathogens. Nature reviews Immunology. 2013;13(11):790-801.

58. Lawley TD, Walker AW. Intestinal colonization resistance. Immunology. 2013;138(1):1-11.

59. van der Waaij D, Berghuis-de Vries JM, Lekkerkerk L-v. Colonization resistance of the digestive tract in conventional and antibiotic-treated mice. The Journal of hygiene. 1971;69(3):405-11.

60. Freter R, Brickner H, Botney M, Cleven D, Aranki A. Mechanisms that control bacterial populations in continuous-flow culture models of mouse large intestinal flora. Infection and immunity. 1983;39(2):676-85.

61. Wilson KH, Perini F. Role of competition for nutrients in suppression of *Clostridium difficile* by the colonic microflora. Infection and immunity. 1988;56(10):2610-4.

62. Bernet MF, Brassart D, Neeser JR, Servin AL. *Lactobacillus acidophilus* LA 1 binds to cultured human intestinal cell lines and inhibits cell attachment and cell invasion by enterovirulent bacteria. Gut. 1994;35(4):483-9.

63. Lee YK, Puong KY, Ouwehand AC, Salminen S. Displacement of bacterial pathogens from mucus and Caco-2 cell surface by lactobacilli. Journal of medical microbiology. 2003;52(Pt 10):925-30.

64. Dabard J, Bridonneau C, Phillipe C, Anglade P, Molle D, Nardi M, et al. Ruminococcin A, a new lantibiotic produced by a *Ruminococcus gnavus* strain isolated from human feces. Applied and environmental microbiology. 2001;67(9):4111-8.

65. Gong HS, Meng XC, Wang H. Mode of action of plantaricin MG, a bacteriocin active against *Salmonella typhimurium*. Journal of basic microbiology. 2010;50 Suppl 1:S37-45.

66. Rea MC, Sit CS, Clayton E, O'Connor PM, Whittal RM, Zheng J, et al. Thuricin CD, a posttranslationally modified bacteriocin with a narrow spectrum of activity against *Clostridium difficile*. Proceedings of the National Academy of Sciences of the United States of America. 2010;107(20):9352-7.

67. Gantois I, Ducatelle R, Pasmans F, Haesebrouck F, Hautefort I, Thompson A, et al. Butyrate specifically down-regulates *Salmonella* pathogenicity island 1 gene expression. Applied and environmental microbiology. 2006;72(1):946-9.

68. Van Deun K, Pasmans F, Van Immerseel F, Ducatelle R, Haesebrouck F. Butyrate protects Caco-2 cells from *Campylobacter jejuni* invasion and translocation. The British journal of nutrition. 2008;100(3):480-4.

69. Hung CC, Garner CD, Slauch JM, Dwyer ZW, Lawhon SD, Frye JG, et al. The intestinal fatty acid propionate inhibits *Salmonella* invasion through the post-translational control of HilD. Molecular microbiology. 2013;87(5):1045-60.

70. Stecher B, Hardt WD. Mechanisms controlling pathogen colonization of the gut. Current opinion in microbiology. 2011;14(1):82-91.

71. Sekirov I, Tam NM, Jogova M, Robertson ML, Li Y, Lupp C, et al. Antibiotic-induced perturbations of the intestinal microbiota alter host susceptibility to enteric infection. Infection and immunity. 2008;76(10):4726-36.

72. Stecher B, Macpherson AJ, Hapfelmeier S, Kremer M, Stallmach T, Hardt WD. Comparison of *Salmonella enterica* serovar Typhimurium colitis in germfree mice and mice pretreated with streptomycin. Infection and immunity. 2005;73(6):3228-41.

73. Meynell GG, Subbaiah TV. Antibacterial mechanisms of the mouse gut. I. Kinetics of infection by *Salmonella typhi-murium* in normal and streptomycin-treated mice studied with abortive transductants. British journal of experimental pathology. 1963;44:197-208.

74. Barthel M, Hapfelmeier S, Quintanilla-Martinez L, Kremer M, Rohde M, Hogardt M, et al. Pretreatment of mice with streptomycin provides a *Salmonella enterica* serovar

Typhimurium colitis model that allows analysis of both pathogen and host. Infection and immunity. 2003;71(5):2839-58.

75. Bohnhoff M, Miller CP. Enhanced susceptibility to *Salmonella* infection in streptomycin-treated mice. The Journal of infectious diseases. 1962;111:117-27.

76. Meynell GG. Antibacterial mechanisms of the mouse gut. II. The role of Eh and volatile fatty acids in the normal gut. British journal of experimental pathology. 1963;44:209-19.

77. Smith MI, Yatsunenko T, Manary MJ, Trehan I, Mkakosya R, Cheng J, et al. Gut microbiomes of Malawian twin pairs discordant for kwashiorkor. Science (New York, NY). 2013;339(6119):548-54.

78. Clavel T, Lagkouvardos I, Blaut M, Stecher B. The mouse gut microbiome revisited: From complex diversity to model ecosystems. International journal of medical microbiology : IJMM. 2016;306(5):316-27.

79. Martz SL, McDonald JA, Sun J, Zhang YG, Gloor GB, Noordhof C, et al. Administration of defined microbiota is protective in a murine *Salmonella* infection model. Scientific reports. 2015;5:16094.

80. Brugiroux S, Beutler M, Pfann C, Garzetti D, Ruscheweyh HJ, Ring D, et al. Genome-guided design of a defined mouse microbiota that confers colonization resistance against *Salmonella enterica* serovar Typhimurium. Nature microbiology. 2016;2:16215.

81. Dewhirst FE, Chien CC, Paster BJ, Ericson RL, Orcutt RP, Schauer DB, et al. Phylogeny of the defined murine microbiota: altered Schaedler flora. Applied and environmental microbiology. 1999;65(8):3287-92.

82. Stecher B, Chaffron S, Kappeli R, Hapfelmeier S, Freedrich S, Weber TC, et al. Like will to like: abundances of closely related species can predict susceptibility to intestinal colonization by pathogenic and commensal bacteria. PLoS pathogens. 2010;6(1):e1000711.

83. Cho I, Blaser MJ. The human microbiome: at the interface of health and disease. Nature reviews Genetics. 2012;13(4):260-70.

84. Sekirov I, Russell SL, Antunes LC, Finlay BB. Gut microbiota in health and disease. Physiological reviews. 2010;90(3):859-904.

85. Zhang S, Kingsley RA, Santos RL, Andrews-Polymenis H, Raffatellu M, Figueiredo J, et al. Molecular pathogenesis of *Salmonella enterica* serotype Typhimurium-induced diarrhea. Infection and immunity. 2003;71(1):1-12.

86. Cummings JH, Pomare EW, Branch WJ, Naylor CP, Macfarlane GT. Short chain fatty acids in human large intestine, portal, hepatic and venous blood. Gut. 1987;28(10):1221-7.

87. Argenzio RA, Southworth M. Sites of organic acid production and absorption in gastrointestinal tract of the pig. The American journal of physiology. 1975;228(2):454-60.

88. Argenzio RA, Southworth M, Stevens CE. Sites of organic acid production and absorption in the equine gastrointestinal tract. The American journal of physiology. 1974;226(5):1043-50.

89. Lawhon SD, Maurer R, Suyemoto M, Altier C. Intestinal short-chain fatty acids alter *Salmonella typhimurium* invasion gene expression and virulence through BarA/SirA. Molecular microbiology. 2002;46(5):1451-64.

90. Huang Y, Suyemoto M, Garner CD, Cicconi KM, Altier C. Formate acts as a diffusible signal to induce *Salmonella* invasion. Journal of bacteriology. 2008;190(12):4233-41.

91. Jiang H, Li P, Gu Q. Heterologous expression and purification of plantaricin NC8, a two-peptide bacteriocin against Salmonella spp. from *Lactobacillus plantarum* ZJ316. Protein expression and purification. 2016;127:28-34.

92. Stevens KA, Sheldon BW, Klapes NA, Klaenhammer TR. Nisin treatment for inactivation of *Salmonella* species and other gram-negative bacteria. Applied and environmental microbiology. 1991;57(12):3613-5.

93. Prouty AM, Gunn JS. *Salmonella enterica* serovar Typhimurium invasion is repressed in the presence of bile. Infection and immunity. 2000;68(12):6763-9.

94. Eade CR, Hung CC, Bullard B, Gonzalez-Escobedo G, Gunn JS, Altier C. Bile Acids Function Synergistically To Repress Invasion Gene Expression in *Salmonella* by Destabilizing the Invasion Regulator HilD. Infection and immunity. 2016;84(8):2198-208.

95. Ridlon JM, Kang DJ, Hylemon PB. Bile salt biotransformations by human intestinal bacteria. Journal of lipid research. 2006;47(2):241-59.

96. Ridlon JM, Hylemon PB. Identification and characterization of two bile acid coenzyme A transferases from *Clostridium scindens*, a bile acid 7alpha-dehydroxylating intestinal bacterium. Journal of lipid research. 2012;53(1):66-76.

97. Masuda N, Oda H, Hirano S, Masuda M, Tanaka H. 7 alpha-Dehydroxylation of bile acids by resting cells of a *Eubacterium lentum*-like intestinal anaerobe, strain c-25. Applied and environmental microbiology. 1984;47(4):735-9.

98. Sridharan GV, Choi K, Klemashevich C, Wu C, Prabakaran D, Pan LB, et al. Prediction and quantification of bioactive microbiota metabolites in the mouse gut. Nature communications. 2014;5:5492.

99. Oh S, Go GW, Mylonakis E, Kim Y. The bacterial signalling molecule indole attenuates the virulence of the fungal pathogen *Candida albicans*. Journal of applied microbiology. 2012;113(3):622-8.

100. Lee J, Attila C, Cirillo SL, Cirillo JD, Wood TK. Indole and 7-hydroxyindole diminish *Pseudomonas aeruginosa* virulence. Microbial biotechnology. 2009;2(1):75-90.

101. Yang Q, Pande GS, Wang Z, Lin B, Rubin RA, Vora GJ, et al. Indole signaling and (micro)algal auxins decrease the virulence of *Vibrio campbellii*, a major pathogen of aquatic organisms. Environmental microbiology. 2017.

102. Vega NM, Allison KR, Khalil AS, Collins JJ. Signaling-mediated bacterial persister formation. Nature chemical biology. 2012;8(5):431-3.

103. Vega NM, Allison KR, Samuels AN, Klempner MS, Collins JJ. *Salmonella typhimurium* intercepts *Escherichia coli* signaling to enhance antibiotic tolerance. Proceedings of the National Academy of Sciences of the United States of America. 2013;110(35):14420-5.

104. Nikaido E, Yamaguchi A, Nishino K. AcrAB multidrug efflux pump regulation in *Salmonella enterica* serovar Typhimurium by RamA in response to environmental signals. The Journal of biological chemistry. 2008;283(35):24245-53.

105. Nikaido E, Giraud E, Baucheron S, Yamasaki S, Wiedemann A, Okamoto K, et al. Effects of indole on drug resistance and virulence of *Salmonella enterica* serovar Typhimurium revealed by genome-wide analyses. Gut pathogens. 2012;4(1):5.

106. Lee J, Zhang XS, Hegde M, Bentley WE, Jayaraman A, Wood TK. Indole cell signaling occurs primarily at low temperatures in *Escherichia coli*. The ISME journal. 2008;2(10):1007-23.

107. Michael B, Smith JN, Swift S, Heffron F, Ahmer BM. SdiA of *Salmonella enterica* is a LuxR homolog that detects mixed microbial communities. Journal of bacteriology. 2001;183(19):5733-42.

108. Wang XD, de Boer PA, Rothfield LI. A factor that positively regulates cell division by activating transcription of the major cluster of essential cell division genes of *Escherichia coli*. The EMBO Journal. 1991;10(11):3363-72.

109. Smith JN, Ahmer BM. Detection of other microbial species by *Salmonella*: expression of the SdiA regulon. Journal of bacteriology. 2003;185(4):1357-66.

110. Sabag-Daigle A, Soares JA, Smith JN, Elmasry ME, Ahmer BM. The acyl homoserine lactone receptor, SdiA, of *Escherichia coli* and *Salmonella enterica* serovar Typhimurium does not respond to indole. Applied and environmental microbiology. 2012;78(15):5424-31.

111. Stecher B, Robbiani R, Walker AW, Westendorf AM, Barthel M, Kremer M, et al. *Salmonella enterica* serovar Typhimurium Exploits Inflammation to Compete with the Intestinal Microbiota. PLoS Biology. 2007;5(10):e244.

112. Winter SE, Thiennimitr P, Winter MG, Butler BP, Huseby DL, Crawford RW, et al. Gut inflammation provides a respiratory electron acceptor for *Salmonella*. Nature. 2010;467(7314):426-9.

113. Price-Carter M, Tingey J, Bobik TA, Roth JR. The alternative electron acceptor tetrathionate supports B12-dependent anaerobic growth of *Salmonella enterica* serovar Typhimurium on ethanolamine or 1,2-propanediol. Journal of bacteriology. 2001;183(8):2463-75.

114. Thiennimitr P, Winter SE, Winter MG, Xavier MN, Tolstikov V, Huseby DL, et al. Intestinal inflammation allows *Salmonella* to use ethanolamine to compete with the microbiota. Proceedings of the National Academy of Sciences of the United States of America. 2011;108(42):17480-5.

115. Hapfelmeier S, Ehrbar K, Stecher B, Barthel M, Kremer M, Hardt WD. Role of the *Salmonella* pathogenicity island 1 effector proteins SipA, SopB, SopE, and SopE2 in *Salmonella enterica* subspecies 1 serovar Typhimurium colitis in streptomycin-pretreated mice. Infection and immunity. 2004;72(2):795-809.

116. Lopez CA, Winter SE, Rivera-Chavez F, Xavier MN, Poon V, Nuccio SP, et al. Phage-mediated acquisition of a type III secreted effector protein boosts growth of *Salmonella* by nitrate respiration. mBio. 2012;3(3).

117. Szabo C, Ischiropoulos H, Radi R. Peroxynitrite: biochemistry, pathophysiology and development of therapeutics. Nature reviews Drug discovery. 2007;6(8):662-80.

118. Barrett EL, Riggs DL. Evidence of a second nitrate reductase activity that is distinct from the respiratory enzyme in *Salmonella typhimurium*. Journal of bacteriology. 1982;150(2):563-71.

119. Barrett EL, Riggs DL. *Salmonella typhimurium* mutants defective in the formate dehydrogenase linked to nitrate reductase. Journal of bacteriology. 1982;149(2):554-60.

120. Fields PI, Swanson RV, Haidaris CG, Heffron F. Mutants of *Salmonella typhimurium* that cannot survive within the macrophage are avirulent. Proceedings of the National Academy of Sciences of the United States of America. 1986;83(14):5189-93.

121. Flannagan RS, Cosio G, Grinstein S. Antimicrobial mechanisms of phagocytes and bacterial evasion strategies. Nature reviews Microbiology. 2009;7(5):355-66.

122. Worley MJ, Ching KH, Heffron F. *Salmonella* SsrB activates a global regulon of horizontally acquired genes. Molecular microbiology. 2000;36(3):749-61.

123. Bijlsma JJ, Groisman EA. The PhoP/PhoQ system controls the intramacrophage type three secretion system of *Salmonella enterica*. Molecular microbiology. 2005;57(1):85-96.

124. Lee AK, Detweiler CS, Falkow S. OmpR regulates the two-component system SsrA-ssrB in *Salmonella* pathogenicity island 2. Journal of bacteriology. 2000;182(3):771-81.

125. Alpuche Aranda CM, Swanson JA, Loomis WP, Miller SI. *Salmonella typhimurium* activates virulence gene transcription within acidified macrophage

phagosomes. Proceedings of the National Academy of Sciences of the United States of America. 1992;89(21):10079-83.

126. Bader MW, Navarre WW, Shiau W, Nikaido H, Frye JG, McClelland M, et al. Regulation of *Salmonella typhimurium* virulence gene expression by cationic antimicrobial peptides. Molecular microbiology. 2003;50(1):219-30.

127. Bader MW, Sanowar S, Daley ME, Schneider AR, Cho U, Xu W, et al. Recognition of antimicrobial peptides by a bacterial sensor kinase. Cell. 2005;122(3):461-72.

128. Cho US, Bader MW, Amaya MF, Daley ME, Klevit RE, Miller SI, et al. Metal bridges between the PhoQ sensor domain and the membrane regulate transmembrane signaling. Journal of molecular biology. 2006;356(5):1193-206.

129. Prost LR, Daley ME, Le Sage V, Bader MW, Le Moual H, Klevit RE, et al. Activation of the bacterial sensor kinase PhoQ by acidic pH. Molecular cell. 2007;26(2):165-74.

130. Hicks KG, Delbecq SP, Sancho-Vaello E, Blanc MP, Dove KK, Prost LR, et al. Acidic pH and divalent cation sensing by PhoQ are dispensable for systemic Salmonellae virulence. eLife. 2015;4:e06792.

131. Chamnongpol S, Cromie M, Groisman EA. Mg2+ sensing by the Mg2+ sensor PhoQ of *Salmonella enterica*. Journal of molecular biology. 2003;325(4):795-807.

132. Alphen WV, Lugtenberg B. Influence of osmolarity of the growth medium on the outer membrane protein pattern of *Escherichia coli*. Journal of bacteriology. 1977;131(2):623-30.

133. Heyde M, Portalier R. Regulation of major outer membrane porin proteins of *Escherichia coli* K 12 by pH. Molecular & general genetics : MGG. 1987;208(3):511-7.

134. Thomas AD, Booth IR. The regulation of expression of the porin gene *ompC* by acid pH. Journal of general microbiology. 1992;138(9):1829-35.

135. Mills SD, Ruschkowski SR, Stein MA, Finlay BB. Trafficking of porin-deficient *Salmonella typhimurium* mutants inside HeLa cells: *ompR* and *envZ* mutants are defective for the formation of *Salmonella*-induced filaments. Infection and immunity. 1998;66(4):1806-11.

136. Chakraborty S, Mizusaki H, Kenney LJ. A FRET-based DNA biosensor tracks OmpR-dependent acidification of *Salmonella* during macrophage infection. PLoS Biology. 2015;13(4):e1002116.

137. Altier C, Suyemoto M, Lawhon SD. Regulation of *Salmonella enterica* serovar Typhimurium Invasion Genes by *csrA*. Infection and immunity. 2000;68(12):6790-7.

138. Santiviago CA, Reynolds MM, Porwollik S, Choi SH, Long F, Andrews-Polymenis HL, et al. Analysis of pools of targeted *Salmonella* deletion mutants identifies novel genes affecting fitness during competitive infection in mice. PLoS pathogens. 2009;5(7):e1000477.

139. Bogomolnaya LM, Santiviago CA, Yang HJ, Baumler AJ, Andrews-Polymenis HL. 'Form variation' of the O12 antigen is critical for persistence of *Salmonella* Typhimurium in the murine intestine. Molecular microbiology. 2008;70(5):1105-19.

140. Linden SK, Sheng YH, Every AL, Miles KM, Skoog EC, Florin TH, et al. MUC1 limits *Helicobacter pylori* infection both by steric hindrance and by acting as a releasable decoy. PLoS pathogens. 2009;5(10):e1000617.

141. Whitt DD, Demoss RD. Effect of microflora on the free amino acid distribution in various regions of the mouse gastrointestinal tract. Applied microbiology. 1975;30(4):609-15.

142. Kingsley RA, Humphries AD, Weening EH, De Zoete MR, Winter S, Papaconstantinopoulou A, et al. Molecular and phenotypic analysis of the CS54 island of *Salmonella enterica* serotype Typhimurium: identification of intestinal colonization and persistence determinants. Infection and immunity. 2003;71(2):629-40.

143. Weening EH, Barker JD, Laarakker MC, Humphries AD, Tsolis RM, Baumler AJ. The *Salmonella enterica* serotype Typhimurium *lpf*, *bcf*, *stb*, *stc*, *std*, and *sth* fimbrial operons are required for intestinal persistence in mice. Infection and immunity. 2005;73(6):3358-66.

144. Lostroh CP, Lee CA. The *Salmonella* pathogenicity island-1 type III secretion system. Microbes and infection. 2001;3(14-15):1281-91.

145. Carter PB, Collins FM. The route of enteric infection in normal mice. The Journal of experimental medicine. 1974;139(5):1189-203.

146. Kanamaru K, Kanamaru K, Tatsuno I, Tobe T, Sasakawa C. SdiA, an *Escherichia coli* homologue of quorum-sensing regulators, controls the expression of virulence factors in enterohaemorrhagic *Escherichia coli* O157:H7. Molecular microbiology. 2000;38(4):805-16.

147. Shimada Y, Kinoshita M, Harada K, Mizutani M, Masahata K, Kayama H, et al. Commensal bacteria-dependent indole production enhances epithelial barrier function in the colon. PloS one. 2013;8(11):e80604.

148. Roediger WE. Role of anaerobic bacteria in the metabolic welfare of the colonic mucosa in man. Gut. 1980;21(9):793-8.

149. Topping DL, Clifton PM. Short-chain fatty acids and human colonic function: roles of resistant starch and nonstarch polysaccharides. Physiological reviews. 2001;81(3):1031-64.

150. Sharma VK, Bearson SM, Bearson BL. Evaluation of the effects of *sdiA*, a *luxR* homologue, on adherence and motility of *Escherichia coli* O157 : H7. Microbiology. 2010;156(Pt 5):1303-12.

151. Ahmer BM, van Reeuwijk J, Timmers CD, Valentine PJ, Heffron F. *Salmonella typhimurium* encodes an SdiA homolog, a putative quorum sensor of the LuxR family, that regulates genes on the virulence plasmid. Journal of bacteriology. 1998;180(5):1185-93.

152. Montagne M, Martel A, Le Moual H. Characterization of the catalytic activities of the PhoQ histidine protein kinase of *Salmonella enterica* serovar Typhimurium. Journal of bacteriology. 2001;183(5):1787-91.

153. Tso WW, Adler J. Negative chemotaxis in *Escherichia coli*. Journal of bacteriology. 1974;118(2):560-76.

154. Oh JK, Perez K, Kohli N, Kara V, Li J, Min Y, et al. Hydrophobically-modified silica aerogels: Novel food-contact surfaces with bacterial anti-adhesion properties. Food Control. 2015;52:132-41.

155. Hansen MC, Palmer RJ, Jr., Udsen C, White DC, Molin S. Assessment of GFP fluorescence in cells of *Streptococcus gordonii* under conditions of low pH and low oxygen concentration. Microbiology. 2001;147(Pt 5):1383-91.

156. Datsenko KA, Wanner BL. One-step inactivation of chromosomal genes in *Escherichia coli* K-12 using PCR products. Proceedings of the National Academy of Sciences of the United States of America. 2000;97(12):6640-5.

157. Yu HS, Alam M. An agarose-in-plug bridge method to study chemotaxis in the Archaeon *Halobacterium salinarum*. FEMS microbiology letters. 1997;156(2):265-9.

158. Adler J. A method for measuring chemotaxis and use of the method to determine optimum conditions for chemotaxis by *Escherichia coli*. Journal of general microbiology. 1973;74(1):77-91.

159. Miller SI, Kukral AM, Mekalanos JJ. A two-component regulatory system (*phoP phoQ*) controls *Salmonella typhimurium* virulence. Proceedings of the National Academy of Sciences of the United States of America. 1989;86(13):5054-8.

160. Stecher B, Hapfelmeier S, Muller C, Kremer M, Stallmach T, Hardt WD. Flagella and chemotaxis are required for efficient induction of *Salmonella enterica* serovar Typhimurium colitis in streptomycin-pretreated mice. Infection and immunity. 2004;72(7):4138-50.

161. Rivera-Chavez F, Winter SE, Lopez CA, Xavier MN, Winter MG, Nuccio SP, et al. *Salmonella* uses energy taxis to benefit from intestinal inflammation. PLoS pathogens. 2013;9(4):e1003267.

162. Stecher B, Barthel M, Schlumberger MC, Haberli L, Rabsch W, Kremer M, et al. Motility allows *S.* Typhimurium to benefit from the mucosal defence. Cellular microbiology. 2008;10(5):1166-80.

163. Trott O, Olson AJ. AutoDock Vina: improving the speed and accuracy of docking with a new scoring function, efficient optimization, and multithreading. Journal of computational chemistry. 2010;31(2):455-61.

164. Grosdidier A, Zoete V, Michielin O. SwissDock, a protein-small molecule docking web service based on EADock DSS. Nucleic acids research. 2011;39(Web Server issue):W270-7.

165. Kitagawa M, Ara T, Arifuzzaman M, Ioka-Nakamichi T, Inamoto E, Toyonaga H, et al. Complete set of ORF clones of *Escherichia coli* ASKA library (A complete set of *E. coli* K-12 ORF archive): Unique resources for biological research. DNA research : an international journal for rapid publication of reports on genes and genomes. 2005;12(5):291-9.

166. Guarnieri MT, Zhang L, Shen J, Zhao R. The Hsp90 inhibitor radicicol interacts with the ATP-binding pocket of bacterial sensor kinase PhoQ. Journal of molecular biology. 2008;379(1):82-93.

167. Guarnieri MT, Blagg BS, Zhao R. A high-throughput TNP-ATP displacement assay for screening inhibitors of ATP-binding in bacterial histidine kinases. Assay and drug development technologies. 2011;9(2):174-83.

168. Bernstein FC, Koetzle TF, Williams GJ, Meyer EF, Jr., Brice MD, Rodgers JR, et al. The Protein Data Bank: a computer-based archival file for macromolecular structures. Journal of molecular biology. 1977;112(3):535-42.

169. Berman HM, Westbrook J, Feng Z, Gilliland G, Bhat TN, Weissig H, et al. The Protein Data Bank. Nucleic acids research. 2000;28(1):235-42.

170. Krivov GG, Shapovalov MV, Dunbrack RL. Improved prediction of protein side-chain conformations with SCWRL4. Proteins. 2009;77(4):778-95.

171. Irwin JJ, Shoichet BK. ZINC--a free database of commercially available compounds for virtual screening. Journal of chemical information and modeling. 2005;45(1):177-82.

172. Irwin JJ, Sterling T, Mysinger MM, Bolstad ES, Coleman RG. ZINC: a free tool to discover chemistry for biology. Journal of chemical information and modeling. 2012;52(7):1757-68.

173. Nakamura Y, Gojobori T, Ikemura T. Codon usage tabulated from international DNA sequence databases: status for the year 2000. Nucleic acids research. 2000;28(1):292.

174. Biasini M, Bienert S, Waterhouse A, Arnold K, Studer G, Schmidt T, et al. SWISS-MODEL: modelling protein tertiary and quaternary structure using evolutionary information. Nucleic acids research. 2014;42(Web Server issue):W252-8. Epub

2014/05/02. doi: 10.1093/nar/gku340. PubMed PMID: 24782522; PubMed Central PMCID: PMCPmc4086089.

175. Tamamis P, Morikis D, Floudas CA, Archontis G. Species specificity of the complement inhibitor compstatin investigated by all-atom molecular dynamics simulations. Proteins. 2010;78(12):2655-67.

176. Tamamis P, Pierou P, Mytidou C, Floudas CA, Morikis D, Archontis G. Design of a modified mouse protein with ligand binding properties of its human analog by molecular dynamics simulations: the case of C3 inhibition by compstatin. Proteins. 2011;79(11):3166-79.

177. Tamamis P, Lopez de Victoria A, Gorham RD, Jr., Bellows-Peterson ML, Pierou P, Floudas CA, et al. Molecular dynamics in drug design: new generations of compstatin analogs. Chemical biology & drug design. 2012;79(5):703-18.

178. Im W, Lee MS, Brooks CL, 3rd. Generalized born model with a simple smoothing function. Journal of computational chemistry. 2003;24(14):1691-702.

179. Harper S, Speicher DW. Purification of proteins fused to glutathione S-tranferase. Methods in molecular biology. 2011;681:259-80.

180. Seeber M, Cecchini M, Rao F, Settanni G, Caflisch A. Wordom: a program for efficient analysis of molecular dynamics simulations. Bioinformatics. 2007;23(19):2625-7.

181. Seeber M, Felline A, Raimondi F, Muff S, Friedman R, Rao F, et al. Wordom: a user-friendly program for the analysis of molecular structures, trajectories, and free energy surfaces. Journal of computational chemistry. 2011;32(6):1183-94.

182. Cock PJ, Whitworth DE. Evolution of prokaryotic two-component system signaling pathways: gene fusions and fissions. Molecular biology and evolution. 2007;24(11):2355-7.

183. Krell T, Lacal J, Busch A, Silva-Jimenez H, Guazzaroni ME, Ramos JL. Bacterial sensor kinases: diversity in the recognition of environmental signals. Annual review of microbiology. 2010;64:539-59.

184. Pullinger GD, van Diemen PM, Dziva F, Stevens MP. Role of two-component sensory systems of *Salmonella enterica* serovar Dublin in the pathogenesis of systemic salmonellosis in cattle. Microbiology. 2010;156(Pt 10):3108-22.

185. Beuzon CR, Meresse S, Unsworth KE, Ruiz-Albert J, Garvis S, Waterman SR, et al. *Salmonella* maintains the integrity of its intracellular vacuole through the action of SifA. The EMBO Journal. 2000;19(13):3235-49.

186. Gunn JS, Ryan SS, Van Velkinburgh JC, Ernst RK, Miller SI. Genetic and functional analysis of a PmrA-PmrB-regulated locus necessary for lipopolysaccharide modification, antimicrobial peptide resistance, and oral virulence of *Salmonella enterica* serovar Typhimurium. Infection and immunity. 2000;68(11):6139-46.

187. Yoon H, McDermott JE, Porwollik S, McClelland M, Heffron F. Coordinated regulation of virulence during systemic infection of *Salmonella enterica* serovar Typhimurium. PLoS pathogens. 2009;5(2):e1000306.

188. Leonardo MR, Forst S. Re-examination of the role of the periplasmic domain of EnvZ in sensing of osmolarity signals in *Escherichia coli*. Molecular microbiology. 1996;22(3):405-13.

APPENDIX

The *Salmonella phoQ* clones were sent for sequencing to Eton Bioscience Inc. in order to verify the presence of desired mutation. The sequences for the correct clones with the two primers: F-CA and pCA24N-gfpR are as follows:

1) Sequence data for pCA24NStmPhoQ, -gfp clone with F-CA primer:

CTTNNCCCATTCACCATCACCATACGGATCCGGCCCTGAGGGCCAATA
AATTTGCTCGCCATTTTCTGCCGCTGTCGCTGCGGGTTCGTTTTTTGCT
GGCGACAGCCGGCGTCGTGCTGGTGCTTTCTTTGGCATATGGCATAGT
GGCGCTGGTCGGCTATAGCGTAAGTTTTGATAAAACCACCTTTCGTTT
GCTGCGCGGCGAAAGCAACCTGTTTTATACCCTCGCCAAATGGGAAA
ATAATAAAATCAGCGTTGAGCTGCCTGAAAATCTGGACATGCAAAGC
CCGACCATGACGCTGATTTACGATGAAACGGGCAAATTATTATGGAC
GCAGCGCAACATTCCCTGGCTGATTAAAAGCATTCAACCGGAATGGT
TAAAAACGAACGGCTTCCATGAAATTGAAACCAACGTAGACGCCACC
AGCACGCTGTTGAGCGAAGACCATTCCGCGCAGGAAAAACTCAAAGA
AGTACGTGAAGATGACGATGATGCCGAGATGACCCACTCGGTAGCGG
TAAATATTTATCCTGCCACGGCGCGGATGCCGCAGTTAACCATCGTGG
TGGTCGATACCATTCCGATAGAACTAAAACGCTCCTATATGGTGTGGA
GCTGGTTCGTATACGTGCTGGCCGCCAATTTACTGTTAGTCATTCCTTT
ACTGTGGATCGCCGCCTGGTGGAGCTTACGCCCTATCGAGGCGCTGG
CGCGGGAAGTCCGCGAGCTTGAAGATCATCACCGCGAAATGCTCAAT

CCGGAGACGACGCGTGAGCTGACCAGCCTTGTGCGCAACCTTAATCA
ACTGCTCAAAAGCGAGCGTGAACGTTATAACAAATACCGCACGACCC
TGACCGACCTGACGCACAGTTTAAAAAACGCCGCTCGCGGGTTTTGC
AGAGTACGTTACGCTCTTTACGCAACGAAAGATGAGCGTCAGCAAAG
CTGAACCGGTGATGCTGGAACAGATCAGCCGGATTTTCCCAGCAGAT
CGGCTATTATCTGCATCGCGCCCAGTATGCGCGGTAGCGGCGTGTTGT
AAANCNGCGAACTGCATCCGGTCGCCGCCGTTGTTAAGAATAAACCC
TG

2) Sequence data for pCA24NStmPhoQ R100A, -gfp clone with F-CA primer:

NCCCTTCCCATGCACCATACGGATCCGGCCCTGAGGGCCAATAAATTT
GCTCGCCATTTTCTGCCGCTGTCGCTGCGGGTTCGTTTTTTGCTGGCGA
CAGCCGGCGTCGTGCTGGTGCTTTCTTTGGCATATGGCATAGTGGCGC
TGGTCGGCTATAGCGTAAGTTTTGATAAAACCACCTTTCGTTTGCTGC
GCGGCGAAAGCAACCTGTTTTATACCCTCGCCAAATGGGAAAATAAT
AAAATCAGCGTTGAGCTGCCTGAAAATCTGGACATGCAAAGCCCGAC
CATGACGCTGATTTACGATGAAACGGGCAAATTATTATGGACGCAGG
CGAACATTCCCTGGCTGATTAAAAGCATTCAACCGGAATGGTTAAAA
ACGAACGGCTTCCATGAAATTGAAACCAACGTAGACGCCACCAGCAC
GCTGTTGAGCGAAGACCATTCCGCGCAGGAAAAACTCAAAGAAGTAC
GTGAAGATGACGATGATGCCGAGATGACCCACTCGGTAGCGGTAAAT
ATTTATCCTGCCACGGCGCGGATGCCGCAGTTAACCATCGTGGTGGTC

GATACCATTCCGATAGAACTAAAACGCTCCTATATGGTGTGGAGCTG
GTTCGTATACGTGCTGGCCGCCAATTTACTGTTAGTCATTCCTTTACTG
TGGATCGCCGCCTGGTGGAGCTTACGCCCTATCGAGGCGCTGGCGCG
GGAAGTCCGCGAGCTTGAAGATCATCACCGCGAAATGCTCAATCCGG
AGACGACGCGTGAGCTGACCAGCCTTGTGCGCAACCTTAATCAACTG
CTCAAAAGCGAGCGTGAACGTTATAACAAATACCGCACGACCCTGAC
CGACCTGACGCACAGTTTAAAAACGCCGCTCGCGGTTTTGCAGAGTA
CGTTACGCTCTTTACGCAACGAAAAGATGAGCGTCAGCAAAGCTGAA
CCGGTGATGCTGGAACAGATCAGCCGGATTTCCCAGCAGATCGGCTA
TTATCTGCATCGCCGCCAGTATGCGCGTAGCGGCGTGTGTTAGCCGCG
AACTGCATCCCGTCGCGCGTGTAGAATACCTGATTTCTGCGCTAAATA
AGTTATCAGCGTAAGGGGTGATATCAGGTATGATATNACCAGAAATC
AGTTTGTCCGCGAGCCAAACGACCTGTCGAGTGATGNNACGNNCTGN
NNANNNTGGANATATGGCCTGGCAGTTGGTCCGAGAATTCCCGGGNN
TNCN

3) Sequence data for pCA24NStmPhoQ R100A, -gfp clone with pCA24N-gfpR primer:

NNGGNTCCGGCGGCAACCGAGCGTTCTCGAACAAATCCAGATGGAGT
TCTGAGGTCATTACTGGATCTATCAACAGGAGTCCAAGCTCAGCTAAT
TAAGCTTGGCTGCAGGTCGACCCTTAGCGGCCGCATAGGCCTTCCTCT
TTCTGTGTGGGATGCTGTCGGCCAAAAACGACCTCCATACGGGCGCC

ACCGAGCAGACTGTCGCTGGCAATGATCTGCCCGGCGTATTGTTCCGT

AATCTCGCGCGCGACAGCCAGCCCCACGCCTTGTCCTGGTCGTAGGGT

ATCGGCGCGCTGACCGCGATCAAACACCAGGGAACGTTTGCTGTGGG

GAATGCCTGGGCCGTCATCTTCGACGAAAATATGCAAATGATCGTCG

GTCTGGCGAGCCGAAATCTCGACAAACTCCAGACAATATTTACAAGC

GTTGTCCAGTACGTTGCCCATCACTTCGACAAAGTCGTTTTGCTCGCC

GACAAAACTGATTTCTGGTGAAATATCCATACTGATATTCACCCCTTT

ACGCTGATAAACTTTATTTAGCGCAGAAATCAGGTTATCTAACAACG

GCGCGACGGGATGCAGTTCGCGGCTTAACAACACGCCGCTACCGCGC

ATACTGGCGCGATGCAGATAATAGCCGATCTGCTGGGAAATCCGGCT

GATCTGTTCCAGCATCACCGGTTCAGCTTTGCTGACGCTCATCTTTTCG

TTGCGTAAAGAGCGTAACGTACTCTGCAAAACCGCGAGCGGCGTTTT

TAAACTGTGCGTCAGGTCGGTCAGGGTCGTGCGGTATTTGTTATAACG

TTCACGCTCGCTTTTGAGCAGTTGATTAAGGTTGCGCACAAGGCTGGT

CAGCTCACGCGTCGTCTCCGGATTGAGCATTTCGCGGTGATGATCTTC

AAGCTCGCGGACTTCCCGCGCCAGCGCCTCGATAGGGCGTAAGCTCC

ACCAGGCGGCGATCCACAGTAAAGGAATGACTACAGTAAATTGGCGG

GCAGCACGTATACGAACCAGCTCCACACCATATAGGAGCGTTTAGTT

CTATCGGAATGGNATCGACCACCACGATGGTAACTGCGCATCCGCGC

CGTGCCAGATAAATATTTACCGCTACGGATGGATCATCTCGNATCATC

GTCATCTNACGTACTTCTTTGAGTTTNCTGGCCCGGAATGNNTTNNNN

NACACGGNCTGG

TGCGNCTACGTTGNNTTCCAANTTTCATATGCGGAAANCNN

4) Sequence data for pCA24NStmPhoQ K115A, -gfp clone with F-CA primer:

ANCNGCGGATGCCGGCCCTGAGGGCCAATAAATTTGCTCGCCATTTTC

TGCCGCTGTCGCTGCGGGTTCGTTTTTTGCTGGCGACAGCCGGCGTCG

TGCTGGTGCTTTCTTTGGCATATGGCATAGTGGCGCTGGTCGGCTATA

GCGTAAGTTTTGATAAAACCACCTTTCGTTTGCTGCGCGGCGAAAGCA

ACCTGTTTTATACCCTCGCCAAATGGGAAAATAATAAAATCAGCGTTG

AGCTGCCTGAAAATCTGGACATGCAAAGCCCGACCATGACGCTGATT

TACGATGAAACGGGCAAATTATTATGGACGCAGCGCAACATTCCCTG

GCTGATTAAAAGCATTCAACCGGAATGGTTAGCGACGAACGGCTTCC

ATGAAATTGAAACCAACGTAGACGCCACCAGCACGCTGTTGAGCGAA

GACCATTCCGCGCAGGAAAAACTCAAAGAAGTACGTGAAGATGACG

ATGATGCCGAGATGACCCACTCGGTAGCGGTAAATATTTATCCTGCCA

CGGCGCGGATGCCGCAGTTAACCATCGTGGTGGTCGATACCATTCCG

ATAGAACTAAAACGCTCCTATATGGTGTGGAGCTGGTTCGTATACGTG

CTGGCCGCCAATTTACTGTTAGTCATTCCTTTACTGTGGATCGCCGCCT

GGTGGAGCTTACGCCCTATCGAGGCGCTGGCGCGGGAAGTCCGCGAG

CTTGAAGATCATCACCGCGAAATGCTCAATCCGGAGACGACGCGTGA

GCTGACCAGCCTTGTGCGCAACCTTAATCAACTGCTCAAAAGCGAGC

GTGAACGTTATAACAAATACCGCACGACCCTGACCGACCTGACGCAC

AGTTTAAAAACGCCGCTCGCGGTTTTGCAGAGTACGTTACGCTCTTTA

CGCAACGAAAAGATGAGCGTCAGCAAAGCTGAACCGGTGATGCTGG

AACAGATCAGCCGGATTTCCCAGCAGATCGGCTATTATCTGCATCGCC

GCCAGTATGCGCGGTAGCGGCGTGTTGTTAGCCGCGAACTGCATCCG

TCGCCGCGTTGTAGAATAACTGATTTCTGCGCTAAATAAAGTTATCAG

CGTAAAGGGGGTGAATATCAGTATGGNTATTTCACCAGAAATCAGNT

TTGTTCGCGAGCAACGACCTTGTCCGAGGTGTATGCACGTACTGNNN

ACGCCGTGGCAAAAT

ATGNNNTGGGAGTTGTGTGCGAGAATTTTCGGNNNNNN

5) Sequence data for pCA24NStmPhoQ K115A, -gfp clone with pCA24N-gfpR primer:

NTTGGGTTTACCATAAAAACGCCCGGCGGCAACCGAGCGTTCTGAAC

AAATCCAGATGGAGTTCTGAGGTCATTACTGGATCTATCAACAGGAG

TCCAAGCTCAGCTAATTAAGCTTGGCTGCAGGTCGACCCTTAGCGGCC

GCATAGGCCTTCCTCTTTCTGTGTGGGATGCTGTCGGCCAAAAACGAC

CTCCATACGGGCGCCACCGAGCAGACTGTCGCTGGCAATGATCTGCC

CGGCGTATTGTTCCGTAATCTCGCGCGCGACAGCCAGCCCCACGCCTT

GTCCTGGTCGTAGGGTATCGGCGCGCTGACCGCGATCAAACACCAGG

GAACGTTTGCTGTGGGGAATGCCTGGGCCGTCATCTTCGACGAAAAT

ATGCAAATGATCGTCGGTCTGGCGAGCCGAAATCTCGACAAACTCCA

GACAATATTTACAAGCGTTGTCCAGTACGTTGCCCATCACTTCGACAA

AGTCGTTTTGCTCGCCGACAAAACTGATTTCTGGTGAAATATCCATAC

TGATATTCACCCCTTTACGCTGATAAACTTTATTTAGCGCAGAAATCA

GGTTATCTAACAACGGCGCGACGGGATGCAGTTCGCGGCTTAACAAC

ACGCCGCTACCGCGCATACTGGCGCGATGCAGATAATAGCCGATCTG

CTGGGAAATCCGGCTGATCTGTTCCAGCATCACCGGTTCAGCTTTGCT

GACGCTCATCTTTTCGTTGCGTAAAGAGCGTAACGTACTCTGCAAAAC

CGCGAGCGGCGTTTTTAAACTGTGCGTCAGGTCGGTCAGGGTCGTGC

GGTATTTGTTATAACGTTCACGCTCGCTTTTGAGCAGTTGATTAAGGT

TGCGCACAAGGCTGGTCAGCTCACGCGTCGTCTCCGGATTGAGCATTT

CGCGGTGATGATCTTCCAAGCTCGCGGACTTCCCGCGCCAGCGCTTCG

ATAGGGCCGTAAGCTCCACCAGGCGGCGATCCACAGTAAAGGAATGA

CTAACAGTAAATTGGCCGGCAAGCACGTATACGACCAGCTCCACACC

ATTATAGGGAGCGTTAGTCTATCGGAATGNNATCGACCACACGGATG

TACTGCGCATCCGCGCGTGCAGGATAANNACGCTACGAGTGNNCATC

CGGCATCATCGCCATCCTNCGTACTCTGANTTTCCTGNCCGATGGTCT

CNNTCAACAGG

6) Sequence data for pCA24NStmPhoQ K186A, -gfp clone with F-CA primer:

NCCATGCGCCATACGGATCCGGCCCTGAGGGCCAATAAATTTGCTCG

CCATTTTCTGCCGCTGTCGCTGCGGGTTCGTTTTTTGCTGGCGACAGCC

GGCGTCGTGCTGGTGCTTTCTTTGGCATATGGCATAGTGGCGCTGGTC

GGCTATAGCGTAAGTTTTGATAAAACCACCTTTCGTTTGCTGCGCGGC

GAAAGCAACCTGTTTTATACCCTCGCCAAATGGGAAAATAATAAAAT

CAGCGTTGAGCTGCCTGAAAATCTGGACATGCAAAGCCCGACCATGA

CGCTGATTTACGATGAAACGGGCAAATTATTATGGACGCAGCGCAAC

ATTCCCTGGCTGATTAAAAGCATTCAACCGGAATGGTTAAAAACGAA

CGGCTTCCATGAAATTGAAACCAACGTAGACGCCACCAGCACGCTGT

TGAGCGAAGACCATTCCGCGCAGGAAAAACTCAAAGAAGTACGTGA

AGATGACGATGATGCCGAGATGACCCACTCGGTAGCGGTAAATATTT

ATCCTGCCACGGCGCGGATGCCGCAGTTAACCATCGTGGTGGTCGAT

ACCATTCCGATAGAACTAGCGCGCTCCTATATGGTGTGGAGCTGGTTC

GTATACGTGCTGGCCGCCAATTTACTGTTAGTCATTCCTTTACTGTGG

ATCGCCGCCTGGTGGAGCTTACGCCCTATCGAGGCGCTGGCGCGGGA

AGTCCGCGAGCTTGAAGATCATCACCGCGAAATGCTCAATCCGGAGA

CGACGCGTGAGCTGACCAGCCTTGTGCGCAACCTTAATCAACTGCTCA

AAAGCGAGCGTGAACGTTATAACAAATACCGCACGACCCTGACCGAC

CTGACGCACAGTTTAAAAACGCCGCTCGCGGTTTTGCAGAGTACGTTA

CGCTCTTTACGCAACGAAAAGATGAGCGTCAGCAAAGCTGAACCGGT

GATGCTGGGAACAGATCAGCCGGATTTCCCAGCAGATCGGCTATATC

TGCATCGCGCCAGTATGCGCGGTAGCGGCGTGTTGTAAGCCGCGAA

CTGCATCCCGTCGCGCGTGTAGATACCTGATTCTGCGCTAATAAAGTT

ATCAGCGTAAGGGTGATATCAGTANNNTATTCACCAGAAATTCANTN

GTCGCGAGCAACGACTTGTCGANNNTGGCACGTACTGGNCAGGCTTG

TTAAAATATTGGNCTGGA

7) Sequence data for pCA24NStmPhoQ K186A, -gfp clone with pCA24N-gfpR primer:

NCGACCCGGCGGCACCGAGCGTTCTGAACAATCCAGATGGAGTTCTG
AGGTCTTACTGGATCTATCAACAGGAGTCCAAGCTCAGCTAATTAAG
CTTGGCTGCAGGTCGACCCTTAGCGGCCGCATAGGCCTTCCTCTTTCT
GTGTGGGATGCTGTCGGCCAAAAACGACCTCCATACGGGCGCCACCG
AGCAGACTGTCGCTGGCAATGATCTGCCCGGCGTATTGTTCCGTAATC
TCGCGCGCGACAGCCAGCCCCACGCCTTGTCCTGGTCGTAGGGTATCG
GCGCGCTGACCGCGATCAAACACCAGGGAACGTTTGCTGTGGGGAAT
GCCTGGGCCGTCATCTTCGACGAAAATATGCAAATGATCGTCGGTCTG
GCGAGCCGAAATCTCGACAAACTCCAGACAATATTTACAAGCGTTGT
CCAGTACGTTGCCCATCACTTCGACAAAGTCGTTTTGCTCGCCGACAA
AACTGATTTCTGGTGAAATATCCATACTGATATTCACCCCTTTACGCT
GATAAACTTTATTTAGCGCAGAAATCAGGTTATCTAACAACGGCGCG
ACGGGATGCAGTTCGCGGCTTAACAACACGCCGCTACCGCGCATACT
GGCGCGATGCAGATAATAGCCGATCTGCTGGGAAATCCGGCTGATCT
GTTCCAGCATCACCGGTTCAGCTTTGCTGACGCTCATCTTTTCGTTGCG
TAAAGAGCGTAACGTACTCTGCAAAACCGCGAGCGGCGTTTTTAAAC
TGTGCGTCAGGTCGGTCAGGGTCGTGCGGTATTTGTTATAACGTTCAC
GCTCGCTTTTGAGCAGTTGATTAAGGTTGCGCACAAGGCTGGTCAGCT
CACGCGTCGTCTCCGGATTGAGCATTTCGCGGTGATGATCTTCAAGCT
CGCGGACTTCCCGCGCCAGCGCCTCGATAGGGCGTAAGCTCCACCAG

GGCGGCGATCCACAGTAAAGGAATGACTACAGTAAATTGGCGGGCCA

GCACGTATACGAACCAGCTCCACACCATATAGGAGCGCCGCT

AGTCTATCGGATGNATCGACCACCCACGATGGTNACTGCGCATCCGC

GCCGTGCCAGATAATATTAACCCGCTACCGAGTGNNCATCTCGNATC

ATCGTCATCCTNNACGTTACCTCTNGNTTNTCTGGGCCCGGATGNNTT

CGCCCCTCCAACAANCNN